

Blind Channel Estimation and Single-User Detection for Multi-Carrier and Spread-Spectrum Systems with Transmit Diversity

Shahrokh Nayeb Nazar



Department of Electrical & Computer Engineering
McGill University
Montreal, Canada

February 2008

A thesis submitted to McGill University in partial fulfillment of the requirements for the
degree of Doctor of Philosophy.

© 2008 Shahrokh Nayeb Nazar



Library and
Archives Canada

Bibliothèque et
Archives Canada

Published Heritage
Branch

Direction du
Patrimoine de l'édition

395 Wellington Street
Ottawa ON K1A 0N4
Canada

395, rue Wellington
Ottawa ON K1A 0N4
Canada

Your file Votre référence
ISBN: 978-0-494-50965-4
Our file Notre référence
ISBN: 978-0-494-50965-4

NOTICE:

The author has granted a non-exclusive license allowing Library and Archives Canada to reproduce, publish, archive, preserve, conserve, communicate to the public by telecommunication or on the Internet, loan, distribute and sell theses worldwide, for commercial or non-commercial purposes, in microform, paper, electronic and/or any other formats.

The author retains copyright ownership and moral rights in this thesis. Neither the thesis nor substantial extracts from it may be printed or otherwise reproduced without the author's permission.

AVIS:

L'auteur a accordé une licence non exclusive permettant à la Bibliothèque et Archives Canada de reproduire, publier, archiver, sauvegarder, conserver, transmettre au public par télécommunication ou par l'Internet, prêter, distribuer et vendre des thèses partout dans le monde, à des fins commerciales ou autres, sur support microforme, papier, électronique et/ou autres formats.

L'auteur conserve la propriété du droit d'auteur et des droits moraux qui protègent cette thèse. Ni la thèse ni des extraits substantiels de celle-ci ne doivent être imprimés ou autrement reproduits sans son autorisation.

In compliance with the Canadian Privacy Act some supporting forms may have been removed from this thesis.

Conformément à la loi canadienne sur la protection de la vie privée, quelques formulaires secondaires ont été enlevés de cette thèse.

While these forms may be included in the document page count, their removal does not represent any loss of content from the thesis.

Bien que ces formulaires aient inclus dans la pagination, il n'y aura aucun contenu manquant.

■*■
Canada

Abstract

The application of transmit diversity techniques such as Space-Time Block Coding (STBC) to the downlink of multiuser wireless communications systems has received considerable attention. The main advantage of such an approach is its ability to provide diversity gains through the use of multiple antennas only at the transmitting side without significantly increasing the complexity at the receiving end. Among the many multiple access techniques proposed, Multi-Carrier (MC) and Direct Sequence (DS) Code Division Multiple Access (CDMA) techniques are known as the most promising candidates for future broadband mobile communication networks. In MC and DS-CDMA systems or combination thereof, employing transmit diversity, the spatial diversity gains can only be realized if the underlying channels are accurately acquired at the receiver. Furthermore, such systems suffer from high computational complexity which should be properly addressed for practical implementations.

Motivated by these observations, in the first part of this dissertation, we introduce the chip-level ST block coding scheme for DS-CDMA systems. For this scheme, we address the problems of single-user detection as well as blind channel estimation, and we show that chip-level coding does not suffer from antenna order ambiguity. Moreover, we demonstrate that chip-level schemes exhibit low decoding delay and allow for the design of adaptive single-user detectors with improved short data-record performance characteristics compared to their symbol-level counterparts.

In the second part of this dissertation, we present a novel transmission scheme for the downlink of MC-CDMA systems with transmit diversity that is based on chip-level Space-Frequency (SF) block coding. For this scheme, we investigate the problem of blind channel estimation when the received signal processing is done (i) pre-Fast Fourier Transform (FFT); and (ii) post-FFT. We propose two blind channel estimation algorithms based on subspace and Minimum Variance Distortionless Response (MVDR) principles. Moreover, we present an analytical performance analysis of the proposed algorithms by investigating the bias as well as the finite data record mean-square error of the channel estimates. Our analysis shows that SFBC MC-CDMA systems do not suffer from antenna order ambiguity. In addition, to benchmark the accuracy of our estimation algorithms, we derive the corresponding Cramér-Rao bounds (CRB) based on a novel approach that assumes the knowledge of only the spreading code of the desired user. Our approach has the advantage of providing lower bounds which are tighter than the CRBs with known signatures.

We also study the problem of single user detection for downlink transmissions to address the issue of multiuser interference. In the case of the post-FFT approach, we take advantage of the SFBC-induced signal structure to derive linear single-user detectors with improved performance in short data-record situations. Finally, in order to address the issue of computational complexity, we exploit the structure of the covariance matrix of the received signal to simplify the computations

involved in estimating the channel, and forming the detector.

Abrégé

Le sujet des techniques de la transmission en diversité, tel que celui du STBC appliqué au canal descendant des télécommunications sans fil à usagers multiples, a reçu une attention considérable. Ici, le gain de diversité obtenu en utilisant de multiples antennes pour la transmission, tout en minimisant la complexité du récepteur, est le principal avantage. Parmi les nombreuses méthodes d'accès multiples, l'utilisation des techniques multiporteuses (MC) et du DS-CDMA, apportent des solutions les plus prometteuses en ce qui concerne le futur des communications mobiles à haut débit. Seuls ou combinés, les systèmes MC et DS-CDMA ne peuvent créer des gains de diversité d'espace que si le récepteur obtient fidèlement les canaux sous-jacents. De plus, la complexité computationnelle est un obstacle à surmonter avant la mise en pratique de tels systèmes.

Motivés par ces observations, nous présentons, dans la première partie de cette dissertation, la technique du codage spatiotemporel (ST) en bloc au niveau de la puce, pour systèmes DS-CDMA. À cette fin, nous soulevons les problèmes de la détection à usagers simples ainsi que de l'estimation aveugle du canal. Notamment, nous faisons remarquer que le codage au niveau de la puce n'est pas affecté par l'ambiguïté d'ordre d'antenne. De plus, nous démontrons que les méthodes, au niveau de la puce, font preuves de décodage rapide et permettent la conception de détecteurs adaptatifs à usagers multiples. Face à leurs homologues au niveau du symbole, ces détecteurs démontrent une performance améliorée pour de courts enregistrements de données.

Dans la seconde partie de cette dissertation, nous présentons une nouvelle méthode de transmission pour le canal descendant des systèmes MC-CDMA. Cette dernière consiste en une diversité de transmission basée sur le codage bloc spatiofréquentiel (SF) au niveau de la puce. C'est ainsi que nous abordons le problème de l'estimation aveugle du canal avec traitement du signal fait (i) avant FFT, et (ii) après FFT. Nous proposons deux algorithmes d'estimation aveugle fondés sur les bases de sous-espace et de réponses à variance minimale sans déformation (MVDR). Par surcroît, nous faisons part de notre travail analytique pour la performance de nos algorithmes en nous penchant sur le biais ainsi que sur l'erreur quadratique moyenne des estimations du canal avec des enregistrements de données finies. Notre travail démontre que les systèmes SFBC MC-CDMA ne sont pas affectés par l'ambiguïté d'ordre d'antenne. D'autre part, afin de coter la performance de nos estimations, nous obtenons les bornes de Cramer-Rao (CRB) grâce à une méthode originale qui ne prend en considération que le code d'étalement de l'utilisateur désiré. Notre approche permet de resserrer les limites du type CRB déjà connues.

Nous abordons également le problème de l'utilisation, pour transmissions descendantes, de détecteurs à usagers simples afin de combattre l'interférence multiusager. Quant à l'approche après FFT, nous utilisons la structure du signal reliée au SFBC afin d'obtenir des détecteurs linéaires à usagers simples qui démontrent des performances supérieures en situations d'enregistrements

de données courts. Pour terminer, nous traitons le cas de la complexité computationnelle. Nous montrons qu'en exploitant la structure de la matrice des covariances du signal reçu, il est possible de simplifier les calculs nécessaires pour l'estimation du canal ainsi que pour définir le détecteur.

Acknowledgments

First of all, I would like to express my sincere thanks to my advisor, Prof. Ioannis Psaromiligkos, for his continued support, guidance, encouragement and trust throughout my Ph.D. studies. I greatly appreciate the respect and the freedom in research that he gave me. He is always available to give me timely and indispensable advice. I can never forget the days and nights that we spent together trying to meet the deadlines of my papers. I believe what I learned during the past few years working with him established a basis that could lead me to the future success.

Next, I would like to thank Prof. Benoit Champagne, and Prof. Benoit Boulet for serving on my proposal committee. Their insightful remarks and comments have made significant contributions to the improvement of my work. Furthermore, I would like to thank the former and current members of Telecommunications and Signal Processing Laboratory in the Department of Electrical & Computer Engineering at McGill University for their help, encouragement and the fruitful discussions. They create a great research environment.

I would like to thank my parents for their unconditional love and support during my academic studies. I attribute all my success in life to their blessings.

Finally, I would like to express my love and appreciation to my wife Farzaneh, to whom I would like to dedicate my thesis. Without her sacrifice and support I would have never been able to complete my studies.

Contents

1	Introduction	1
1.1	Background and Literature Review	1
1.2	Thesis Contribution	7
1.3	Thesis Organization	11
1.4	Published Work	11
2	Chip-Level Space-Time Block Coded DS/CDMA systems	13
2.1	Introduction	13
2.2	System Description	15
2.3	Single-User Detection Algorithms	18
2.3.1	Disjoint ST Decoding and Symbol Detection	18
2.3.2	Joint ST Decoding and Symbol Detection	21
2.4	Blind Channel Estimation	24
2.4.1	Symbol-level vs. Chip-level STBC	25
2.4.2	Subspace-based Channel Estimation Algorithms	27
2.5	Simulations Studies	30
3	Space-Frequency Block Coded MC-CDMA: A Pre-FFT Approach	34
3.1	Introduction	34
3.2	System Model	38
3.2.1	Equivalent Single-Input-Single-Output Representation	40
3.3	Single-User Detection	42
3.3.1	Disjoint SF Decoding and Symbol Detection	43
3.3.2	Joint SF Decoding and Symbol Detection	45
3.3.3	Simulations Studies	47
3.4	Subspace-based Blind Channel Estimation	49

3.4.1	Identifiability	51
3.4.2	SFBC vs. STBC	55
3.4.3	Finite Data Record Performance Analysis	56
3.4.4	Cramer-Rao Bound	59
3.4.5	Simulations Studies	64
3.5	MVDR-type Blind Channel Estimation	67
3.5.1	Performance Analysis	70
3.5.2	Cramer-Rao Bound	73
3.5.3	Simulations Studies	75
4	Space-Frequency Block Coded MC-CDMA: A Post-FFT Approach	79
4.1	Introduction	79
4.2	System Model	81
4.2.1	Equivalent Single-Input-Single-Output Representation	81
4.3	Second-Order-Statistics-based Channel Estimation Methods: Background and Simplifications	83
4.3.1	MVDR Channel Estimator	85
4.3.2	Subspace Channel Estimator	86
4.4	Improved Blind Channel Estimation Algorithms	87
4.4.1	Identifiability	90
4.5	Performance Analysis	92
4.5.1	MVDR Algorithm Mean-Squared Error Performance	92
4.5.2	Subspace Algorithm Mean-Squared Error Performance	95
4.6	Cramer-Rao Bounds	96
4.7	Detection Algorithms	101
4.8	Simulations Studies	103
5	Conclusions and Future Research	112
5.1	Future Research	113
	References	116

List of Figures

2.1	Combined STBC and DS/CDMA transmission and reception.	16
2.2	Receiver structure (a) Disjoint ST block decoding and single-user detection, (b) Joint ST block decoding and single-user detection.	19
2.3	Normalized cross-correlation between the channel vector \mathbf{h} and the channel estimate $\hat{\mathbf{h}}$ as a function of the data record size M	30
2.4	Bit-error-rate of disjoint single-user detection algorithms as a function of the SNR of the user of interest for flat fading channels.	31
2.5	Bit-error-rate of joint single-user detection algorithms as a function of the SNR of the user of interest for multipath fading channels.	32
2.6	Bit-error-rate of joint single-user detection algorithms for frequency selec- tive fading channels as a function of the number of the samples for channel estimation and the sample average estimate.	33
3.1	Combined space-frequency block coding and MC-CDMA transmitter for downlink transmissions.	38
3.2	Combined space-time block coding and MC-CDMA transmitter.	40
3.3	Receiver structure of the disjoint space-frequency block decoding and single- user detection.	43
3.4	Receiver structure of the joint space-frequency block decoding and single- user detection.	45
3.5	Bit-error-rate of both chip-level and symbol-level detection algorithms as a function of the SNR of the user of interest.	48
3.6	Bit-error-rate of both chip-level and symbol-level detection algorithms as a function of the number of the samples used for estimating the autocorrelation matrix.	49
3.7	The MSE as a function of the SNR.	64

3.8	The MSE as a function of the number of samples used for estimating the autocorrelation matrix.	65
3.9	The MSE as a function of the SNR of the desired user.	66
3.10	The MSE as a function of the number of users in the system.	67
3.11	The MSE as a function of the Near-Far Ratio.	68
3.12	The MSE as a function of the number of users in the system.	75
3.13	The MSE as a function of the SNR.	76
3.14	The MSE as a function of the data record size.	77
3.15	The MSE as a function of the Near-Far Ratio.	78
4.1	The MVDR method MSE performance as a function of the SNR.	104
4.2	The subspace method MSE performance as a function of the SNR.	105
4.3	The MVDR method MSE performance as a function of the SNR of the desired user.	106
4.4	The subspace method MSE performance as a function of the SNR of the desired user.	107
4.5	The MSE performance of both MVDR and subspace methods as a function of the number of samples used for estimating the covariance matrix.	108
4.6	The MSE performance of both MVDR and subspace methods as a function of the number of users in the system.	109
4.7	The MSE performance of both MVDR and subspace methods as a function of the Near-Far Ratio.	110
4.8	The BER of the MVDR detector as a function of SNR.	111

List of Acronyms

BCRB	Biased Cramer-Rao Bound
BER	Bit Error Ratio
CP	Cyclic Prefix
CRB	Cramer-Rao Bound
CSI	Channel State Information
DS-CDMA	Direct Sequence Code Division Multiple Access
EVD	Eigen-Value Decomposition
FFT	Fast Fourier Transform
FIM	Fisher Information Matrix
IBI	Inter-Block Interference
IFFT	Inverse Fast Fourier Transform
ISI	Inter-Symbol Interference
OFDM	Orthogonal Frequency Division Multiplexing
MC-CDMA	Multi-Carrier Code Division Multiple Access
MIMO	Multiple Input Multiple Output
MISO	Multiple Input Single Output
MRC	Maximum Ratio Combining
MSE	Mean Squared Error
MUI	Multi-User Interference
MVDR	Minimum Variance Distortionless Response
SC-FDE	Single-Carrier Frequency-Domain Equalized
SFBC	Space Frequency Block Code
SISO	Single Input Single Output
SMI	Sample Matrix Inversion
SNR	Signal-to-Noise Ratio

SOS	Second Order Statistics
STBC	Space Time Block Code
SVD	Singular-Value Decomposition
TR	Time-Reversal
WCDMA	Wideband Code Division Multiple Access
WiMAX	Worldwide Interoperability for Microwave Access
ZP	Zero Padding

Chapter 1

Introduction

1.1 Background and Literature Review

The next generation of broadband wireless communication systems is expected to provide high bit rates and to increase system capacity in order to cope with the increasing demand for wireless broadband services and applications such as high speed Internet access, cellular base stations, streaming video, mobile computing, wireless IPTV, distance learning and digital cinema, among many others. However, there are probably many critical performance limiting obstacles that must be overcome before this goal can be attained. The co-channel interference and mobile-radio channel impairments, such as multipath fading and Doppler spread, are among the factors with destructive impact on the performance of any wireless communication system. In general, high rate transmission in the wireless channels can be achieved by applying one or a combination of the following techniques [1]:

- Increase transmission power: Power is a key issue for mobile wireless applications. In fact, increasing transmission power in mobile clients significantly reduces battery life, increases the co-channel interference, and more importantly, increases the non-desirable effects of the nonlinearity of power amplifiers. Regarding the latter, the high power amplifiers must be driven as close to their saturation point as possible but still within their linear region in order to make their operation power efficient. Among the conventional approaches to address this problem are to back-off the operating point of the nonlinear amplifier or to use a linear amplifier. However, both schemes achieve linear operation at the expense of power efficiency.
- Increase transmission bandwidth: Due to the significant costs and limitations associ-

ated with bandwidth expansion, this technique is probably the most inefficient way to increase the transmission rate. Indeed, bandwidth is an expensive commodity and wireless service providers generally have to pay in order to be authorized to exploit a segment of the radio spectrum. This is in addition to the regulatory issues which further limits the availability of communications bandwidth. Besides, increasing the bandwidth of the signal relative to the coherence bandwidth of the wireless channel could increase the intersymbol interference (ISI).

- Use of spectrally efficient modulation schemes: The primary objective of this technique is to maximize the bandwidth efficiency (i.e., to increase data throughput for a given channel bandwidth) by designing algorithms which can be readily extended to large constellations or to signals of high dimension. However, this approach leads to increased susceptibility to the channel noise and interference, and consequently, to performance degradation.
- Use of multiple transmit and/or receive antennas: Exploiting the spatial dimension, Multiple-Input Multiple-Output (MIMO) wireless systems can significantly increase (depending on the application) the data rate by spatially multiplexing independent data streams, provide spatial diversity and array gains for improved link reliability, and combat co-channel interference in multiple-access environments.

Should the complexity and the cost issues of MIMO implementation be overcome, among all the above-mentioned techniques, the MIMO systems seem to be among the most promising methods in supporting reliable, high-data-rate transmissions [2]. The high implementation cost of MIMO systems are due to the requirement for multiple RF chains, extra hardware and sophisticated receiver algorithms associated with multiple antennas. Spatial diversity techniques constitute a particular implementation of multiple-antenna communications systems. These techniques can mitigate channel fading without necessarily sacrificing bandwidth resources and significantly increase the capacity over Single-Input Single-Output (SISO) systems. Depending on whether the multiple antennas are deployed at the transmitter or at the receiver, two types of spatial diversity can be configured: transmit-antenna diversity and receive-antenna diversity. Conventional maximum ratio combining (MRC) is probably the most widely applied receive antenna diversity technique. In this method, the multiple receive antennas collect and coherently combine separate replicas of the transmitted signals to mitigate channel fading by maximizing the received signal-to-noise ratio.

However, due to the size/complexity limitations at the mobile units, transmit-antenna diversity appears to be more favorable than receive-antenna diversity for the downlink (from base-station to mobile) transmissions. In addition, transmit-antenna diversity schemes have the advantage of transferring complexity from the receiver to the transmitter. Among all the transmit diversity schemes, orthogonal Space-Time Block Coding (STBC) [3], [4] is of particular interest because of its attractive features¹. More specifically:

- It does not require channel state information (CSI) at the transmitter. This feature eliminates the need for a potentially unreliable feedback link in fast time-varying environments.
- It achieves maximum diversity gain at full transmission rate for any (real or complex) signal constellation when employing only two antennas at the transmitter and one antenna at the receiver².
- Due to its orthogonal code structure, decoding and detection require only low-complexity linear processing at the receiver.

Transmit diversity in the form of STBC proposed by Alamouti [3] has already found its way into a number of wireless standards including 3G/WCDMA, WiMax/IEEE 802.16e and WiFi/IEEE 802.11n.; thus, one would expect it to be an integral part of future broadband communications systems.

Although offering attractive features, there are two major obstacles associated with practical STBC implementations. First, since STBC was initially designed for flat fading scenarios, its successful implementation over frequency-selective channels requires a carefully designed mechanism to overcome Inter-Symbol Interference (ISI) effects. Indeed, as shown in [6], an error floor occurs when ST encoded signals are transmitted over frequency-selective fading channels unless one incorporates a carefully designed equalizer at the receiving side. Previous research efforts that have successfully addressed this problem can be categorized into three major approaches:

- Time-Reversal (TR) STBC [7]: This method applies STBC at the block level instead of the symbol level and can effectively deal with ISI through zero padding (ZP) of the transmitted blocks. The technique involves time reversal of symbols at both

¹For a detailed survey of space-time coding please see [5].

²We note that in [4], full-diversity orthogonal STBC schemes are designed for more than two transmit antennas. However, the resulting rates are less than one.

transmitter and receiver which implies that the input-output relationship involves a time-reversal of the channel taps. However, it requires complex receiver equalization.

- Single-Carrier Frequency-Domain-Equalized (SC FDE) STBC [8], [9]: This scheme combines the advantages of the Alamouti scheme with the low complexity property of frequency domain equalizers to effectively combat ISI.
- Orthogonal Frequency Division Multiplexing (OFDM) STBC [10]: In this scheme, OFDM is employed to convert the frequency selective channels into a set of parallel independent flat fading sub-channels; STBC is then applied to each sub-channel. This method is particularly attractive due to its decoding simplicity.

The second major problem related to the use of STBC in practice, can be attributed to the single-user communication assumption [11], [12]. In fact, ST coding transmitter diversity impairs the system's interference suppression ability in a multiuser situation because it generates multiple signals that appear independent at the receiver. To cope with multiuser interference (MUI), the use of a robust multiple access scheme along with an interference rejection method is among the best solutions. Addressing the above mentioned issues is key to bringing the STBC techniques into the practical arena of wireless communications.

Since its initial proposal, considerable research efforts have aimed at bringing the space-time coding advantages to multiple access systems by integrating transmit diversity techniques into multiple access schemes [12], [13]. Among the many multiple access techniques proposed, direct-sequence code-division-multiple-access (DS/CDMA) has emerged as the predominant multiple access technique for third-generation (3G) cellular systems. These systems principally rely on the orthogonality of the spreading codes pre-assigned to each active user at the transmitter to separate the different user signals at the receiver. By far, the most common approach in DS/CDMA systems employing STBC is to perform ST block coding either at the symbol level or at the block level while DS/CDMA is used for the transmission of the resulting ST encoded signals [12], [14]. However, this approach has several drawbacks. First, the corresponding receivers have a decoding delay of at least M information symbol intervals (where M is the number of transmit antennas). Second, linear joint ST decoding and multiuser detection algorithms (as the one in [15]) require the use of very long filters (of length at least equal to $M \times L$ where L is the system processing gain). More importantly, however, performing ST block coding at the symbol level or at the block level requires the assignment of M CDMA signatures to each user if blind

channel estimation without ambiguity is to be performed [16], [15]. It is worthwhile noting that antenna order ambiguity (also known as permutation ambiguity) arises in any multi-channel blind estimation problem and reflects the fact that a system employing multiple antennas cannot distinguish between the subchannels (i.e., the communications channels between the multiple transmit and receive antennas). In DS/CDMA systems with transmit diversity, this ambiguity can be resolved either by assigning different spreading codes (one for each transmit antenna) to each user or by transmitting a training sequence, though both approaches come with the penalty of requiring extra resources. Indeed, in the former case, the assignment of more than one signature to each user severely limits the maximum number of users that can be accommodated in the system, whereas the latter case results in an inefficient use of bandwidth. Finally, they cannot be used with fast fading channels where the channel may vary during one symbol period. Indeed, because of the quasi-static channel assumption of the employed ST block codes, symbol-level schemes require that the channel remains constant over many information symbol periods. This requirement becomes an even greater limitation for block-level schemes as the number of symbols per block increases.

Despite its wide deployment in the 3G cellular wireless communications systems, DS-CDMA is not the technology of choice for future broadband transmissions. The time-dispersive nature of the multipath channel destroys the orthogonality among the users' signatures for high chip rates, giving rise to Multi-User Interference (MUI), which dramatically deteriorates the performance. This type of interference is even more severe in the presence of transmit diversity, as multiple independent signals are transmitted. Due to the above mentioned limitation of DS/CDMA systems, Multi-Carrier Code Division Multiple Access (MC-CDMA) is emerging as one of the most promising candidates for the downlink of future broadband wireless communications systems as it exploits the advantages of both OFDM multicarrier modulation and Direct-Sequence Spread Spectrum (DSSS) techniques. As opposed to DS/CDMA systems that do not make full use of the received signal energy scattered in the time domain due to the multi-path effect, the MC-CDMA systems have the advantage of collecting all the received signal energy scattered in the frequency domain. This can be attributed to the fact that an MC-CDMA system employs the frequency domain spreading and despreading of the data symbols to exploit the frequency-selectivity of the channel. Moreover, thanks to its multicarrier origin, MC-CDMA can substantially combat the adverse effects of multipath fading channels, while maintaining high transmission rates.

To enable an additional dimension, namely, frequency domain, in MC-CDMA systems block coding can be performed across the spatial and the frequency dimension instead of the temporal dimension. This approach is called Space-Frequency Block Coding (SFBC) and its application to OFDM systems has been well studied in the past [17]- [18]. Compared to STBC OFDM systems which show performance degradation in the mobile wireless channel environment SFBC-OFDM systems have the clear advantage of being robust in such an environment. There are, however, a number of drawbacks associated with the traditional SFBC OFDM approach³. First, this scheme fails to exploit the frequency diversity available in a time-dispersive MIMO channel [19]. Therefore, we cannot achieve the maximum theoretically achievable diversity order in the MIMO multipath channels which is quantified by the product of the number of transmit antennas, the number of receive antennas, and the number of delay paths. One approach to achieve higher diversity order in such systems is the design of a completely new SF code [19]. Among the schemes which have recently been proposed to achieve multipath diversity in an OFDM-based framework are the works in [18] and [20]. In [20], a class of SF codes for an OFDM system was provided which achieves full spatial and frequency diversity at the expense of the bandwidth efficiency. Later, in [18], a simple mapping scheme was proposed for transforming any full-diversity ST code into a full-diversity SF code but still the resulting SF codes cannot achieve full rate. From a system performance point of view, both aforementioned methods involve some kind of tradeoff between the diversity order and the coding rate or the symbol rate. The second shortcoming of the SFBC OFDM systems is their susceptibility to the channel nulls caused by deep fades in wireless channels. In fact, symbol recovery (in the case of detection) and channel identifiability (in the case of blind channel estimation) are not guaranteed when the channel has nulls on (or close to) some subcarriers [10], [21]. To increase robustness against channel nulls, the authors of [21] and [22] suggested transceiver designs based on the redundant transmitter precoding at the expense of loss in bandwidth efficiency. Finally, SFBC OFDM suffers from channel order ambiguity.

Motivated by the aforementioned problems that are inherent to the symbol/block level ST coding approach, in the first part of this thesis, we consider a chip-level ST block coding scheme for downlink transmissions in DS/CDMA systems. For this method, we apply STBC at the chip level (after code spreading) rather than the symbol-level. We show that the application of this scheme can alleviate most of the aforementioned shortcomings of

³We note that traditional approach refers to the extension of the Alamouti STBC [3] to a space-frequency block coding architecture.

symbol/block level ST coding schemes. Then, as an alternative to SFBC OFDM methods, we focus on a SFBC MC-CDMA scheme in the second part of this thesis. This technique which can be regarded as the extension of our chip-level approach to the frequency-selective channels enjoys all the advantages that had previously been reserved for chip-level scheme. Moreover, in the case of the MC-CDMA this scheme enables us to extract frequency diversity without any additional redundancy or bandwidth expansion by spreading the original data stream over different subcarriers in the frequency domain using a spreading code. We show that, due to the inherent structure imposed by spreading codes and SFBC, the SFBC MC-CDMA schemes assure symbol recovery and blind channel estimation regardless of channel zeros locations and without utilizing extra resources such as spreading codes or bandwidth.

We note that even compared with their STBC MC-CDMA counterparts [13], [23], there are several unique features associated with the SFBC MC-CDMA approach. For instance, SFBC MC-CDMA is inherently resistant against permutation ambiguity even when a single spreading code is assigned to each user, while STBC MC-CDMA requires that, for each user, a distinct signature being used corresponding to each transmitting antenna. Moreover, STBC MC-CDMA is only applicable under the assumption that the channel remains quasi-static over several consecutive OFDM symbol durations. Consequently, the latter suffers from the severe time selectivity of the wireless mobile fading channel. On the other hand, the SFBC MC-CDMA approach requires that the neighboring subcarriers experience highly correlated channels. Nevertheless, the undesirable effects of frequency-selectivity of the channel can be effectively overcome in SFBC MC-CDMA by increasing the frequency resolution (i.e., increasing the FFT size) whereas the spatial diversity gain in STBC MC-CDMA is severely reduced for rapidly fading channels and there is no straightforward solution for this shortcoming of STBC MC-CDMA.

1.2 Thesis Contribution

The main objective of our research is to investigate efficient schemes which exploit transmit diversity in wireless communication systems. In particular, we introduce two transmit diversity-assisted receiver structures for DS/CDMA and MC-CDMA systems, respectively, which we believe have the potential to outperform most of the widely used receivers with transmit diversity in terms of performance or computational complexity. For these schemes, we try to address the problem of detection and channel estimation along with the cor-

responding analytical performance analysis. The main results and contributions can be summarized as follows:

- We introduce a combined STBC CDMA scheme in which ST block coding is performed at the chip level, i.e., after code spreading. The receiver structures based on the proposed chip-level STBC CDMA scheme provide the following advantages over their symbol-level counterparts for a two-antenna receiver in the downlink transmission:
 - They exhibit a decoding delay of only one information symbol period which is about half that of symbol-level implementations.
 - By performing the decoding operation within one symbol, they only require about half of the decoder memory needed for the symbol-level schemes. This property results in lower complexity at the receiver.
 - Since the decision variables are completely determined within one symbol period, the channel variations between successive symbol periods do not degrade the performance. This is in contrast to the symbol-level schemes whose performance heavily relies on the channel to remain constant over several symbol periods.

For the proposed chip-level STBC CDMA scheme, we develop and analyze so called disjoint and joint ST block decoding and information bit detection algorithms that utilize linear interference suppression structures based on matched, decorrelating-type and Minimum-Variance-Distortionless-Response (MVDR)-type filtering criteria and we show that:

- For the case of joint receiver, a linear filter of length almost equal to the processing gain is needed which is about half the length of that required by symbol-level schemes. This leads to a lower computational complexity.
- The joint detector based on the decorrelating filtering criterion exhibits similar performance to that of the symbol-level approach for the case of flat fading channels. This suggests that the advantages of the proposed approach do not come at the expense of performance degradation.
- The linear detectors based on MVDR filtering criterion provide superior performance for the same data record size over their symbol-level counterparts. This is principally due to the fact that the autocorrelation matrix used by the MVDR

algorithm in symbol-level schemes is twice the size of that needed for chip-level techniques.

- The joint and disjoint receivers based on decorrelating-type filtering criteria exhibit identical performance for the case of flat fading channels.

Furthermore, exploiting the signal structure imposed by the chip-level ST block coding, we establish that blind channel multipath estimation (with only a scalar ambiguity) is feasible, even with the assignment of a single code vector to each user. This leads to significant user capacity improvements in systems with limited available signatures.

- To extend the application of our chip-level approach to ISI channels, transmit diversity in the form of SFBC for the downlink of MC-CDMA systems is considered. When compared with STBC MC-CDMA systems, the proposed SFBC MC-CDMA approach possesses all the advantages of chip-level STBC CDMA systems. Furthermore, when compared to SFBC OFDM, the proposed scheme has several advantages including:
 - The SFBC MC-CDMA systems are capable of enhancing receiver performance by providing multipath diversity gain in frequency selective channels, unlike SFBC OFDM systems that fail to exploit frequency diversity.
 - Symbol recovery and blind channel estimation are always feasible in SFBC MC-CDMA systems, even in the situations where the channel nulls are located on the subcarriers. This is not the case for SFBC OFDM systems which are extremely susceptible to channel nulls.
 - In SFBC MC-CDMA systems, blind channel estimation can be performed without permutation ambiguity while SFBC OFDM schemes rely on pilot signals or differential modulation for resolving such an ambiguity.

For the proposed SFBC MC-CDMA scheme, we consider two scenarios, namely, a pre-FFT approach and a post-FFT approach. The former refers to manipulation of the received signal in the time domain whereas the latter takes the frequency-domain received signal for processing. For each scenario, we develop:

- A linear formulation for the complex modulated received signals which reduces

the multichannel estimation problem to a single-input single-output (SISO) problem.

- Linear single-user decoding and detection algorithms that exhibit low complexity, low decoding delay and enhanced performance for frequency-selective fading channels compared to that of the STBC MC-CDMA schemes.
- Two alternative second-order statistics-based blind channel estimation techniques including: (i) a MVDR-type channel estimator, and (ii) a subspace-based channel estimator.
- Identifiability conditions for each estimator along with the necessary and sufficient conditions under which the channel estimates are unique (within a complex scalar ambiguity).
- Analytical closed-form expressions for the bias and mean-square-error (MSE) of each estimator.
- Novel formulations of the Cramer-Rao bounds (CRBs) for both unbiased and biased estimators in the downlink transmissions which provide tighter bounds on their corresponding channel MSEs than the conventional CRBs.
- A novel closed form bias expression caused by the additive noise for MVDR channel estimator that unlike the traditional approaches [24] does not rely on the existence of the noise subspace and accurately approximates the actual bias regardless of the system setup (e.g. in the case of heavy system loading or small processing gain).

We also establish that

- The presented blind channel estimators do not suffer from antenna order ambiguity (also known as permutation ambiguity).
- Channel identifiability is always guaranteed, regardless of the channel zeros location (within a complex scalar ambiguity).
- As opposed to its pre-FFT channel estimator counterpart, the post-FFT approach has the advantage of fully exploiting the inherent structure imposed by SFBC to further improve the performance and lower the computational complexity required for practical systems.

- Unlike the subspace approach, the MVDR-type estimator is applicable to medium or highly loaded systems.

1.3 Thesis Organization

The rest of this thesis is organized as follows. In Chapter 2, a combined STBC CDMA scheme in which ST block coding is performed at the chip level is introduced. For this scheme, we develop and analyze so called disjoint and joint ST block decoding and information symbol detection algorithms as well as blind channel estimation algorithms. In Chapter 3, the design principles of the proposed chip-level ST block coded CDMA systems is first extended to MC-CDMA systems to obtain a novel chip-level Space-Frequency Block Coded (SFBC) MC-CDMA scheme for downlink transmissions. Then, we investigate the problem of blind channel estimation and single-user symbol detection for SFBC MC-CDMA systems. Chapter 4 is focused on more efficient techniques for blind channel estimation and symbol detection for SFBC MC-CDMA systems by fully exploiting the inherent structure imposed by SFBC to improve the performance and lower the computational complexity required for practical systems. Also in Chapters 4 and 5, a comprehensive performance analysis of the presented blind channel estimation algorithms is provided. Finally, Chapter 5 includes a concluding discussion and topics for future work.

1.4 Published Work

The contents of this thesis have been partly published in journals and presented at a number of international conferences. These publications are listed below.

Journal Articles

- J1) S. Nayeb Nazar and I. N. Psaromiligkos, "Minimum variance channel estimation in MC-CDMA systems: bias analysis and Cramer-Rao bound," *IEEE Transactions on Signal Processing*, vol. 55, no. 6, pp. 3143-3148, Jun. 2007.
- J2) S. Nayeb Nazar and I. N. Psaromiligkos, "Performance of blind channel estimation algorithms for space-frequency block coded MC-CDMA systems," to appear in *IEE Proceeding Communications*.

Peer-Reviewed Conference Papers

- C1) S. Nayeb Nazar and I. N. Psaromiligkos, "Efficient second-order statistics-based channel estimation algorithms for MC-CDMA systems using transmit diversity," in *Proc. IEEE GLOBECOM Conference 2006*, San Francisco, CA, USA, Nov. 2006.
- C2) S. Nayeb Nazar, and I. N. Psaromiligkos, "Efficient minimum-variance receivers for MC-CDMA systems using transmit diversity," in *Proc. 40th IEEE Asilomar Conference on Signals, Systems, and Computers*, Pacific Grove, CA, Oct. 2006.
- C3) S. Nayeb Nazar and I. N. Psaromiligkos, "Further results on the performance of minimum variance channel estimation algorithms for MC-CDMA systems," in *Proc. IEEE VTC Fall 2006 - Vehicular Technology Conference*, Montreal, QC, Sept. 2006.
- C4) S. Nayeb Nazar, and I.N. Psaromiligkos, "Performance analysis of the MVDR channel estimator for space-frequency block coded MC-CDMA systems," in *Proc. IEEE WCNC 2006 - Wireless Commun. and Networking Conference*, Las Vegas, NV, USA, Apr. 2006, pp. 2029-2034.
- C6) S. Nayeb Nazar, and I. N. Psaromiligkos, "On subspace-based blind channel estimation algorithms for SFBC MC-CDMA systems," in *Proc. 39th IEEE Asilomar Conference on Signals, Systems, and Computers*, Pacific Grove, CA, Oct. 2005, pp. 1089-1093.
- C7) S. Nayeb Nazar and I. N. Psaromiligkos, "Detection and channel estimation algorithms for chip-level space-frequency block coded MC-CDMA systems," in *Proc. IEEE WiMob 2005 - International Conference on Wireless and Mobile Computing, Networking and Communications*, Montreal, QC, Canada, Aug. 2005, pp. 145-152.
- C9) S. Nayeb Nazar and I. N. Psaromiligkos, "Single-user detection algorithms for space-time block coded DS/CDMA transmissions over multipath fading channels," in *Proc. IEEE VTC Fall 2003 - Vehicular Technology Conference*, Orlando, FL, Oct. 2003, pp. 1084-1088.
- C10) S. Nayeb Nazar, and I. N. Psaromiligkos, "Blind channel estimation and single-user detection algorithms for ST block coded DS/CDMA systems," in *Proc. CISS 2003 - Conference on Information Sciences and Systems*, Johns Hopkins University, Baltimore, MD, March 2003.

Chapter 2

Chip-Level Space-Time Block Coded DS/CDMA systems

2.1 Introduction

In recent years, space-time block coding (STBC) [3], [4], has emerged as a practical way to mitigate channel fading and increase the capacity in wireless communications without necessarily sacrificing bandwidth resources. When deployed with CDMA systems, STBC techniques will allow us to realize increased data rates and improved coverage to satisfy the ever growing demands of multimedia services and applications [12], [13]. The common characteristic of all schemes presented by far in the literature is that ST block coding is performed either at the symbol level or at the block level while DS/CDMA is used for the transmission of the resulting ST encoded signals [12], [14]. One major assumption in STBC schemes is that the channel remains static over the length of the entire codeword. However, the so-called “quasi-static channel” assumption may potentially limit the practical use of symbol-level space-time codes in fast fading environments. On the other hand, the frequency selectivity of the channel severely limits the performance of STBCs in high data rate wireless communications where delay spread of the channel generally exceeds the symbol duration [25]. Other shortcomings of the symbol-level approach are that the corresponding receivers have a long decoding delay and that the linear joint ST decoding and multiuser detection require the use of very long filters. Alternatively, we may attempt to apply space-time coding at the chip-level, thus alleviating many of the limitations associated with the symbol-level approach as we will demonstrate in this thesis.

In this chapter, we develop and analyze single-user detection and blind channel estimation algorithms for a chip-level scheme that employs the popular and well-studied orthogonal STBCs. More specifically, we develop so called disjoint and joint ST block decoding and information bit detection algorithms for flat fading and frequency-selective channels, respectively. The proposed algorithms utilize linear interference suppression structures based on matched, decorrelating-type and Minimum-Variance-Distortionless-Response (MVDR)-type filtering criteria. All the proposed filters have a length almost equal to the processing gain (as suggested in [26], short-data-record situations favor the use of short filters) and have a decoding delay of only one information symbol period. We also present an analytical performance comparison between the symbol-level STBC decorrelator of [15] and the proposed chip-level STBC decorrelator. We show that there is no performance loss due to the chip-level ST block coding. In addition, we show analytically that the proposed joint and disjoint decorrelating-type detectors exhibit identical performance. These results suggest that the advantages of the proposed receivers do not come at the expense of detection performance.

Furthermore, in the multipath fading channel case, a subspace-based channel estimation algorithm is proposed. We address the issue of channel identifiability and we derive necessary and sufficient conditions under which the channel estimate is unique. It is also shown that unlike their symbol-level counterparts which require more than one signature to be assigned to each user for blind channel estimation without antenna order ambiguity, for the chip-level schemes the channel can be uniquely identified even in the case when there is only one signature assigned to each user.

It is acknowledged that, in independent works parallel to this work¹, the authors in [27] and [28] have also studied the application of chip-level ST block coding to the downlink of wideband CDMA system. In [27], considerable diversity gain and performance improvements in time-varying flat fading channel due to the use of chip-level ST block coding were reported. In [28], the combination of channel chip equalization and STBCs (at both chip-level and symbol-level) was considered. However, in contrast to the present work, both [27] and [28] consider only matched-filter-type multiuser detectors and assume perfect knowledge of the channel state information.

The rest of this chapter is organized as follows. In Section 2.2, we introduce the com-

¹Much of Chapter 2 was presented at the Conference on Information Sciences and Systems (CISS 2003), Johns Hopkins University, Baltimore, MD, March 2003, and at the 58th IEEE Vehicular Technology Conference (VTC 2003-Fall), Orlando, Florida, September 2003.

bined chip-based STBC/CDMA scheme. Linear single-user joint and disjoint ST block decoding and detection algorithms are investigated in Section 2.3. A blind channel estimation algorithm is developed and analyzed in Section 2.4. Also in Section 2.4, a comparison between the proposed chip-level scheme and the traditional symbol-level scheme is presented. Finally, Section 2.5 contains simulation studies.

2.2 System Description

We consider the downlink of a wireless system with K synchronous² mobile users where the base station is equipped with two antennas and each mobile user with a single antenna³. Downlink transmissions take place using the combined chip-level STBC and DS/CDMA scheme depicted in Fig. 2.1 and described herein. The information bit $b_k \in \{\pm 1\}$ to be transmitted to the k th user, $k = 1, \dots, K$, is first spread using the pre-assigned code signature vector \mathbf{s}_k given by⁴

$$\mathbf{s}_k \triangleq [s_k[1], s_k[2], \dots, s_k[L]]^T, \quad (2.1)$$

where L is the system processing gain, and $s_k[i] \in \{\pm 1/\sqrt{L}\}$. The vectors $\{\mathbf{s}_k\}_{k=1, \dots, K}$ are assumed to be linearly independent. After spreading, the composite vector \mathbf{x} is formed as follows

$$\mathbf{x} \triangleq \sum_{k=1}^K b_k \mathbf{s}_k = [x[1], x[2], \dots, x[L]]^T, \quad (2.2)$$

and then is transmitted using the orthogonal STBC scheme of Alamouti [3]. More specifically, \mathbf{x} is divided into $L/2$ blocks $\mathbf{c}_l \triangleq [x[2l-1], x[2l]]^T$, $l = 1, \dots, L/2$, of length⁵ 2. Each block \mathbf{c}_l , $l = 1, \dots, L/2$, is transmitted over two chip intervals. During the first chip interval, the elements $x[2l-1]$ and $x[2l]$ are transmitted from transmit antenna 1 (Tx1) and transmit antenna 2 (Tx2), respectively. During the second chip interval, the elements

²Unlike uplink transmissions, the downlink transmissions are typically coordinated, which lead to synchronous DS/CDMA systems.

³Our preliminary studies show that extension to multiple receive antennas and more than two transmit antennas is feasible.

⁴In this thesis, $(\cdot)^T$, $(\cdot)^H$, $(\cdot)^*$, $(\cdot)^\dagger$, $\text{tr}(\cdot)$, and \otimes denote transpose, Hermitian, conjugate, pseudo-inverse, trace, and Kronecker product, respectively.

⁵We assume that L is an even number. Cases where L is an odd number can be treated in a straightforward manner (e.g., constructing an even number by appending a +1).

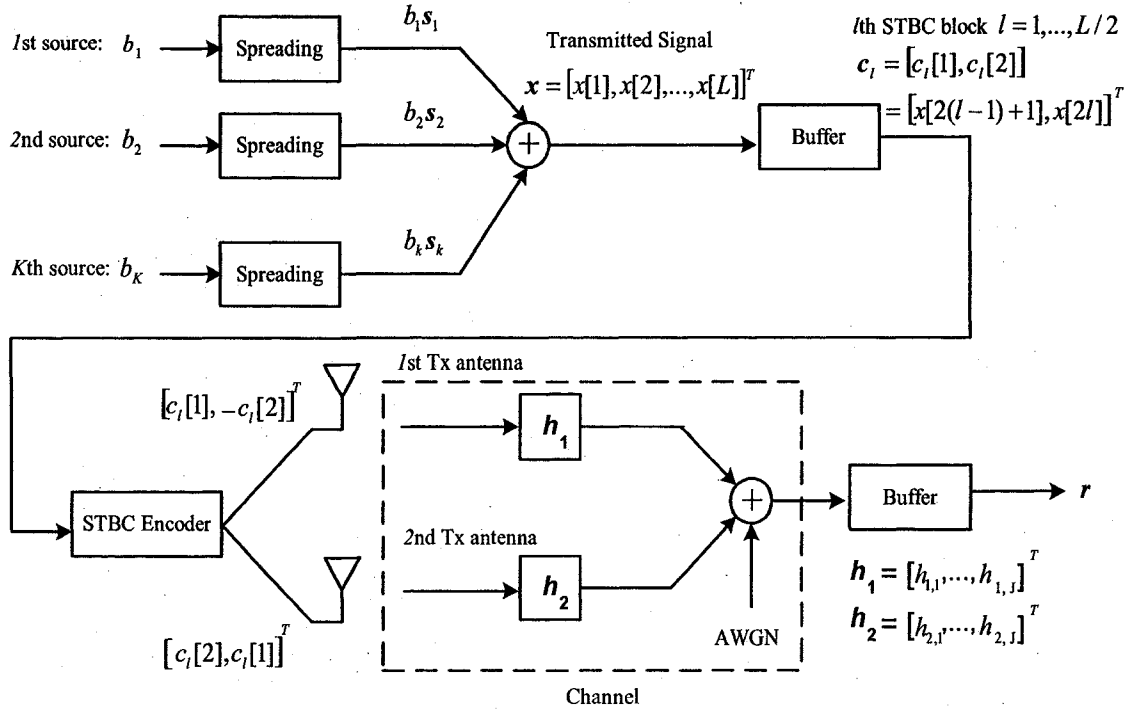


Fig. 2.1 Combined STBC and DS/CDMA transmission and reception.

$-x[2l]^*$ and $x[2l-1]^*$ are transmitted from Tx1 and Tx2, respectively.⁶

The communication channel consists of 2 parallel, independent, multipath Rayleigh fading sub-channels. The sub-channels between the p th antenna and the single receive antenna are modeled as finite impulse response (FIR) filters with J distinct paths with an impulse response given by

$$h_p(t) \triangleq \sum_{j=1}^J h_{p,j} \delta(t - jT_c), \quad p = 1, 2. \quad (2.3)$$

In (2.3), $h_{p,j}$, $p = 1, 2$, $j = 1, \dots, J$, is the complex path coefficient of the j th path of the p th subchannel, $\delta(\cdot)$ denotes the kronecker delta function, while T_c is the chip duration. The path coefficients, $h_{p,j}$, are assumed to be independent, complex Gaussian random variables with zero mean and variance σ_c^2 .

From the perspective of each individual mobile user, signals from all users pass through

⁶We note that the transmitted symbol as well as the user codes are assumed to be real in this chapter; therefore, we can ignore the complex conjugation operation during the second chip interval.

the same channel in the downlink. At the mobile, after chip-matched filtering and chip rate sampling, the discrete-time received signal that corresponds to a single transmitted symbol for each user and composed of the $L/2$ transmitted blocks is given in vector form by

$$\mathbf{r} = [r[1], r[2], \dots, r[L + J - 1]]^T = \sum_{k=1}^K b_k \mathbf{S}_k \mathbf{h} + \mathbf{n} = \sum_{k=1}^K b_k \mathbf{g}_k + \mathbf{n}, \quad (2.4)$$

where $\mathbf{h} \triangleq [h_{1,1}, \dots, h_{1,J}, h_{2,1}, \dots, h_{2,J}]^T$ is the composite channel vector, \mathbf{n} is additive white Gaussian noise (AWGN) with zero-mean and covariance matrix $\sigma^2 \mathbf{I}_{L+J-1}$. In addition, the $(L + J - 1) \times 2J$ matrices \mathbf{S}_k , $k = 1, \dots, K$ are defined by

$$\mathbf{S}_k \triangleq \begin{bmatrix} s_k[1] & 0 & \dots & 0 & s_k[2] & 0 & \dots & 0 \\ -s_k[2] & s_k[1] & & & s_k[1] & s_k[2] & & \\ \vdots & -s_k[2] & \ddots & \vdots & \vdots & s_k[1] & \ddots & \vdots \\ s_k[L-1] & \vdots & \ddots & s_k[1] & s_k[L] & \vdots & \ddots & s_k[2] \\ -s_k[L] & s_k[L-1] & \ddots & -s_k[2] & s_k[L-1] & s_k[L] & \ddots & s_k[1] \\ 0 & -s_k[L] & \ddots & \vdots & 0 & s_k[L-1] & \ddots & \vdots \\ \vdots & \vdots & & s_k[L-1] & \vdots & \vdots & & s_k[L] \\ 0 & 0 & \dots & -s_k[L] & 0 & 0 & \dots & s_k[L-1] \end{bmatrix}, \quad (2.5)$$

and

$$\mathbf{g}_k \triangleq \mathbf{S}_k \mathbf{h} = [g_k[1], g_k[2], \dots, g_k[L + J - 1]]^T. \quad (2.6)$$

Since the maximum delay spread of the channel is usually small compared to the symbol period, we assumed that the channel order is much less than the processing gain, i.e., $J \ll L$. Thus, we can safely assume that the inter-symbol interference (ISI) is very small compared to the multiple-access interference (MAI) [29]. For this reason and for simplicity in presentation, we will ignore ISI in the presentation of the theoretical developments and we will only consider the dominant MAI. However, in the simulation results presented in Section 2.5 we consider a realistic DS/CDMA system where ISI is explicitly taken into account.

2.3 Single-User Detection Algorithms

At the k th mobile, the receiver's ultimate task is to perform single-user detection, i.e., to detect the transmitted bit b_k given the received vector \mathbf{r} without any knowledge of the other users' signatures. In this section, we investigate two single-user detection approaches. The first one, called *disjoint* ST decoding and information bit detection, is to perform the exact inverse of the transmission scheme in Fig. 2.1. As a result, detection algorithms that follow this approach consist of two stages. The first stage performs the ST block decoding of the transmitted blocks while the second stage performs the despreading and information bit detection. With respect to the second stage, we focus on linear structures that consist of a linear filter followed by a sign detector. Due to the well-known limitations of the orthogonal ST block codes, we assume that the channels are flat, i.e., $\mathbf{h} = [h_1, h_2]^T$. The second approach, called *joint* ST decoding and information bit detection, merges the decoding and detection stages into a single one through the use of a linear filter. In contrast to disjoint algorithms, joint decoding and detection algorithms implicitly equalize the received signal and, therefore, can handle frequency selective channels.

Throughout this section the only quantities assumed known to the receiver are the spreading code associated with the user of interest and the channel vector \mathbf{h} . Algorithms for channel estimation will be considered in the next section.

2.3.1 Disjoint ST Decoding and Symbol Detection

Without loss of generality, we will assume that the user of interest is $k = 1$. The disjoint receiver structure is shown in Fig. 2.2(a). The received signal due to the l th transmitted block \mathbf{c}_l , $l = 1, \dots, L/2$, can be written in vector form as

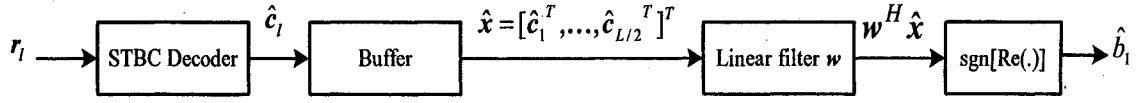
$$\mathbf{r}_l \triangleq \begin{bmatrix} r_l[1] \\ r_l[2] \end{bmatrix} = \begin{bmatrix} h_1 & h_2 \\ h_2 & -h_1 \end{bmatrix} \begin{bmatrix} c_l[1] \\ c_l[2] \end{bmatrix} + \begin{bmatrix} n_l[1] \\ n_l[2] \end{bmatrix}, \quad (2.7)$$

where $n_l[p]$, $p = 1, 2$ denotes additive white Gaussian noise (AWGN) with zero-mean and variance σ^2 .

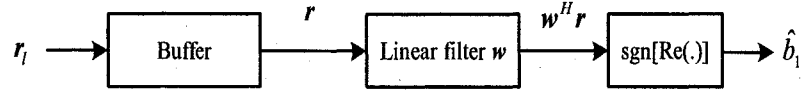
Then, the corresponding *soft* output of the STBC decoder is $\hat{\mathbf{c}}_l \triangleq [\hat{c}_l[1], \hat{c}_l[2]]^T$, where [3]

$$\hat{c}_l[1] = h_1^* r_l[1] + h_2 r_l^*[2] \quad (2.8)$$

$$\hat{c}_l[2] = h_2^* r_l[1] - h_1 r_l^*[2]. \quad (2.9)$$



(a)



(b)

Fig. 2.2 Receiver structure (a) Disjoint ST block decoding and single-user detection, (b) Joint ST block decoding and single-user detection.

By stacking $L/2$ decoder output blocks, we obtain the decoded vector $\hat{\mathbf{x}} \triangleq [\hat{c}_1^T, \dots, \hat{c}_{L/2}^T]^T$ which can be written as

$$\begin{aligned} \hat{\mathbf{x}} &= (|h_1|^2 + |h_2|^2)\mathbf{x} + \tilde{\mathbf{n}} \\ &= E \sum_{k=1}^K b_k \mathbf{s}_k + \tilde{\mathbf{n}}, \end{aligned} \quad (2.10)$$

where $E = (|h_1|^2 + |h_2|^2)$, and $\tilde{\mathbf{n}} \sim \mathcal{N}(0, E\sigma^2 \mathbf{I}_L)$. We observe that the decoded vector $\hat{\mathbf{x}}$ has the form of a DS/CDMA signal. Hence, the transmitted bit b_1 can be detected using a linear filter \mathbf{w} of length L as follows:

$$\hat{b}_1 = \text{sgn}[\text{Re}(\mathbf{w}^H \hat{\mathbf{x}})]. \quad (2.11)$$

For the linear filter \mathbf{w} we consider the following alternatives:

1. *Matched Filter*

The spreading code of the desired user \mathbf{s}_1 can be chosen as the weight vector of a filter matched to the signal of interest, i.e.,

$$\mathbf{w}_{mf} = \mathbf{s}_1. \quad (2.12)$$

2. *Minimum-Variance-Distortionless-Response (MVDR) Filter*

The MVDR filter $\mathbf{w}_{mvd r}$ minimizes the variance/energy $\mathbb{E}\{|\mathbf{w}_{mvd r}^H \mathbf{r}|^2\}$ at its output while being distortionless in the direction of the signal of interest \mathbf{s}_1 , i.e., $\mathbf{w}_{mvd r}^H \mathbf{s}_1 = 1$. It is given by [24]

$$\mathbf{w}_{mvd r} = \frac{\mathbf{R}_x^{-1} \mathbf{s}_1}{\mathbf{s}_1^T \mathbf{R}_x^{-1} \mathbf{s}_1}. \quad (2.13)$$

In (2.13), $\mathbf{R}_x \triangleq \mathbb{E}\{\hat{\mathbf{x}}\hat{\mathbf{x}}^H\}$ is the autocorrelation matrix of the input vector $\hat{\mathbf{x}}$. In practice, the autocorrelation matrix \mathbf{R}_x is not known and it is sample-average estimated from M received vectors $\hat{\mathbf{x}}(i)$, $i = 1, \dots, M$, as follows:

$$\hat{\mathbf{R}}_x \triangleq \frac{1}{M} \sum_{i=1}^M \hat{\mathbf{x}}(i)\hat{\mathbf{x}}(i)^H. \quad (2.14)$$

Substituting $\hat{\mathbf{R}}_x$ in place of \mathbf{R}_x in (2.13), we obtain sample-matrix-inversion (SMI) estimate of $\mathbf{w}_{mvd r}$, $\hat{\mathbf{w}}_{mvd r}$:

$$\hat{\mathbf{w}}_{mvd r} = \frac{\hat{\mathbf{R}}_x^{-1} \mathbf{s}_1}{\mathbf{s}_1^T \hat{\mathbf{R}}_x^{-1} \mathbf{s}_1}. \quad (2.15)$$

3. Decorrelating Filter

The decorrelating filter \mathbf{w}_{dec} aims at completely eliminating the MAI, and is given by

$$\mathbf{w}_{dec} = \mathbf{S} \mathbf{R}_s^{-1} \mathbf{e}_1. \quad (2.16)$$

where $\mathbf{S} = [\mathbf{s}_1, \mathbf{s}_2, \dots, \mathbf{s}_K]$ denotes the signature matrix and $\mathbf{e}_1 = [1, 0, \dots, 0]^T \in \mathcal{R}^K$. In (2.16), $\mathbf{R}_s = \mathbf{S}^T \mathbf{S}$ is the signature cross-correlation matrix which is assumed to be nonsingular. We note that alternative implementations of the decorrelating detector can be employed that do not require the prior knowledge of the interferers' signature waveforms [30], [31], [32]. Under the assumption of perfectly known input statistics the decorrelating structures in [30] and [31] perform identically to the filter in (2.16). The same holds true upon convergence for the algorithm in [32]. However, for simplicity in presentation, we chose to define the decorrelator using the expression in (2.16) even though the latter requires knowledge of the interfering users' signatures.

The following lemma identifies the performance of the decorrelating detector.

Lemma 1 *The probability of detection error of the decorrelator in (2.16) is given by*

$$P_e(\mathbf{w}_{dec}) = Q\left(\frac{\sqrt{2E}}{\sigma\sqrt{[\mathbf{R}_s^{-1}]_{1,1}}}\right) \quad (2.17)$$

where $[\mathbf{R}_s^{-1}]_{1,1}$ is the (1, 1)-element of \mathbf{R}_s^{-1} .

Proof: The output of the decorrelating filter is

$$z = \mathbf{w}_{dec}^H \hat{\mathbf{x}} = Eb_1 + v \quad (2.18)$$

where $v \triangleq \mathbf{w}_{dec}^H \tilde{\mathbf{n}} \sim \mathcal{N}(0, E\sigma^2 \|\mathbf{w}_{dec}\|^2)$.

Therefore, the probability of detection error for the proposed scheme can be computed as

$$\begin{aligned} P_e(\mathbf{w}_{dec}) &= P(\text{Re}\{z\} < 0 \mid b_1 = 1) \\ &= P(\text{Re}\{v\} < -E) = Q\left(\frac{\sqrt{2E}}{\sigma \|\mathbf{w}_{dec}\|}\right) \\ &= Q\left(\frac{\sqrt{2E}}{\sigma\sqrt{[\mathbf{R}_s^{-1}]_{1,1}}}\right) \end{aligned} \quad (2.19)$$

■

Comparing (2.19) with Eq. (32) in [15], we see that the decorrelator in (2.13) and the disjoint decorrelator of [15] have the same performance. Therefore, there is no performance loss incurred by chip-level ST block coding compared to symbol-level scheme.

2.3.2 Joint ST Decoding and Symbol Detection

The proposed joint scheme is illustrated in Fig. 2.2(b). To perform single-user detection in multipath fading channels, we first form the modified received vector $\tilde{\mathbf{r}}$ as follows

$$\begin{aligned} \tilde{\mathbf{r}} &\triangleq [r[1], r^*[2], \dots, r[L+J-2], r^*[L+J-1]]^T \\ &= b_1 \tilde{\mathbf{g}}_1 + \sum_{k=2}^K b_k \tilde{\mathbf{g}}_k + \tilde{\mathbf{n}}, \end{aligned} \quad (2.20)$$

where $\tilde{\mathbf{n}} \triangleq [n[1], n^*[2], \dots, n[L+J-2], n^*[L+J-1]]^T$ is a noise vector with the same statistics as the noise vector \mathbf{n} in (2.4). In (2.20), $\tilde{\mathbf{g}}_k$ is the effective signature of the k th user, $k = 1, \dots, K$, formed by conjugating the even numbered elements of the vector \mathbf{g}_k (given by (2.6)), i.e.,

$$\tilde{\mathbf{g}}_k \triangleq [g_k[1], g_k^*[2], \dots, g_k[L+J-2], g_k^*[L+J-1]]^T. \quad (2.21)$$

The first term in (2.20) represents the desired signal while the second term represents the multiple access interference (MAI).

In the proposed methods, the transmitted bit b_1 is recovered from the received signal $\tilde{\mathbf{r}}$ by means of a linear filter $\tilde{\mathbf{w}}$ of length $L+J-1$. The estimate of the transmitted bit b_1 of the user of interest can be found as

$$\hat{b}_1 = \text{sgn}[\text{Re}(\tilde{\mathbf{w}}^H \tilde{\mathbf{r}})]. \quad (2.22)$$

Similarly to the disjoint algorithms, we consider the following alternatives for the linear filter $\tilde{\mathbf{w}}$:

1. *Matched Filter*

$$\tilde{\mathbf{w}}_{mf} = \tilde{\mathbf{g}}_1. \quad (2.23)$$

2. *Minimum-Variance-Distortionless-Response (MVDR) Filter*

$$\tilde{\mathbf{w}}_{mvd} = \frac{\tilde{\mathbf{R}}^{-1} \tilde{\mathbf{g}}_1}{\tilde{\mathbf{g}}_1^H \tilde{\mathbf{R}}^{-1} \tilde{\mathbf{g}}_1}. \quad (2.24)$$

In (2.24), $\tilde{\mathbf{R}} \triangleq \mathbb{E}\{\tilde{\mathbf{r}}\tilde{\mathbf{r}}^H\}$ is the autocorrelation matrix of the input vector $\tilde{\mathbf{r}}$. As before, since the autocorrelation matrix $\tilde{\mathbf{R}}$ is not known in practice, it is sample-average estimated from M received vectors $\tilde{\mathbf{r}}(n)$, $n = 1, \dots, M$.

3. *Decorrelating Filter*

$$\tilde{\mathbf{w}}_{dec} = \tilde{\mathbf{G}}\mathbf{X}^{-1}\mathbf{e}_1. \quad (2.25)$$

In (2.25), $\tilde{\mathbf{G}} = [\tilde{\mathbf{g}}_1, \tilde{\mathbf{g}}_2, \dots, \tilde{\mathbf{g}}_K]$ denotes the effective signature matrix, $\mathbf{X} = \tilde{\mathbf{G}}^H \tilde{\mathbf{G}}$ the effective signature cross-correlation matrix, and $\mathbf{e}_1 = [1, 0, \dots, 0]^T \in \mathcal{R}^K$. Here, it is

assumed that the matrix \mathbf{X} is invertible, which requires that the matrix $\tilde{\mathbf{G}}$ be full column rank, i.e. $\text{Rank}(\tilde{\mathbf{G}}) = K$.

We next examine the performance of the disjoint decorrelating detector versus the joint one. Lemma 2 below shows the relationship between the joint and disjoint decorrelating detector weight vectors for flat fading channels. Note that the joint decoding and detection algorithm for flat fading channels is the special case of the algorithm presented in the previous subsection with $J = 1$.

Lemma 2 *For a 2-antenna system, the weight vector of the joint decorrelating detector $\tilde{\mathbf{w}}_{dec}$ is related to that of the disjoint detector \mathbf{w}_{dec} by*

$$\tilde{\mathbf{w}}_{dec} = \frac{1}{\|\tilde{\mathbf{h}}\|^2} (\mathbf{I}_{L/2} \otimes \mathbf{H}) \mathbf{w}_{dec}. \quad (2.26)$$

where $\mathbf{H} \triangleq [\tilde{\mathbf{h}}, \bar{\mathbf{h}}]$, $\tilde{\mathbf{h}} \triangleq [h_1, h_2^*]^T$, $\bar{\mathbf{h}} \triangleq [h_2, -h_1^*]^T$, and \otimes denotes the Kronecker product.

Proof: It is straightforward to verify that the matrix $\tilde{\mathbf{G}}$ in (2.25) can be written as

$$\tilde{\mathbf{G}} = (\mathbf{I}_{L/2} \otimes \mathbf{H}) \mathbf{S} \quad (2.27)$$

Now, we may rewrite (2.25) as

$$\begin{aligned} \tilde{\mathbf{w}}_{dec} &= \tilde{\mathbf{G}} (\tilde{\mathbf{G}}^H \tilde{\mathbf{G}})^{-1} \mathbf{e}_1 \\ &= [(\mathbf{I}_{L/2} \otimes \mathbf{H}) \mathbf{S}] \left([(\mathbf{I}_{L/2} \otimes \mathbf{H}) \mathbf{S}]^H [(\mathbf{I}_{L/2} \otimes \mathbf{H}) \mathbf{S}] \right)^{-1} \mathbf{e}_1 \\ &= [(\mathbf{I}_{L/2} \otimes \mathbf{H}) \mathbf{S}] (\mathbf{S}^H (\mathbf{I}_{L/2} \otimes \mathbf{H}^H) (\mathbf{I}_{L/2} \otimes \mathbf{H}) \mathbf{S})^{-1} \mathbf{e}_1 \\ &= \frac{1}{\|\tilde{\mathbf{h}}\|^2} [(\mathbf{I}_{L/2} \otimes \mathbf{H}) \mathbf{S}] (\mathbf{S}^H \mathbf{S})^{-1} \mathbf{e}_1 \\ &= \frac{1}{\|\tilde{\mathbf{h}}\|^2} (\mathbf{I}_{L/2} \otimes \mathbf{H}) [\mathbf{S} (\mathbf{S}^H \mathbf{S})^{-1} \mathbf{e}_1] \\ &= \frac{1}{\|\tilde{\mathbf{h}}\|^2} (\mathbf{I}_{L/2} \otimes \mathbf{H}) \mathbf{w}_{dec} \end{aligned} \quad (2.28)$$

which concludes the proof. ■

Using the above result, the following proposition compares the performance of joint and disjoint decorrelating detectors.

Proposition 1 *For a 2-antenna system, the probability of detection error for the joint decorrelator is equal to that of disjoint decorrelator.*

Proof: From Lemma 2 we have

$$\begin{aligned}
\| \tilde{\mathbf{w}}_{dec} \|^2 &= \tilde{\mathbf{w}}_{dec}^H \tilde{\mathbf{w}}_{dec} \\
&= \frac{1}{\| \tilde{\mathbf{h}} \|^4} \mathbf{w}_{dec}^H (\mathbf{I}_{L/2} \otimes \mathbf{H})^H (\mathbf{I}_{L/2} \otimes \mathbf{H}) \mathbf{w}_{dec} \\
&= \frac{1}{\| \tilde{\mathbf{h}} \|^4} \mathbf{w}_{dec}^H (\| \tilde{\mathbf{h}} \|^2 \mathbf{I}_L) \mathbf{w}_{dec} \\
&= \frac{1}{\| \tilde{\mathbf{h}} \|^2} \| \mathbf{w}_{dec} \|^2
\end{aligned} \tag{2.29}$$

or equivalently

$$\| \tilde{\mathbf{w}}_{dec} \| = \frac{\| \mathbf{w}_{dec} \|}{\sqrt{E}}. \tag{2.30}$$

The output of the decorrelating filter for the joint scheme is

$$\tilde{z} = \tilde{\mathbf{w}}_{dec}^H \tilde{\mathbf{r}} = b_1 + u, \tag{2.31}$$

where $u \triangleq \tilde{\mathbf{w}}_{dec}^H \tilde{\mathbf{r}} \sim \mathcal{N}(0, \sigma^2 \| \tilde{\mathbf{w}}_{dec} \|^2)$. Therefore, the probability of detection error can be evaluated as

$$\begin{aligned}
P_e(\tilde{\mathbf{w}}_{dec}) &= P(\text{Re}\{\tilde{z}\} < 0 \mid b_1 = 1) \\
&= P(\text{Re}\{u\} < -1) = Q\left(\frac{\sqrt{2}}{\sigma \| \tilde{\mathbf{w}}_{dec} \|}\right).
\end{aligned} \tag{2.32}$$

Comparing (2.32) with (2.19), it is seen that both detectors have identical performance. ■

The single-user detection algorithms presented in this section assume knowledge of the channel vector \mathbf{h} . In practice, the channel state information is not known and has to be estimated. In the next section, we consider exactly this problem.

2.4 Blind Channel Estimation

In this section, we develop subspace-type channel estimation algorithms that require knowledge of only the code vector \mathbf{s}_1 of the user of interest, the total number of users K , and the channel order J . As such, the proposed algorithms are blind, i.e., they do not require the transmission of a known training sequence. However, when it comes to the blind channel estimation, it would be insightful to first identify the main feature of the chip-level scheme

introduced in this thesis compared with its traditional symbol-level counterpart [15] which is discussed next.

2.4.1 Symbol-level vs. Chip-level STBC

To keep the notation simple and the discussion brief we will focus on single-user transmissions over flat fading channels. Specifically, we consider a system where the user of interest (user 1) transmits a block of two information symbols $b_1(1), b_1(2) \in \{\pm 1\}$ over a flat fading channel using the symbol-level scheme described in [15]. Denoting by $\mathbf{s}_1 \in \mathcal{R}^L$ the code vector assigned to user 1, the $2L$ -long discrete-time received signal over a time period spanning two information symbol periods can be written as [15]

$$\mathbf{r}' = b_1(1) \begin{pmatrix} h_1 \mathbf{s}_1 \\ h_2 \mathbf{s}_1 \end{pmatrix} + b_1(2) \begin{pmatrix} h_2 \mathbf{s}_1 \\ -h_1 \mathbf{s}_1 \end{pmatrix} + \mathbf{n} \quad (2.33)$$

where $\mathbf{n} \sim \mathcal{CN}(\mathbf{0}, \sigma^2 \mathbf{I}_{2L})$. In (2.33), h_p , $p = 1, 2$, is the single path coefficient of the p th subchannel, i.e., the channel vector is $\mathbf{h} = [h_1, h_2]^T$. Furthermore, in the case when $\mathbf{h} = [h_2, -h_1]^T$ the received vector is given by

$$\mathbf{r}'' = b_1(1) \begin{pmatrix} h_2 \mathbf{s}_1 \\ -h_1 \mathbf{s}_1 \end{pmatrix} + b_1(2) \begin{pmatrix} -h_1 \mathbf{s}_1 \\ -h_2 \mathbf{s}_1 \end{pmatrix} + \mathbf{n}. \quad (2.34)$$

Next, to shed some light on the statistical properties of the received vectors $\mathbf{r}' = [r'(1), r'(2)]^T$ and $\mathbf{r}'' = [r''(1), r''(2)]^T$, we examine the probability density function (pdf) of each received vector. More specifically, the conditional probability density function (pdf) of the received signals \mathbf{r}' and \mathbf{r}'' are given by

$$p(\mathbf{r}' | h_1, h_2, b_1(1), b_1(2)) = \frac{1}{(2\pi\sigma^2)^L} \exp\left(-\frac{\mu_1}{2\sigma^2}\right), \quad (2.35)$$

and

$$p(\mathbf{r}'' | h_1, h_2, b_1(1), b_1(2)) = \frac{1}{(2\pi\sigma^2)^L} \exp\left(-\frac{\mu_2}{2\sigma^2}\right), \quad (2.36)$$

respectively, where

$$\mu_1 = \left\| \begin{pmatrix} r'(1) \\ r'(2) \end{pmatrix} - \begin{pmatrix} \mathbf{s}_1 & 0 \\ 0 & \mathbf{s}_1 \end{pmatrix} \begin{pmatrix} h_1 & h_2 \\ h_2 & -h_1 \end{pmatrix} \begin{pmatrix} b_1(1) \\ b_1(2) \end{pmatrix} \right\|^2, \quad (2.37)$$

and

$$\mu_2 = \left\| \begin{pmatrix} r''(1) \\ r''(2) \end{pmatrix} - \begin{pmatrix} \mathbf{s}_1 & 0 \\ 0 & \mathbf{s}_1 \end{pmatrix} \begin{pmatrix} h_2 & -h_1 \\ -h_1 & -h_2 \end{pmatrix} \begin{pmatrix} b_1(1) \\ b_1(2) \end{pmatrix} \right\|^2. \quad (2.38)$$

It is now easy to verify that since $r''(1) = r'(2)$ and $r''(2) = -r'(1)$, we have: $\mu_1 = \mu_2$; therefore, the probability density functions (pdfs) of the received vectors \mathbf{r}' and \mathbf{r}'' in (2.33) and (2.34) are identical. Based on the above observation, we conclude that it would be impossible for a blind receiver to distinguish between the two cases, namely the channel \mathbf{h} being $[h_1, h_2]^T$ or $[h_2, -h_1]^T$, which implies that no blind channel estimation algorithm can provide a unique channel estimate. This inability to uniquely estimate the channel in a symbol-level STBC system is commonly referred to as the channel order or channel ambiguity problem.

We can arrive at a different (but equivalent) interpretation of this problem by rewriting (2.33) as

$$\begin{aligned} \mathbf{r}' &= h_1 \begin{pmatrix} b_1(1)\mathbf{s}_1 \\ -b_1(2)\mathbf{s}_1 \end{pmatrix} + h_2 \begin{pmatrix} b_1(2)\mathbf{s}_1 \\ b_1(1)\mathbf{s}_1 \end{pmatrix} + \mathbf{n} \\ &= h_1 \mathbf{x}'_1 + h_2 \mathbf{x}'_2 + \mathbf{n}, \end{aligned} \quad (2.39)$$

where \mathbf{x}'_1 and \mathbf{x}'_2 are the discrete time signals transmitted from antenna 1 and antenna 2, respectively. In the case when the transmitted block is $b_1(2), -b_1(1)$ the received vector is given by

$$\begin{aligned} \mathbf{r}'' &= h_1 \begin{pmatrix} b_1(2)\mathbf{s}_1 \\ b_1(1)\mathbf{s}_1 \end{pmatrix} + h_2 \begin{pmatrix} -b_1(1)\mathbf{s}_1 \\ b_1(2)\mathbf{s}_1 \end{pmatrix} + \mathbf{n} \\ &= h_1 \mathbf{x}''_1 + h_2 \mathbf{x}''_2 + \mathbf{n}. \end{aligned} \quad (2.40)$$

where, as before, \mathbf{x}''_1 and \mathbf{x}''_2 are the discrete time signals transmitted from antenna 1 and antenna 2, respectively. Clearly, $\mathbf{x}''_1 = \mathbf{x}'_2$ and $\mathbf{x}''_2 = -\mathbf{x}'_1$ which imply that the pdf of the signal transmitted from the 1st (2nd) antenna when the transmitted bits are $b_1(1), b_1(2)$ is the same to the pdf of the signal transmitted from the 2nd (1st) antenna when the

transmitted bits are $b_1(2), -b_1(1)$. In other words, a blind channel estimator that does not have knowledge of the transmitted bits can not differentiate the signals transmitted from the two antennas and will be unable to distinguish between the two cases of \mathbf{h} being $[h_1, h_2]^T$ or $[h_2, -h_1]^T$.

In the case when the chip-level scheme is employed, the L -long received vector \mathbf{r} due to the transmission of a single bit $b_1(1)$ is given by

$$\mathbf{r} = h_1 b_1(1) \bar{\mathbf{s}}_1 + h_2 b_1(1) \tilde{\mathbf{s}}_1 + \mathbf{n}, \quad (2.41)$$

where $\bar{\mathbf{s}}_1 \triangleq [s_1[1], -s_1[2], \dots, s_1[L-1], -s_1[L]]^T$ and $\tilde{\mathbf{s}}_1 \triangleq [s_1[2], s_1[1], \dots, s_1[L], s_1[L-1]]^T$. We observe that the antennas transmit signals with distinct pdfs which implies that it is possible to differentiate between the two transmit antennas and the corresponding subchannels and thus avoid the channel ambiguity problem. Motivated by this observation, we develop in the next subsection a blind subspace-based channel estimation method and identify necessary and sufficient conditions for the unique identification of the channel.

2.4.2 Subspace-based Channel Estimation Algorithms

Let us denote as \mathbf{G} the $(L+J-1) \times K$ matrix whose columns are the K vectors $\mathbf{g}_1, \dots, \mathbf{g}_K$, i.e.,

$$\mathbf{G} \triangleq [\mathbf{g}_1 \ \mathbf{g}_2 \ \dots \ \mathbf{g}_K]. \quad (2.42)$$

We recall that $\mathbf{g}_k = \mathbf{S}_k \mathbf{h}$, $k = 1, \dots, K$ where \mathbf{S}_k is given by (2.5). The autocorrelation matrix, \mathbf{R} , of the received vector \mathbf{r} in (2.4) can now be expressed as

$$\mathbf{R} = \mathbf{G}\mathbf{G}^H + \sigma^2 \mathbf{I}_{L+J-1}. \quad (2.43)$$

Let the eigenvalue decomposition (ED) of \mathbf{R} be $\mathbf{R} = \mathbf{Q}\mathbf{\Lambda}\mathbf{Q}^H$, where $\mathbf{\Lambda} \triangleq \text{diag}(\lambda_1, \lambda_2, \dots, \lambda_{L+J-1})$, $\lambda_1 \geq \dots \geq \lambda_K > \lambda_{K+1} = \dots = \lambda_{L+J-1} = \sigma^2$, are the eigenvalues of \mathbf{R} in descending order, and $\mathbf{Q} \triangleq [\mathbf{q}_1, \dots, \mathbf{q}_{L+J-1}]$ is the matrix of the corresponding eigenvectors. Finally, let

$$\mathbf{Q}_n \triangleq [\mathbf{q}_{L+J-K}, \dots, \mathbf{q}_{L+J-1}], \quad (2.44)$$

where $\mathbf{q}_{L+J-K}, \dots, \mathbf{q}_{L+J-1}$ are the eigenvectors that span the noise subspace.

The orthogonality between the noise subspace and the signal subspace implies that for the user of interest (user 1), \mathbf{g}_1 is orthogonal to all the vectors $\mathbf{q}_{L+J-K}, \dots, \mathbf{q}_{L+J-1}$ that

span the noise subspace. Thus, we have

$$\mathbf{Q}_n^H \mathbf{g}_1 = \mathbf{Q}_n^H \mathbf{S}_1 \mathbf{h} = \mathbf{0} \quad (2.45)$$

Equivalently, we can write

$$\mathbf{h}^H \boldsymbol{\Omega} \mathbf{h} = 0, \quad (2.46)$$

where

$$\boldsymbol{\Omega} = \mathbf{S}_1^T \mathbf{Q}_n \mathbf{Q}_n^H \mathbf{S}_1. \quad (2.47)$$

Therefore, the desired user can estimate the channel vector \mathbf{h} as the eigenvector that corresponds to the zero eigenvalue of the $2J \times 2J$ matrix $\boldsymbol{\Omega}$ in (2.47), provided that the rank of $\boldsymbol{\Omega}$ is $2J - 1$.

The following theorem presents sufficient and necessary conditions that guarantee unique identifiability (within a scalar ambiguity) of the channel vector \mathbf{h} .

Theorem 1 *The sufficient and necessary conditions for the channel vector \mathbf{h} in (2.46) to be identifiable with a scalar ambiguity are as follows*

- **(Sufficient)** *The matrix $[\mathbf{S}_1 \ \mathbf{g}_2 \ \mathbf{g}_3 \ \dots \ \mathbf{g}_K]$ has full column rank*
- **(Necessary)** $L \geq J + K$.

Proof: It suffices to show that there does not exist \mathbf{h}' linearly independent from \mathbf{h} such that $\mathbf{g}' \in \mathbf{Q}_s$, where $\mathbf{g}' = \mathbf{S}_1 \mathbf{h}'$, and $\mathbf{Q}_s \triangleq [\mathbf{q}_1, \dots, \mathbf{q}_K]$ is the matrix formed by the eigenvectors that span the signal subspace. Similarly to [24], we will prove the sufficient condition by contradiction. Let the matrix $[\mathbf{S}_1 \ \mathbf{g}_2 \ \mathbf{g}_3 \ \dots \ \mathbf{g}_K]$ be full column rank and both $\mathbf{S}_1 \mathbf{h} \in \mathbf{Q}_s$ and $\mathbf{S}_1 \mathbf{h}' \in \mathbf{Q}_s$ for $\mathbf{h}' \neq \mathbf{h}$. Since $\text{span}\{\mathbf{Q}_s\} = \text{span}\{\mathbf{G}\}$, there exist parameters α and β such that

$$\mathbf{S}_1 \mathbf{h}' = [\mathbf{g}_2 \ \dots \ \mathbf{g}_K] \alpha + \beta \mathbf{g}_1. \quad (2.48)$$

Substituting $\mathbf{g}_1 = \mathbf{S}_1 \mathbf{h}$ in (2.48), we obtain

$$\mathbf{S}_1 \tilde{\mathbf{h}} = [\mathbf{g}_2 \ \dots \ \mathbf{g}_K] \alpha, \quad (2.49)$$

where $\tilde{\mathbf{h}} \triangleq (\mathbf{h}' - \beta \mathbf{h})$. If \mathbf{h} and \mathbf{h}' are linearly independent, then $\tilde{\mathbf{h}} \neq \mathbf{0}$, and (2.49) contradicts the full rank assumption of the matrix $[\mathbf{S}_1 \ \mathbf{g}_2 \ \mathbf{g}_3 \ \dots \ \mathbf{g}_K]$.

To prove the necessary condition, we use the fact that the channel is identifiable only if the $2J \times 2J$ matrix Ω in (2.47) be rank deficient by one. Then, there exists only one eigenvector that corresponds to the one zero eigenvalue. Therefore, we should have

$$\text{Rank}(\Omega) = \text{Rank}(\mathbf{S}_1^T \mathbf{Q}_n \mathbf{Q}_n^H \mathbf{S}_1) = 2J - 1. \quad (2.50)$$

For any matrix $\mathbf{A} \in \mathbb{C}^{m \times n}$ with rank r , we have

$$\text{Range}(\mathbf{A}) = \text{Range}(\mathbf{A}\mathbf{A}^H), \quad (2.51)$$

$$\text{Rank}(\mathbf{A}) = \text{Rank}(\mathbf{A}\mathbf{A}^H) = r, \quad (2.52)$$

Hence, we may write

$$\text{Range}(\mathbf{S}_1^T \mathbf{Q}_n \mathbf{Q}_n^H \mathbf{S}_1) = \text{Range}(\mathbf{S}_1^T \mathbf{Q}_n). \quad (2.53)$$

Using (2.50) - (2.53), it follows that

$$\text{Rank}(\Omega) = \text{Rank}(\mathbf{S}_1^T \mathbf{Q}_n) = 2J - 1. \quad (2.54)$$

Since $\mathbf{S}_1^T \mathbf{Q}_n$ is a $2J \times (L + J - 1 - K)$ matrix, the result in (2.54) suggests that

$$\min(2J, L + J - 1 - K) \geq 2J - 1, \quad (2.55)$$

or equivalently

$$L \geq J + K. \quad (2.56)$$

■

The above theorem reveals that due to the signal structure imposed by the chip-level ST block coding the channel can be uniquely identified even in the case when there is only one signature assigned to each user. On the other hand, in symbol-level schemes identifiability can only be guaranteed if each user is assigned a total number of signatures equal to the number of transmit antennas. As a result, use of chip-level ST block coding can lead to significant user capacity improvements compared to symbol-level block coding.

In practice, \mathbf{R} is not available and is estimated through sample-averaging over M re-

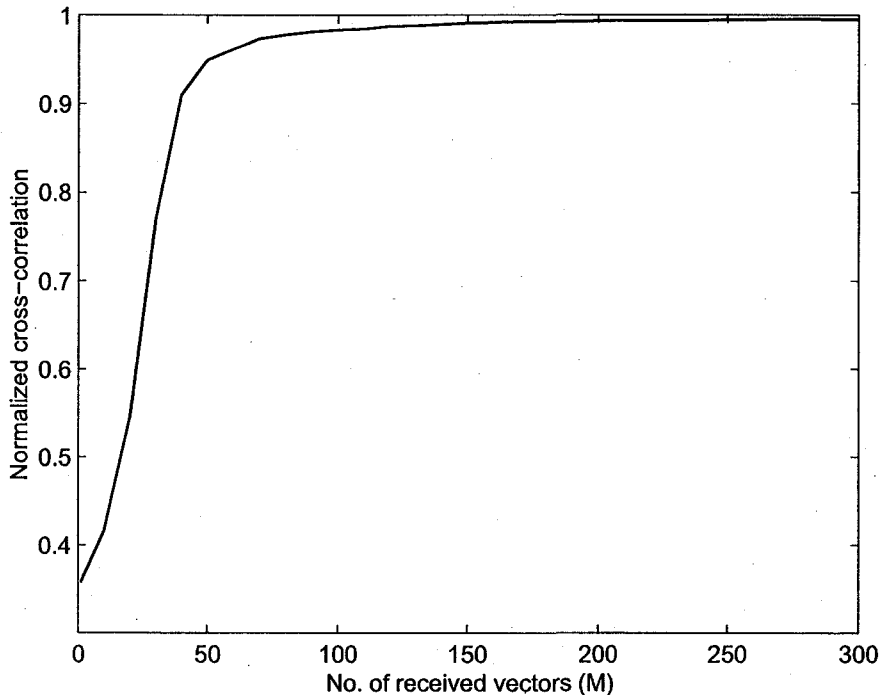


Fig. 2.3 Normalized cross-correlation between the channel vector \mathbf{h} and the channel estimate $\hat{\mathbf{h}}$ as a function of the data record size M .

ceived vectors $\mathbf{r}(1), \dots, \mathbf{r}(M)$. The sample average estimate $\hat{\mathbf{R}}$ is given by

$$\hat{\mathbf{R}} \triangleq \frac{1}{M} \sum_{n=1}^M \mathbf{r}(n)\mathbf{r}(n)^H. \quad (2.57)$$

In this case, the channel vector $\hat{\mathbf{h}}$ is obtained as the eigenvector that corresponds to the smallest eigenvalue of the matrix $\hat{\mathbf{\Omega}} \triangleq \mathbf{S}_1^T \hat{\mathbf{Q}}_n \hat{\mathbf{Q}}_n^H \mathbf{S}_1$, where $\hat{\mathbf{Q}}_n$ is the $(L+J-1) \times (L+J-K-1)$ matrix whose columns are the eigenvectors that correspond to the $L+J-K-1$ smallest eigenvalues of $\hat{\mathbf{R}}$.

2.5 Simulations Studies

As a representative case study, we consider a DS-CDMA system with 25 users utilizing code sequences of length⁷ 32. All interfering users are assumed to have SNR of 10 dB.

⁷Constructed from Gold sequences of length 31 by appending a +1.

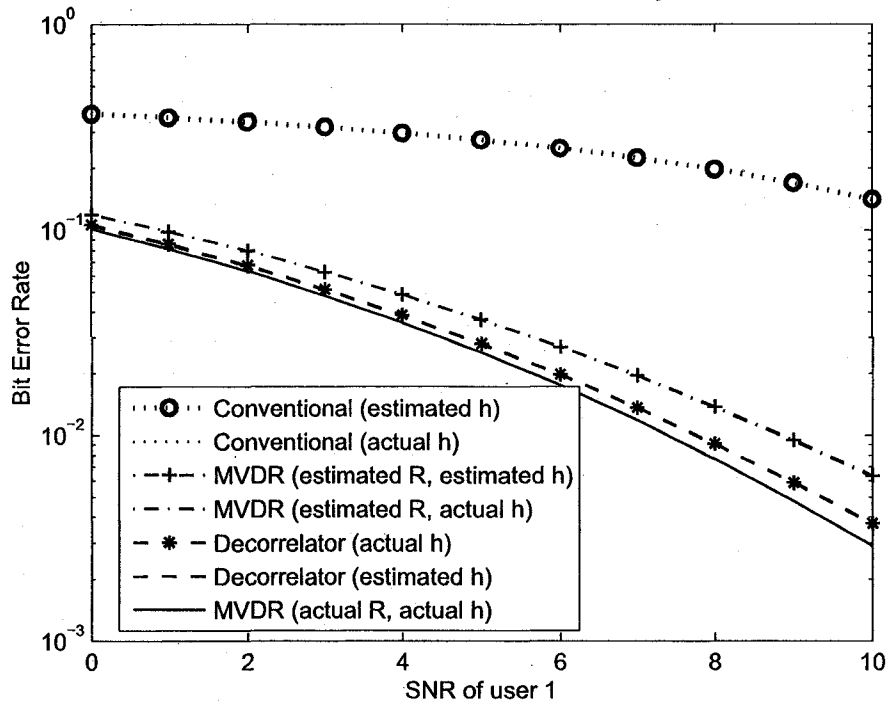


Fig. 2.4 Bit-error-rate of disjoint single-user detection algorithms as a function of the SNR of the user of interest for flat fading channels.

The transmitter and the receiver are equipped with 2 and 1 antennas, respectively, while the STBC employed is the real orthogonal block code of [3] explained in Section 2.2. For the multipath case, we have considered a channel with 3 paths. Each path coefficient has variance $\sigma_c^2 = 1$. The presented results are averages over 100 independent experiments.

In Fig. 2.3, we plot the normalized cross-correlation of the channel vector estimate $\hat{\mathbf{h}}$ and the actual channel vector \mathbf{h} as a function of the number of received vectors M used to form the autocorrelation matrix estimate in (2.57). In this study, the SNRs of all users in the system including the user of interest is fixed at 10 dB.

The performance of the disjoint single-user detection algorithms for flat fading channels described in Section III is given in Fig. 2.4. For comparison, Fig. 2.4 also includes the BER curves of the detectors that use the channel estimate instead of the actual channel. Here, the estimation of the channel vector and the MVDR filter is based on $M = 400$ received vectors. In all cases, the performance of the ideal receiver is almost equivalent to that of their counterparts employing the channel estimate. In Fig. 2.5, we plot the BER

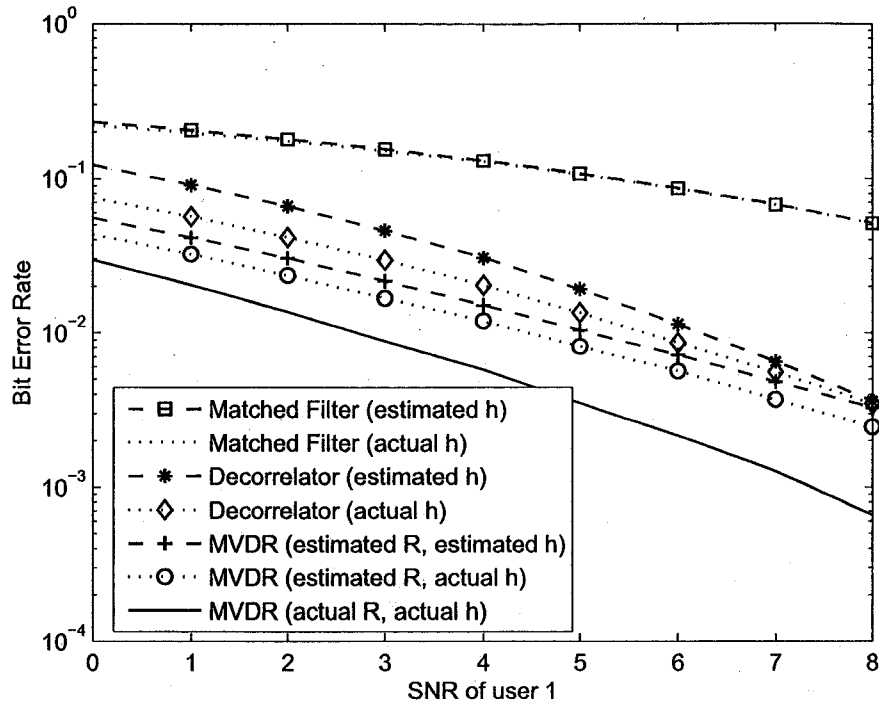


Fig. 2.5 Bit-error-rate of joint single-user detection algorithms as a function of the SNR of the user of interest for multipath fading channels.

of the joint single-user detection algorithms for frequency-selective fading channels, as a function of the SNR of the user of interest. As before, the estimation of the channel vector and the sample average estimate of \mathbf{R} is based on $M = 400$ received vectors. We see that in the multipath scenario since the number of received samples taken to form the sample average estimate of \mathbf{R} is not sufficient (for perfect channel estimation), the performance of the detectors using the channel estimate is a few dB away from that of the ideal receiver.

Finally, the BER performance of the joint algorithms versus number of the received samples for multipath fading channels is illustrated in Fig. 2.6. The SNRs of all users including the user of interest are fixed at 10 dB. As can be seen from this experiment, by increasing the data record size, there is a considerable improvement on the performance of the detectors using the channel estimate.

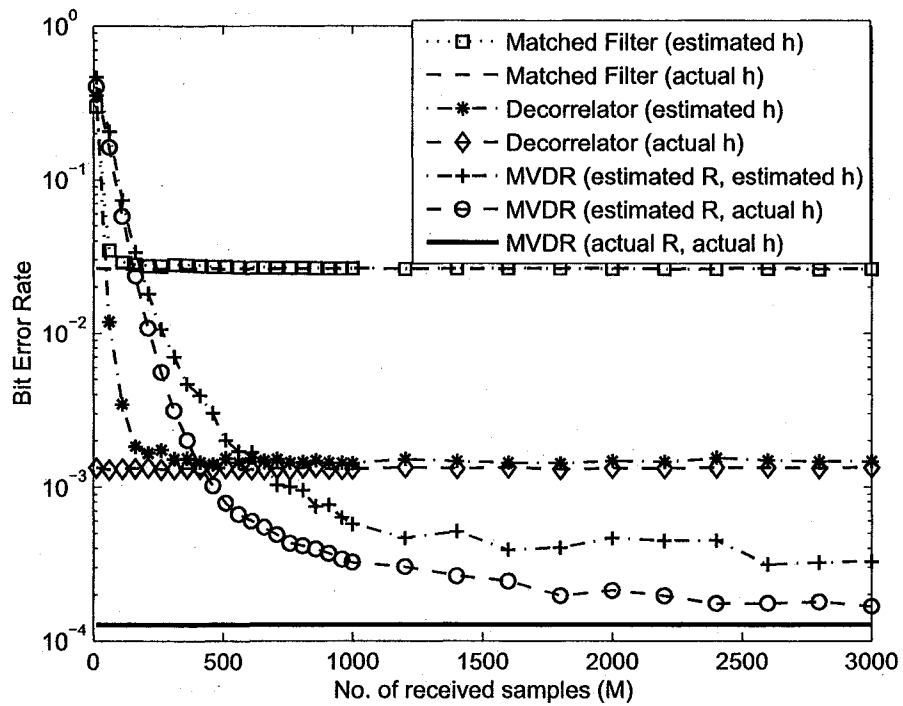


Fig. 2.6 Bit-error-rate of joint single-user detection algorithms for frequency selective fading channels as a function of the number of the samples for channel estimation and the sample average estimate.

Chapter 3

Space-Frequency Block Coded MC-CDMA: A Pre-FFT Approach

3.1 Introduction

Among the many multiple access techniques proposed, Multi-Carrier Code Division Multiple Access (MC-CDMA) is one of the most promising candidates for the downlink of future wireless communications systems as it exploits the advantages of both Orthogonal Frequency Division Multiplexing (OFDM) multicarrier modulation and Direct-Sequence Spread Spectrum (DSSS) techniques. In fact, the combined scheme allows different users share the same bandwidth at the same time by applying different user specific spreading codes (thanks to the spread spectrum mechanism); whereas offers the advantage of reducing the amount of ISI by lowering the symbol rate (thanks to the multicarrier modulation).

In MC-CDMA systems with cyclic prefix (CP) or zero-padding (ZP) [33], a frequency-selective fading channel is transformed into a number of parallel flat-fading channels. Therefore, ST block coding techniques, which were originally designed for flat fading channels, can effectively be applied to MC-CDMA systems to combat fading and achieve coding gains even in the case of multipath fading channels with large delay spreads. Alternatively, in MC-CDMA systems, block coding can be performed across the spatial and the frequency dimension instead of the temporal dimension. This approach is called Space-Frequency Block Coding (SFBC) and can provide significant performance improvements over STBC in situations where the channel is time-varying [34]. In fact, the STBC MC-CDMA systems are generally designed under the assumption that the channel is static over the duration

of a ST codeword. Consequently, they are very sensitive to the high time selectivity of the wireless mobile fading channel. One potential application of SFBC MC-CDMA could be in the emerging mobile broadband standards such as IEEE 802.16e and IEEE 802.20 in which the quasi-static channel assumption is no longer valid.

Examples of some recent research activities that focus on combining the benefits of STBC and MC-CDMA include [23], [13], [35], and [36]. In [23], the orthogonality property of STBC and the multicarrier modulation of MC-CDMA have been exploited to design a low complexity optimal multiuser receiver under a Bayesian framework. Iterative receiver structures for joint semiblind multiuser detection and decoding in a STBC MC-CDMA system have been presented in [13]. The bit-error rate (BER) performance and capacity of asynchronous STBC MC-CDMA systems in the presence of carrier frequency offset (CFO) between the transmitter and receiver oscillators have been studied in [35].

The common characteristic of the schemes in [23], [13], [35], and [36] is that ST block coding is performed at the information symbol level while MC-CDMA is used for the transmission of the resulting ST encoded symbols. However, this approach suffers from the exact same drawbacks as its DS-CDMA counterpart discussed in Chapter 2. First, the corresponding receivers have a decoding delay of at least M_t information symbol intervals (where M_t is the number of transmit antennas). Second, linear joint ST decoding and multiuser detection algorithms (as the one in [13]) require the use of very long filters (of length at least equal to $M_t \times L$ where L is the system processing gain). More importantly, however, performing ST block coding at the information symbol level requires the assignment of M_t CDMA signatures to each user if blind channel estimation without ambiguity is to be performed [16], [15]. The assignment of more than one signature to each user severely limits the maximum number of users that can be accommodated in the system. Finally, they cannot be used over fast fading channels where the channel may vary during one symbol period. Indeed, because of the quasi-static channel assumption of the employed ST block codes, symbol-level schemes require that the channel remains constant over many information symbol periods.

In this chapter, in an attempt to alleviate all of the aforementioned shortcomings, we apply the design principles of chip-level ST block coded CDMA systems developed in Chapter 2 to MC-CDMA systems and we obtain a novel chip-level Space-Frequency Block Coded (SFBC) MC-CDMA scheme for downlink transmissions. For this scheme, we develop so called disjoint and joint SF block decoding and information symbol detection algorithms for frequency-selective fading channels. The proposed joint algorithms utilize linear inter-

ference suppression structures based on matched, and Minimum-Variance-Distortionless-Response (MVDR)-type filtering criteria. Both proposed filters have a length equal to the processing gain plus the size of zero padding (as suggested in [26], short filters exhibit superior performance in short data-record situations) and have a decoding delay of only one OFDM block.

Since coherent detection/decoding of SFBC MC-CDMA transmissions require channel state information (CSI) at the receiver, channel estimation algorithms are also studied in this chapter. The diversity and coding gains that are possible in MC-CDMA systems with transmit diversity can only be realized if the underlying channels are accurately acquired at the receiver. Indeed, it is shown in [37], [38] that in the case of imperfect channel estimation, the performance of systems employing transmit diversity techniques is severely degraded. This motivates our effort to develop reliable channel estimation algorithms for MC-CDMA systems with transmit diversity. Examples of methods that exploit STBC for blind channel estimation in a multicarrier framework include the ones found in [10], [39], [23] and [36]. For example in [36], a subspace-based blind channel identification algorithm and the associated identifiability conditions for STBC MC-CDMA has been investigated. However, to our best knowledge, no channel estimation algorithm has been proposed or analyzed for SFBC MC-CDMA in the literature.

In this chapter¹, as a first step in filling that gap, we also investigate the problem of blind channel estimation for SFBC MC-CDMA systems. We utilize a system model for complex modulation schemes (such as QAM) that enables us to treat the links between the multiple transmit antennas and the single receive antenna as a single channel and, thus, reduces the multichannel estimation problem to a single-input single-output (SISO) problem. This allows us to develop two second-order-statistics-based channel estimation methods, namely, a subspace-based channel estimator and a Minimum Variance Distortionless Response (MVDR)-type channel estimator. For these methods, we address the issue of channel identifiability and we investigate the necessary and sufficient conditions under which the channel estimates are unique (within a complex scalar). Our studies reveal two interesting properties of SFBC MC-CDMA systems: First, unlike STBC-based systems that suffer from antenna order ambiguity unless a different spreading code is assigned to

¹Chapter 3 was presented in part at the IEEE Wireless and Mobile Computing, Networking and Communications Conference (WiMob 2005), Montreal, QC, Aug. 2005, at the 39th IEEE Asilomar Conference on Signals, Systems, and Computers, Pacific Grove, CA, Oct. 2005, and at the IEEE Wireless Communications and Networking Conference (WCNC 2006), Las Vegas, NV, Apr. 2006.

each user for each transmit antenna, the signal structure imposed by the SFBC removes such an ambiguity even though only one code is assigned to each user. Hence, we maintain the same total number of spreading codes available in the system as in a single transmit antenna case. Second, channel identifiability is guaranteed, regardless of the channel zeros location.

Moreover, we investigate the performance of the aforementioned algorithms in the case where only a finite number of received data vectors are available to perform the estimation of the channel. More specifically, we first establish the unbiasedness of the subspace-based channel estimator and the biasedness of the MVDR-type channel estimator and then we derive the analytical closed-form expressions for the variances of the channel estimates based on the eigenvalue decomposition (EVD) of the autocorrelation matrix of the received signal. As numerical studies verify, this approach provides analytical expressions for the mean-square-errors (MSEs) that are closer approximations to their corresponding actual MSEs in low SNRs than expressions based on the singular-value decomposition (SVD) (see [40], [41]).

Finally, to benchmark the accuracy of our estimation algorithms we also derive the Cramer-Rao bounds (CRBs) for both unbiased and biased channel estimators for the down-link of MC-CDMA systems. In [42], [43], the CRB was derived under the assumption of knowledge of all users' spreading codes. However, this assumption is not valid for down-link transmission where the signature waveform of only the desired user is available at the receiver. Therefore, the corresponding CRB cannot be adopted as a valid benchmark for the error variance of estimators of the forward channel. In this thesis, by treating the interfering users' signature waveforms as unknown deterministic quantities, we provide the CRBs which are tighter than the CRB with known signatures.

The rest of this chapter is organized as follows. In Section 3.2, we describe the combined SFBC MC-CDMA system model. Linear single-user SF block decoding and detection algorithms are investigated in Section 3.3, followed by presenting a subspace-based blind channel estimation algorithm in Section 3.4. Also in Section 3.4, we analyze the performance of the derived channel estimation algorithm by providing the MSE and the CRB. Finally, in Section 3.5 we present a MVDR-type blind channel estimation scheme along with its comprehensive performance analysis.

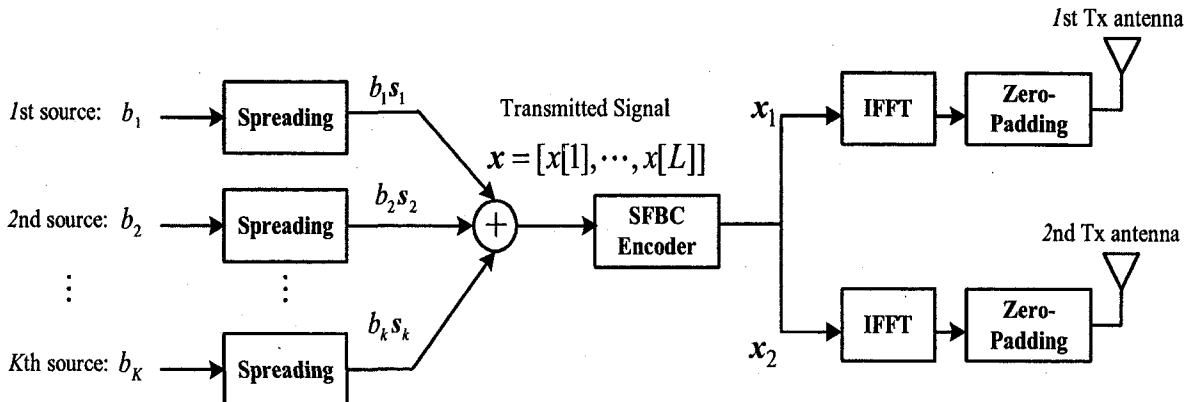


Fig. 3.1 Combined space-frequency block coding and MC-CDMA transmitter for downlink transmissions.

3.2 System Model

We consider the downlink of a wireless system with K synchronous mobile users where the base station is equipped with two antennas and each mobile user with a single antenna². The communication channel consists of 2 parallel, independent, multipath Rayleigh fading sub-channels. The sub-channels between the p th antenna, $p = 1, 2$, and the single receive antenna are modeled as finite impulse response (FIR) filters with J distinct paths whose impulse responses are given by

$$h_p(t) \triangleq \sum_{j=1}^J h_{p,j} \delta(t - jT_c), \quad p = 1, 2. \quad (3.1)$$

In (3.1), $h_{p,j}$, $p = 1, 2$, $j = 1, \dots, J$, is the complex path coefficient of the j th path of the p th subchannel, $\delta(\cdot)$ denotes the Kronecker delta function, and T_c is the chip duration. The path coefficients, $h_{p,j}$, are assumed to be independent, complex Gaussian random variables with zero mean and variance σ_c^2 . We will denote the p th subchannel vector as $\mathbf{h}_p \triangleq [h_{p,1}, \dots, h_{p,J}]^T$, $p = 1, 2$.

Downlink transmissions take place using the combined SFBC and MC-CDMA scheme depicted in Fig. 3.1 and described herein. The complex QPSK data symbol b_k to be transmitted to the k th user, $k = 1, \dots, K$, is first spread using the preassigned code signature

²Based on our preliminary studies extension to multiple receive antennas and more than two transmit antennas is feasible.

vector \mathbf{s}_k given by

$$\mathbf{s}_k \triangleq [s_k[1], s_k[2], \dots, s_k[L]]^T, \quad (3.2)$$

where L is the system processing gain and $s_k[i] \in \{\pm\sqrt{E_k/L}\}$ with E_k denoting the symbol energy of k th user. The vectors $\{\mathbf{s}_k\}_{k=1,\dots,K}$ are assumed to be linearly independent. After spreading, we form the complex vector \mathbf{x} as follows

$$\mathbf{x} \triangleq \sum_{k=1}^K b_k \mathbf{s}_k = [x[1], x[2], \dots, x[L]]^T, \quad (3.3)$$

on which we apply an Alamouti-type [3] orthogonal SF block encoding technique. More specifically, at any given symbol period, the encoded blocks sent to the transmit antenna 1 (Tx1) and transmit antenna 2 (Tx2) are $\mathbf{x}_1 = [x[1], -x^*[2], \dots, x[L-1], -x^*[L]]^T$, and $\mathbf{x}_2 = [x[2], x^*[1], \dots, x[L], x^*[L-1]]^T$, respectively. Finally, at each antenna, each encoded block is multicarrier modulated by applying the Inverse Fast Fourier Transform (IFFT) of size equal to the processing gain L and then zero-padded with a block of Z trailing zeros. In this work, we make the common assumption that Z has to be longer than the multipath channel spread J to completely eliminate the inter-block interference (IBI) [33].

From the perspective of each individual mobile station, signals from all users pass through the same channel in the downlink. At the mobile user, the discrete-time $P \times 1$ ($P \triangleq L + Z$) received vector due to the transmission of \mathbf{x} in (3.3) is given by

$$\mathbf{r} = \mathbf{H}_1 \mathbf{F}^H \mathbf{x}_1 + \mathbf{H}_2 \mathbf{F}^H \mathbf{x}_2 + \mathbf{n}, \quad (3.4)$$

where \mathbf{H}_1 and \mathbf{H}_2 are the $P \times L$ channel Toeplitz matrices with their first column as $[h_{1,1}, \dots, h_{1,J}, 0, \dots, 0]^T$, and $[h_{2,1}, \dots, h_{2,J}, 0, \dots, 0]^T$, respectively, \mathbf{F}^H is the $L \times L$ IFFT matrix whose (m, n) th entry is equal to $\exp\{j2\pi(m-1)(n-1)/L\}/\sqrt{L}$, and \mathbf{n} is additive white Gaussian noise (AWGN).

It is worthwhile noting that the maximum diversity order that can be achieved with optimal SFBC MC-CDMA transceiver design in rich scattering environments is $JM_t M_r$, where M_t (M_r) is the number of transmit (receive) antennas, and J is the number of taps corresponding to each FIR channel. Alternatively, the same transmit diversity order can be achieved by using STBC (see Fig. 3.2). In STBC MC-CDMA systems, the ST block encoder first maps each user's incoming symbol stream into multiple ST-coded streams.

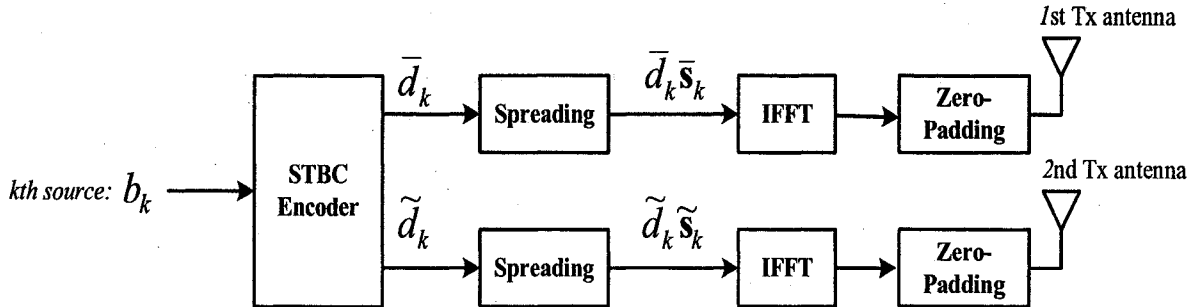


Fig. 3.2 Combined space-time block coding and MC-CDMA transmitter.

Next, each of the ST-coded streams is spread by a distinctive spreading code and subsequently multiplexed into L parallel substreams (where L is the number of subcarriers). Finally, the IFFT of the spread signal is computed (to perform OFDM modulation) which after CP insertion or zero-padding produces the transmitted signal.

3.2.1 Equivalent Single-Input-Single-Output Representation

To explicitly express the received vector in terms of the unknown channel vector \mathbf{h} that we wish to estimate, we rewrite \mathbf{r} in (3.4) by separating the real and imaginary components of each user's transmitted symbol. The received vector \mathbf{r} in (3.4) can be expressed as

$$\begin{aligned}
 \mathbf{r} &= \sum_{k=1}^K (\mathbf{S}_{k,r} \mathbf{h} \Re(b_k) + \mathbf{S}_{k,i} \mathbf{h} \Im(b_k)) + \mathbf{n}, \\
 &= \sum_{k=1}^K (\mathbf{g}_{k,r} \Re(b_k) + \mathbf{g}_{k,i} \Im(b_k)) + \mathbf{n},
 \end{aligned} \tag{3.5}$$

where $\mathbf{h} \triangleq [\mathbf{h}_1^T, \mathbf{h}_2^T]^T = [h_{1,1}, \dots, h_{1,J}, h_{2,1}, \dots, h_{2,J}]^T$ is the channel vector³, $\Re(b_k)$ and $\Im(b_k)$ indicate the real and imaginary parts of b_k , respectively, and $\mathbf{S}_{k,r}$ and $\mathbf{S}_{k,i}$ are the $P \times 2J$

³For the rest of this thesis, the channel vector will be assumed to be normalized (i.e., $\|\mathbf{h}\| = 1$).

matrices defined by

$$\mathbf{S}_{k,r} \triangleq \begin{bmatrix} \tilde{s}_{k,r}[1] & \dots & 0 & \bar{s}_{k,r}[1] & \dots & 0 \\ \vdots & & & & & \vdots \\ \tilde{s}_{k,r}[L] & \ddots & 0 & \tilde{s}_{k,r}[L] & \ddots & 0 \\ 0 & \ddots & \tilde{s}_{k,r}[1] & 0 & \ddots & \bar{s}_{k,r}[1] \\ \vdots & & \vdots & \vdots & & \vdots \\ 0 & \dots & \tilde{s}_{k,r}[L] & 0 & \dots & \bar{s}_{k,r}[L] \end{bmatrix}, \quad (3.6)$$

$$\mathbf{S}_{k,i} \triangleq \begin{bmatrix} \tilde{s}_{k,i}[1] & \dots & 0 & \bar{s}_{k,i}[1] & \dots & 0 \\ \vdots & & & & & \vdots \\ \tilde{s}_{k,i}[L] & \ddots & 0 & \tilde{s}_{k,i}[L] & \ddots & 0 \\ 0 & \ddots & \tilde{s}_{k,i}[1] & 0 & \ddots & \bar{s}_{k,i}[1] \\ \vdots & & \vdots & \vdots & & \vdots \\ 0 & \dots & \tilde{s}_{k,i}[L] & 0 & \dots & \bar{s}_{k,i}[L] \end{bmatrix}. \quad (3.7)$$

with

$$\begin{aligned} \tilde{\mathbf{s}}_{k,r} &= \mathbf{F}^H \mathbf{D}_1 \mathbf{s}_k, & \tilde{\mathbf{s}}_{k,i} &= \mathbf{F}^H \mathbf{D}_2 \mathbf{s}_k, \\ \bar{\mathbf{s}}_{k,r} &= \mathbf{F}^H \mathbf{D}_3 \mathbf{s}_k, & \bar{\mathbf{s}}_{k,i} &= \mathbf{F}^H \mathbf{D}_4 \mathbf{s}_k. \end{aligned} \quad (3.8)$$

In (3.8), the $L \times L$ precoding matrices \mathbf{D}_1 , \mathbf{D}_2 , \mathbf{D}_3 , \mathbf{D}_4 are given by

$$\mathbf{D}_1 \triangleq (\mathbf{I}_{M/2} \otimes \mathbf{A}); \quad \mathbf{A} = \begin{bmatrix} 1 & 0 \\ 0 & -1 \end{bmatrix}, \quad (3.9)$$

$$\mathbf{D}_2 \triangleq j\mathbf{I}_M, \quad (3.10)$$

$$\mathbf{D}_3 \triangleq (\mathbf{I}_{M/2} \otimes \mathbf{B}); \quad \mathbf{B} = \begin{bmatrix} 0 & 1 \\ 1 & 0 \end{bmatrix}, \quad (3.11)$$

$$\mathbf{D}_4 \triangleq (\mathbf{I}_{M/2} \otimes \mathbf{C}); \quad \mathbf{C} = \begin{bmatrix} 0 & j \\ -j & 0 \end{bmatrix}. \quad (3.12)$$

In (3.5), the vectors $\mathbf{g}_{k,r} \triangleq \mathbf{S}_{k,r} \mathbf{h}$ and $\mathbf{g}_{k,i} \triangleq \mathbf{S}_{k,i} \mathbf{h}$ are the effective signatures of the k th user, $k = 1, \dots, K$, corresponding to the real and imaginary parts of its transmitted symbol, respectively. As we can see, the real and imaginary parts of b_k modulate different effective signatures which is exactly what led us to treat them separately in (3.5). By closely

examining the SFBC-imposed structures of the signature matrices $\mathbf{S}_{k,r}$ and $\mathbf{S}_{k,i}$ defined by (3.6) and (3.7), respectively, it can be seen that for a given k , the spreading code \mathbf{s}_k is transformed to a set of linearly independent vectors $\tilde{\mathbf{s}}_{k,r}$, $\tilde{\mathbf{s}}_{k,i}$, $\bar{\mathbf{s}}_{k,r}$, and $\bar{\mathbf{s}}_{k,i}$. The vectors $\tilde{\mathbf{s}}_{k,r}$, $\bar{\mathbf{s}}_{k,r}$ are used for the transmission of the real part of b_k from antenna 1 and 2, respectively. The vectors $\tilde{\mathbf{s}}_{k,i}$, $\bar{\mathbf{s}}_{k,i}$ are used for the transmission of the imaginary part of b_k in a similar manner. Since these vectors are distinct, the receiver is able to distinguish the signals transmitted from each antenna and, therefore, can perform blind channel estimation with no order/permutation ambiguity. This is perhaps the most distinctive feature of SFBC MC-CDMA systems compared to their STBC counterparts. In STBC systems, blind channel estimation with no order ambiguity is only possible if each user is assigned two spreading codes⁴ (one for each transmit antenna).

The main advantage of representing the received signal as in (3.5) is that it reduces the problem of multi-channel estimation to a single-input single-output (SISO) channel estimation problem by treating the links between multiple transmit antennas and single receive antenna as a single channel.

3.3 Single-User Detection

At the k th mobile, the receiver's ultimate task is to detect the transmitted symbol b_k given the received vector \mathbf{r} without any knowledge of the other users' signatures. One way to perform single-user detection is to follow the exact inverse of the transmission scheme in Fig. 3.1. In Chapter 2, we called this technique which is shown in Fig. 3.3 as *disjoint* SF decoding and symbol detection. In other words, at the first stage, one may apply the overlap-add technique on the received vector to transform the linear convolution of the channel into circular convolution. As the second stage, FFT can be used to transform a frequency-selective fading channel into a number of parallel flat-fading channels. Then, space-frequency block decoding is performed followed by a single-user detector.

An alternative approach is *joint* SF decoding and information symbol detection which merges all the steps including multicarrier demodulation, SF decoding and single-user detection stages into a single one through the use of a linear filter. This technique which

⁴Intuitively, the basic DS/CDMA system is a natural special case of MC-CDMA with FFT size equal to one. Thus, our discussion on channel order ambiguity in Section 2.4.1 is valid for a MC-CDMA scenario as well.



Fig. 3.3 Receiver structure of the disjoint space-frequency block decoding and single-user detection.

conceptually is similar to the one presented in Chapter 2 implicitly equalizes the received signal and, therefore, can handle frequency selective channels in situations where the length of trailing zeros is less than the delay spread of the dispersive channel (i.e., $J > Z$). In that case, disjoint algorithms cannot cope with the ISI and Inter-Carrier Interference (ICI) caused by multipath channels and use of (potentially complex) equalizers are necessary. In what follows, first we give a brief overview of the disjoint scheme and then the joint technique is presented.

Throughout this section the only quantities assumed known to the receiver are the spreading code associated with the user of interest and the channel vector \mathbf{h} . Algorithms for channel estimation will be considered in the next section.

3.3.1 Disjoint SF Decoding and Symbol Detection

Without loss of generality, we will assume that the user of interest is $k = 1$. The disjoint receiver structure is shown in Fig. 3.3. To transform the linear convolution of the channel into circular convolution and thus facilitate diagonalization of the associated channel matrix, we apply the widely used overlap-add technique on the received vector. In this method, the last Z samples of the received vector are added to the first ones to form the modified received vector $\tilde{\mathbf{r}}$, as shown by

$$\begin{aligned}
 \tilde{\mathbf{r}} &\triangleq \mathbf{r}_u + \begin{bmatrix} \mathbf{r}_l \\ \mathbf{0}_{(L-Z) \times 1} \end{bmatrix}, \\
 &= \tilde{\mathbf{H}}_1 \mathbf{F}^H \mathbf{x}_1 + \tilde{\mathbf{H}}_2 \mathbf{F}^H \mathbf{x}_2 + \tilde{\mathbf{n}},
 \end{aligned} \tag{3.13}$$

where \mathbf{r}_u and \mathbf{r}_l represent the upper $L \times 1$ part and the lower $Z \times 1$ part of the received vector \mathbf{r} in (3.4), respectively; $\tilde{\mathbf{n}}$ denotes the $L \times 1$ AWGN vector. Finally, $\tilde{\mathbf{H}}_1$ and $\tilde{\mathbf{H}}_2$ are the $L \times L$ circulant matrices corresponding to the channel matrices \mathbf{H}_1 and \mathbf{H}_2 , respectively,

given by

$$\tilde{\mathbf{H}}_1 \triangleq \text{Circ}_L(h_{1,1} \ 0 \ \dots \ 0 \ h_{1,J} \ \dots \ h_{1,2}), \quad (3.14)$$

$$\tilde{\mathbf{H}}_2 \triangleq \text{Circ}_L(h_{2,1} \ 0 \ \dots \ 0 \ h_{2,J} \ \dots \ h_{2,2}). \quad (3.15)$$

where $\text{Circ}_L(\boldsymbol{\nu})$ denotes a square circulant matrix of size L with $\boldsymbol{\nu}$ as its first row.

In principal, the circulant matrices can be diagonalized by pre-multiplication and post-multiplication by the FFT and IFFT matrix, respectively. Therefore, pre-multiplying $\tilde{\mathbf{r}}$ in (3.13) by the $L \times L$ FFT matrix \mathbf{F} we get

$$\begin{aligned} \mathbf{y} &= \mathbf{F}\tilde{\mathbf{H}}_1\mathbf{F}^H\mathbf{x}_1 + \mathbf{F}\tilde{\mathbf{H}}_2\mathbf{F}^H\mathbf{x}_2 + \mathbf{F}\tilde{\mathbf{n}}, \\ &= \boldsymbol{\Lambda}_1\mathbf{x}_1 + \boldsymbol{\Lambda}_2\mathbf{x}_2 + \mathbf{F}\tilde{\mathbf{n}}, \end{aligned} \quad (3.16)$$

where $\boldsymbol{\Lambda}_1$ and $\boldsymbol{\Lambda}_2$ are the $L \times L$ diagonal matrices with vectors $\tilde{\mathbf{h}}_1 \triangleq \sqrt{L}\mathbf{F}[h_{1,1}, \dots, h_{1,J}, 0, \dots, 0]^T$ and $\tilde{\mathbf{h}}_2 \triangleq \sqrt{L}\mathbf{F}[h_{2,1}, \dots, h_{2,J}, 0, \dots, 0]^T$ as their diagonal, respectively.

Let \mathbf{x}_o and \mathbf{x}_e be two $L/2$ vectors denoting the odd and the even component vectors of \mathbf{x} , i.e.,

$$\mathbf{x}_o \triangleq [x[1], x[3], \dots, x[L-1]]^T, \quad (3.17)$$

$$\mathbf{x}_e \triangleq [x[2], x[4], \dots, x[L]]^T. \quad (3.18)$$

Assuming the channel vectors are known at the receiver, the space-frequency block decoder output provides the *soft* estimates of \mathbf{x}_o and \mathbf{x}_e as [3]

$$\hat{\mathbf{x}}_o = \boldsymbol{\Lambda}_{1,o}^*\mathbf{y}_o + \boldsymbol{\Lambda}_{2,e}\mathbf{y}_e^*, \quad (3.19)$$

$$\hat{\mathbf{x}}_e = \boldsymbol{\Lambda}_{2,o}^*\mathbf{y}_o - \boldsymbol{\Lambda}_{1,e}\mathbf{y}_e^*, \quad (3.20)$$

where $\boldsymbol{\Lambda}_{1,o}$, $\boldsymbol{\Lambda}_{1,e}$, $\boldsymbol{\Lambda}_{2,o}$, $\boldsymbol{\Lambda}_{2,e}$, denote the odd and the even diagonal submatrices of $\boldsymbol{\Lambda}_1$ and $\boldsymbol{\Lambda}_2$, respectively, and \mathbf{y}_o and \mathbf{y}_e are the odd and the even component vectors of \mathbf{y} , respectively.

Adopting the principle assumption of STBC MC-CDMA systems wherein the channel is assumed to be approximately constant during two consecutive OFDM symbol durations, we assume that the channel is approximately constant over two neighboring OFDM subcarriers,

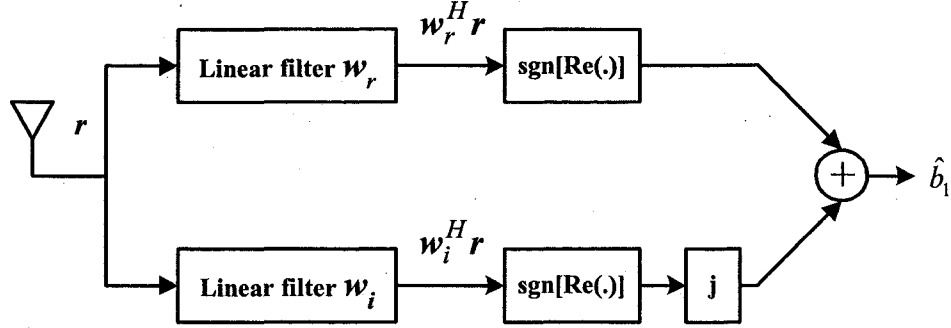


Fig. 3.4 Receiver structure of the joint space-frequency block decoding and single-user detection.

i.e., $\Lambda_{1,o} = \Lambda_{1,e}$ and $\Lambda_{2,o} = \Lambda_{2,e}$, we obtain

$$\hat{\mathbf{x}}_o = (|\Lambda_{1,o}|^2 + |\Lambda_{2,o}|^2)\mathbf{x}_o + \mathbf{z}_o, \quad (3.21)$$

$$\hat{\mathbf{x}}_e = (|\Lambda_{1,e}|^2 + |\Lambda_{2,e}|^2)\mathbf{x}_e + \mathbf{z}_e, \quad (3.22)$$

where \mathbf{z}_o and \mathbf{z}_e are the odd and the even component vectors of the AWGN noise vector \mathbf{z} . Equivalently, we may write the output of the decoder as

$$\hat{\mathbf{x}} = (|\Lambda_1|^2 + |\Lambda_2|^2)\mathbf{x} + \mathbf{z}, \quad (3.23)$$

$$= (|\Lambda_1|^2 + |\Lambda_2|^2) \sum_{k=1}^K b_k \mathbf{s}_k + \mathbf{z}. \quad (3.24)$$

Clearly, the decoded vector $\hat{\mathbf{x}}$ in (3.24) has the form of a DS/CDMA signal. Hence, the transmitted symbol b_1 can be detected using a single-user detector such as matched filter, decorrelator or MVDR-type filter as explained in section 2.3.1.

3.3.2 Joint SF Decoding and Symbol Detection

The proposed joint scheme is illustrated in Fig. 3.4. To perform single-user detection, the real and imaginary parts of the complex transmitted symbol b_1 are separately recovered from the received signal \mathbf{r} in (3.5) by means of two different linear filters \mathbf{w}_r and \mathbf{w}_i of length P . In other words, the estimate of the complex data symbol b_1 of the user of interest is obtained as

$$\hat{b}_1 = \text{sgn}[\Re(\mathbf{w}_r^H \mathbf{r})] + j \text{sgn}[\Re(\mathbf{w}_i^H \mathbf{r})]. \quad (3.25)$$

In the sequel, we present two alternative choices for the linear filters \mathbf{w}_r and \mathbf{w}_i :

1. MATCHED FILTER

The effective signatures of the desired user $\mathbf{g}_{1,r}$ and $\mathbf{g}_{1,i}$ can be chosen as the tap weight vectors of two filters matched to the real and imaginary parts of the signal of interest, respectively, i.e.,

$$\mathbf{w}_{\text{mf},r} = \mathbf{g}_{k,r} \quad \text{and} \quad \mathbf{w}_{\text{mf},i} = \mathbf{g}_{k,i}. \quad (3.26)$$

2. MINIMUM-VARIANCE-DISTORTIONLESS-RESPONSE (MVDR) FILTER

The conventional matched filter receivers suffer from the multiple access interference (MAI) and inter-symbol interference (ISI). Alternatively, we may use the MVDR filters $\mathbf{w}_{\text{mv},r}$ and $\mathbf{w}_{\text{mv},i}$ that minimize the variance/energy at their outputs, while being distortionless in the direction of the real and imaginary parts of the signal of interest, respectively. They are given by

$$\mathbf{w}_{\text{mv},r} = \frac{\mathbf{R}^{-1} \mathbf{g}_{k,r}}{\mathbf{g}_{k,r}^H \mathbf{R}^{-1} \mathbf{g}_{k,r}}, \quad (3.27)$$

and

$$\mathbf{w}_{\text{mv},i} = \frac{\mathbf{R}^{-1} \mathbf{g}_{k,i}}{\mathbf{g}_{k,i}^H \mathbf{R}^{-1} \mathbf{g}_{k,i}}, \quad (3.28)$$

where $\mathbf{R} \triangleq \mathbb{E}\{\mathbf{r}\mathbf{r}^H\}$ is the autocorrelation matrix of the input vector \mathbf{r} . In practice, the autocorrelation matrix \mathbf{R} is not known and it is sample-average estimated from N received vectors $\mathbf{r}(i)$, $i = 1, \dots, N$, as follows:

$$\hat{\mathbf{R}} \triangleq \frac{1}{N} \sum_{i=1}^N \mathbf{r}(i)\mathbf{r}(i)^H. \quad (3.29)$$

Substituting $\hat{\mathbf{R}}$ in place of \mathbf{R} in (3.28), we obtain sample-matrix-inversion (SMI) estimates of $\mathbf{w}_{\text{mv},r}$ and $\mathbf{w}_{\text{mv},i}$:

$$\hat{\mathbf{w}}_{\text{mv},r} = \frac{\hat{\mathbf{R}}^{-1} \mathbf{g}_{k,r}}{\mathbf{g}_{k,r}^H \hat{\mathbf{R}}^{-1} \mathbf{g}_{k,r}}, \quad (3.30)$$

and

$$\hat{\mathbf{w}}_{mv,i} = \frac{\hat{\mathbf{R}}^{-1} \mathbf{g}_{k,i}}{\mathbf{g}_{k,i}^H \hat{\mathbf{R}}^{-1} \mathbf{g}_{k,i}}. \quad (3.31)$$

As can be seen from the presented joint detection/decoding algorithms, in SFBC MC-CDMA schemes the transmitted blocks \mathbf{x}_1 and \mathbf{x}_2 are being multiplexed simultaneously across all subcarriers. Following are the key observations regarding such an approach.

- The scheme performs SF decoding within one OFDM symbol, therefore there is a decoding delay of only one symbol and it only requires half of the decoder memory needed for STBC MC-CDMA of the same block size.
- The decision variables in a SFBC detector are completely determined from a single received block hence the corresponding detector requires a shorter filter for detection and performs better than STBC in fast fading channels [34].
- There is no need for the channel to remain constant for more than one symbol duration. Instead, the scheme requires that two adjacent subcarriers experience the same channel [19] (we note that this requirement can be easily satisfied by increasing the FFT size).
- A similar approach can be followed to design a MVDR filter for the STBC MC-CDMA receivers. However, the autocorrelation matrix used by the MVDR algorithm in the SFBC MC-CDMA scheme is half the size of the one needed for the STBC MC-CDMA implementation. This can be attributed to the fact that the latter requires the received vector to be comprised from two consecutive OFDM symbols. This increases complexity and reduces the accuracy of the STBC-based SMI MVDR filter estimator. We demonstrate this important issue later in our numerical studies.

3.3.3 Simulations Studies

As a representative case study, we consider a MC-CDMA system with 15 users utilizing code sequences of length⁵ 32 which is assumed to be equal to the number of subcarriers. We used zero padding of length 8 which is 1/4th of the FFT size. Five of the interfering

⁵Constructed from Gold sequences of length 31 by appending a +1.

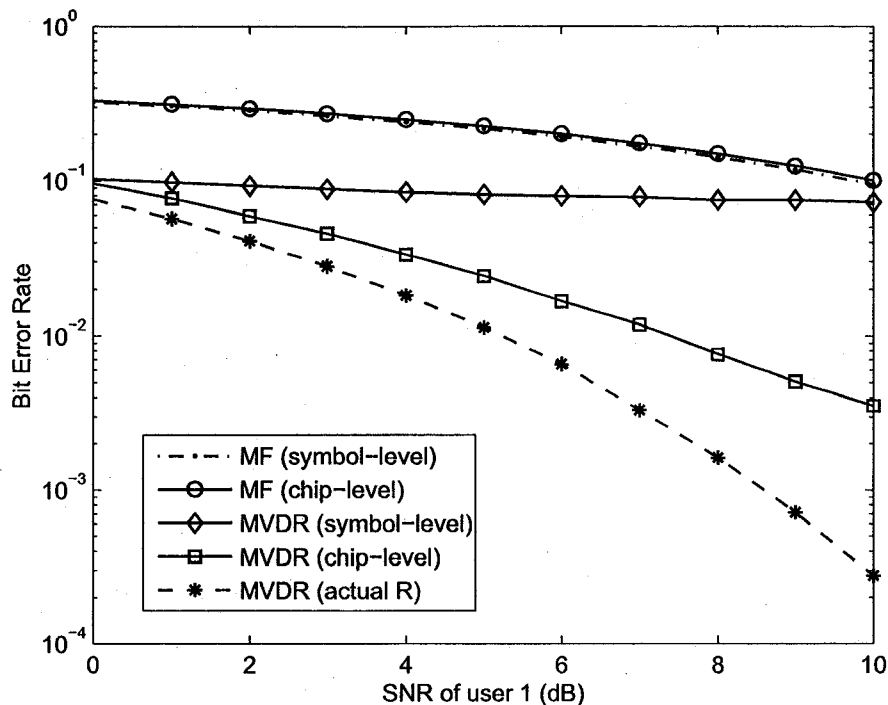


Fig. 3.5 Bit-error-rate of both chip-level and symbol-level detection algorithms as a function of the SNR of the user of interest.

users are assumed to have SNR⁶ of 10 dB, five have SNR of 15 dB and the rest of them have SNR of 20 dB. The transmitter and the receiver are equipped with 2 and 1 antennas, respectively, while the SFBC employed is the orthogonal block code of [3]. Each multipath channel \mathbf{h}_p , $p = 1, 2$, consists of 3 paths where each path coefficient is modeled as a complex Gaussian random variable with zero mean and variance of $\sigma_c^2 = 1$. In what follows, the presented results are averages over 100 independent channel realizations.

Fig. 3.5 and 3.6 depict the BER performance of the joint MVDR receivers versus the SNR of the user of interest and the number of samples used to form the autocorrelation matrix estimate in (3.29), respectively, for both chip-level and symbol-level schemes. The BER performance of the corresponding MF receivers is also shown as a reference. The SNR of the desired user in Fig. 3.6 is fixed at 10 dB. From these experiments, we infer that the use of chip-level technique leads to significant performance gains for short data records. In fact, in Fig. 3.5, we have considered a data record of 500 received samples, but

⁶The SNR of the k th user is defined as E_k/σ^2 , $k = 1, \dots, K$.

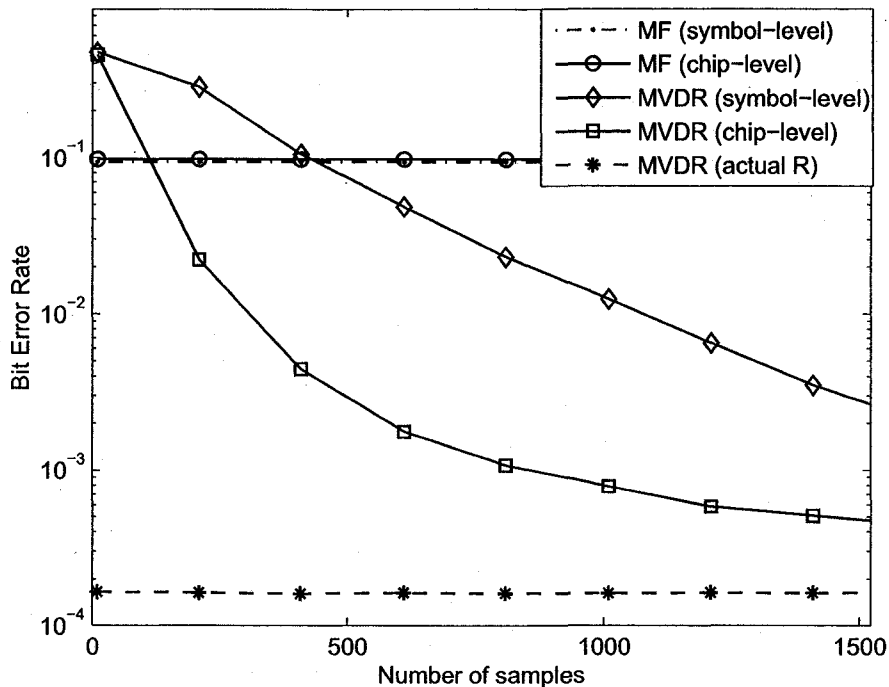


Fig. 3.6 Bit-error-rate of both chip-level and symbol-level detection algorithms as a function of the number of the samples used for estimating the autocorrelation matrix.

the chip-level method still affords a significant gain compared to the symbol level one.

3.4 Subspace-based Blind Channel Estimation

Among the many blind multichannel estimation algorithms (see [44] and references therein), subspace-based estimation algorithms are particularly attractive due to their accuracy and simplicity (they require only second-order statistics of the received signal). In the rest of this section, we derive and analyze a simple intuitive subspace-based channel estimation algorithm. We understand that more sophisticated channel estimation algorithms for SFBC MC-CDMA systems may be derived but this is not the purpose of this section. Instead, we aim at a comprehensive study and performance evaluation of the algorithm derived herein. These studies identify important properties of SFBC MC-CDMA systems and also provide useful performance benchmarks for future developments.

For the derivation of the subspace channel estimation algorithm presented in this section the only parameters assumed known are: (i) the spreading code of the user of interest (assumed to be user 1); (ii) the total number of users K , and (iii) the channel order J . Knowledge of the last two parameters allows accurate signal and noise subspace separation and it is a common assumption for many subspace channel identification methods [45]. If the number of users K needs to be estimated, this can be done through the use of information theoretic criteria as in [46]. Similarly, the channel length J can also be estimated by applying a rank test criterion to the received signal autocorrelation matrix as in [47].

Under the assumption that each user's information symbols are independent and identically distributed (i.i.d.) and the symbol streams of the users are independent, the autocorrelation matrix \mathbf{R} of the received vector \mathbf{r} in (3.5) can be written as

$$\mathbf{R} \triangleq \mathbb{E}\{\mathbf{r}\mathbf{r}^H\} = \mathbf{G}\mathbf{G}^H + \sigma^2\mathbf{I}_P, \quad (3.32)$$

where the $P \times 2K$ matrix \mathbf{G} is the effective signature matrix given by

$$\mathbf{G} \triangleq [\mathbf{g}_{1,r} \ \mathbf{g}_{2,r} \ \cdots \ \mathbf{g}_{K,r} \ \mathbf{g}_{1,i} \ \mathbf{g}_{2,i} \ \cdots \ \mathbf{g}_{K,i}]. \quad (3.33)$$

Applying the eigenvalue decomposition (EVD) to the autocorrelation matrix \mathbf{R} we obtain

$$\mathbf{R} = \mathbf{Q}\mathbf{\Lambda}\mathbf{Q}^H = [\mathbf{Q}_s \ \mathbf{Q}_n] \begin{bmatrix} \mathbf{\Lambda}_s & \mathbf{0} \\ \mathbf{0} & \mathbf{\Lambda}_n \end{bmatrix} \begin{bmatrix} \mathbf{Q}_s^H \\ \mathbf{Q}_n^H \end{bmatrix}, \quad (3.34)$$

where $\mathbf{\Lambda} \triangleq \text{diag}[\mathbf{\Lambda}_s \ \mathbf{\Lambda}_n] = \text{diag}(\lambda_1, \lambda_2, \dots, \lambda_P)$, $\lambda_1 \geq \dots \geq \lambda_{2K} > \lambda_{2K+1} = \dots = \lambda_P = \sigma^2$ contains in its diagonal the eigenvalues of \mathbf{R} in descending order, and $\mathbf{Q} \triangleq [\mathbf{Q}_s \ \mathbf{Q}_n]$ is the matrix of the corresponding eigenvectors. In (3.34), the columns of $\mathbf{Q}_s \triangleq [\mathbf{q}_1, \dots, \mathbf{q}_{P-2K}]$ span the signal subspace, whereas the columns of $\mathbf{Q}_n \triangleq [\mathbf{q}_{P-2K+1}, \dots, \mathbf{q}_P]$ span the noise subspace.

The orthogonality between the noise subspace and the signal subspace gives rise to a special property of the channel vector \mathbf{h} identified in the following Proposition.

Proposition 2 *Let $\mathbf{S}_{1,r}$ and $\mathbf{S}_{1,i}$ be defined by (3.6) and (3.7), respectively, with $k = 1$. Then, the channel vector \mathbf{h} satisfies*

$$\mathbf{h}^H \mathbf{\Omega}_{ss} \mathbf{h} = 0, \quad (3.35)$$

where Ω_{ss} is the $2J \times 2J$ matrix given by

$$\Omega_{ss} \triangleq \mathbf{S}_{1,r}^H \mathbf{Q}_n \mathbf{Q}_n^H \mathbf{S}_{1,r} + \mathbf{S}_{1,i}^H \mathbf{Q}_n \mathbf{Q}_n^H \mathbf{S}_{1,i}. \quad (3.36)$$

Proof: Due to the orthogonality between the noise subspace and the signal subspace, both effective signatures of the desired user $\mathbf{g}_{1,r}$ and $\mathbf{g}_{1,i}$ are orthogonal to the columns of $\mathbf{Q}_n = [\mathbf{q}_{P-2K+1}, \dots, \mathbf{q}_P]$ that span the noise subspace. Therefore, we have

$$\|\mathbf{Q}_n^H \mathbf{g}_{1,r}\|^2 + \|\mathbf{Q}_n^H \mathbf{g}_{1,i}\|^2 = 0. \quad (3.37)$$

Moreover, since both real and imaginary parts of the complex transmitted symbol are passing through the same channel filter, the latter equation is equivalent to

$$\mathbf{h}^H \mathbf{S}_{1,r}^H \mathbf{Q}_n \mathbf{Q}_n^H \mathbf{S}_{1,r} \mathbf{h} + \mathbf{h}^H \mathbf{S}_{1,i}^H \mathbf{Q}_n \mathbf{Q}_n^H \mathbf{S}_{1,i} \mathbf{h} = 0. \quad (3.38)$$

or

$$\mathbf{h}^H (\mathbf{S}_{1,r}^H \mathbf{Q}_n \mathbf{Q}_n^H \mathbf{S}_{1,r} + \mathbf{S}_{1,i}^H \mathbf{Q}_n \mathbf{Q}_n^H \mathbf{S}_{1,i}) \mathbf{h} = 0. \quad (3.39)$$

■

The above proposition implies that the channel vector \mathbf{h} can be identified as the eigenvector that corresponds to the zero eigenvalue of the matrix Ω_{ss} in (3.36), provided that this eigenvector is unique, i.e., the rank of Ω_{ss} is $2J - 1$. The identifiability conditions of the channel estimator are discussed next.

3.4.1 Identifiability

The following theorem presents sufficient and necessary conditions for the unique identifiability (always with a scalar ambiguity) of the channel vector \mathbf{h} .

Theorem 2 *Under the assumption that the effective signature matrix \mathbf{G} has full column rank, sufficient and necessary conditions for the channel vector \mathbf{h} in (3.35) to be uniquely identifiable up to an unknown complex scalar are as follows*

- **(Sufficient)** The following matrix has full column rank:

$$\mathbf{\Gamma} \triangleq \begin{bmatrix} \mathbf{S}_{1,r} & \tilde{\mathbf{G}} & \mathbf{0} \\ \mathbf{S}_{1,i} & \mathbf{0} & \bar{\mathbf{G}} \end{bmatrix} \quad (3.40)$$

where

$$\tilde{\mathbf{G}} \triangleq [\mathbf{g}_{2,r} \ \cdots \ \mathbf{g}_{K,r} \ \mathbf{g}_{1,i} \ \mathbf{g}_{2,i} \ \cdots \ \mathbf{g}_{K,i}], \quad (3.41)$$

$$\bar{\mathbf{G}} \triangleq [\mathbf{g}_{1,r} \ \mathbf{g}_{2,r} \ \cdots \ \mathbf{g}_{K,r} \ \mathbf{g}_{2,i} \ \cdots \ \mathbf{g}_{K,i}]. \quad (3.42)$$

- **(Necessary)** $P > J + 2K - 1$.

Proof: The unique identifiability of the channel vector \mathbf{h} in (3.35) can be guaranteed only if the equation

$$\mathbf{h}^H [\mathbf{S}_{1,r}^H \ \mathbf{S}_{1,i}^H] \begin{bmatrix} \mathbf{Q}_n \mathbf{Q}_n^H & \mathbf{0} \\ \mathbf{0} & \mathbf{Q}_n \mathbf{Q}_n^H \end{bmatrix} \begin{bmatrix} \mathbf{S}_{1,r} \\ \mathbf{S}_{1,i} \end{bmatrix} \mathbf{h} = \mathbf{0}, \quad (3.43)$$

has a unique solution. Correspondingly, for (3.43) to have a unique solution, we should show that $\mathbf{\Gamma}$ in (3.40), or equivalently, the matrices $\mathbf{\Gamma}_r \triangleq [\mathbf{S}_{1,r} \ \tilde{\mathbf{G}}]$ and $\mathbf{\Gamma}_i \triangleq [\mathbf{S}_{1,i} \ \bar{\mathbf{G}}]$ have full column rank. Without loss of generality, we focus on $\mathbf{\Gamma}_r$. Similarly to [24], we will prove the sufficient condition by contradiction. Hence, it suffices to show that there does not exist \mathbf{h}' linearly independent from \mathbf{h} such that $\mathbf{S}_{1,r} \mathbf{h}' \in \mathbf{Q}_s$. Let the matrix $\mathbf{\Gamma}_r$ be full column rank and both $\mathbf{S}_{1,r} \mathbf{h} \in \mathbf{Q}_s$ and $\mathbf{S}_{1,r} \mathbf{h}' \in \mathbf{Q}_s$ for $\mathbf{h}' \neq \mathbf{h}$. Since $\text{span}\{\mathbf{Q}_s\} = \text{span}\{\mathbf{G}\}$, there exist parameters α and β such that

$$\mathbf{S}_{1,r} \mathbf{h}' = [\mathbf{g}_{2,r} \ \cdots \ \mathbf{g}_{K,r} \ \mathbf{g}_{1,i} \ \mathbf{g}_{2,i} \ \cdots \ \mathbf{g}_{K,i}] \alpha + \beta \mathbf{g}_{1,r}. \quad (3.44)$$

Substituting $\mathbf{g}_{1,r} = \mathbf{S}_{1,r} \mathbf{h}$ in (3.44), we obtain

$$\mathbf{S}_{1,r} \tilde{\mathbf{h}} = [\mathbf{g}_{2,r} \ \cdots \ \mathbf{g}_{K,r} \ \mathbf{g}_{1,i} \ \mathbf{g}_{2,i} \ \cdots \ \mathbf{g}_{K,i}] \alpha, \quad (3.45)$$

where $\tilde{\mathbf{h}} \triangleq (\mathbf{h}' - \beta \mathbf{h})$. If \mathbf{h} and \mathbf{h}' are linearly independent, then $\tilde{\mathbf{h}} \neq \mathbf{0}$, and (3.45) contradicts the full rank assumption of the matrix $\mathbf{\Gamma}_r$.

To prove the necessary condition, we use the fact that the channel is identifiable only if the $2J \times 2J$ matrix $\mathbf{\Omega}_{ss}$ in (3.36) is rank deficient by one. Then, there exists only one

eigenvector that corresponds to the one zero eigenvalue. Therefore, we should have

$$\text{Rank}(\mathbf{\Omega}_{\text{SS}}) = 2J - 1. \quad (3.46)$$

For any two matrices $\mathbf{A}, \mathbf{B} \in \mathbb{C}^{m \times n}$, we have

$$\text{Rank}(\mathbf{A} + \mathbf{B}) \leq \text{Rank}(\mathbf{A}) + \text{Rank}(\mathbf{B}). \quad (3.47)$$

Therefore, we may write

$$\text{Rank}(\mathbf{\Omega}_{\text{SS}}) \leq \text{Rank}(\mathbf{S}_{k,r}^H \mathbf{Q}_n \mathbf{Q}_n^H \mathbf{S}_{k,r}) + \text{Rank}(\mathbf{S}_{k,i}^H \mathbf{Q}_n \mathbf{Q}_n^H \mathbf{S}_{k,i}). \quad (3.48)$$

Also, we have

$$\text{Range}(\mathbf{S}_{k,r}^H \mathbf{Q}_n \mathbf{Q}_n^H \mathbf{S}_{k,r}) = \text{Range}(\mathbf{S}_{k,r}^H \mathbf{Q}_n), \quad (3.49)$$

$$\text{Range}(\mathbf{S}_{k,i}^H \mathbf{Q}_n \mathbf{Q}_n^H \mathbf{S}_{k,i}) = \text{Range}(\mathbf{S}_{k,i}^H \mathbf{Q}_n). \quad (3.50)$$

Using (3.46) - (3.50), it follows that

$$\text{Rank}(\mathbf{\Omega}_{\text{SS}}) \leq \text{Rank}(\mathbf{S}_{k,r}^H \mathbf{Q}_n) + \text{Rank}(\mathbf{S}_{k,i}^H \mathbf{Q}_n). \quad (3.51)$$

Since both $\mathbf{S}_{k,r}^H \mathbf{Q}_n$ and $\mathbf{S}_{k,i}^H \mathbf{Q}_n$ are $2J \times (P - 2K)$ matrices, the result in (3.51) suggests that

$$2J - 1 \leq \min(2J, P - 2K) + \min(2J, P - 2K), \quad (3.52)$$

or equivalently

$$P \geq J + 2K - 1/2 > J + 2K - 1. \quad (3.53)$$

■

An interesting observation from the above theorem is that channel identifiability is guaranteed, regardless of the channel zeros location as long as the sufficient conditions hold. This property does not apply to OFDM systems, in which channel identifiability is not guaranteed when the channels have nulls on the subcarriers [39]. In fact, as opposed to the OFDM systems for the channel to be identifiable in MC-CDMA systems, the channel matrix $[\mathbf{H}_1 \ \mathbf{H}_2]$ need not full rank, instead, the full rank condition should be satisfied for the matrix $\mathbf{\Gamma}$ in (3.40).

It is also worth noting that the necessary condition $P > J + 2K - 1$ imposes the upper bound $(P - J + 1)/2$ on the number of active users in the system. This limitation, which is a direct consequence of the complex modulation scheme employed (QPSK), can be overcome by using a real modulation scheme (e.g., BPSK). In the case of real modulation schemes the received signal in (3.5) can be written as:

$$\mathbf{r}' = \sum_{k=1}^K b'_k \mathbf{g}_{k,r} + \mathbf{n}. \quad (3.54)$$

Consequently, the channel vector \mathbf{h} can be identified as the zero eigenvector of

$$\mathbf{\Omega}'_{ss} \triangleq \mathbf{S}_{1,r}^H \mathbf{Q}'_n \mathbf{Q}'_n{}^H \mathbf{S}_{1,r}, \quad (3.55)$$

where \mathbf{Q}'_n contains as its columns the eigenvectors of $\mathbf{R}' \triangleq \mathbb{E}\{\mathbf{r}'\mathbf{r}'^H\}$ that span the noise subspace. The following proposition identifies necessary and sufficient conditions for the identifiability of \mathbf{h} . The proof is similar to the proof of Theorem 2 and is thus omitted.

Proposition 3 *Under the assumption that the effective signature matrix $\mathbf{G}' \triangleq [\mathbf{g}_{1,r} \dots \mathbf{g}_{K,r}]$ has full column rank, sufficient and necessary conditions for the channel vector \mathbf{h} in (3.55) to be uniquely identifiable up to an unknown complex scalar are as follows*

- **(Sufficient)** *The matrix $[\mathbf{S}_{1,r} \ \mathbf{g}_{2,r} \ \dots \ \mathbf{g}_{K,r}]$ has full column rank.*
- **(Necessary)** $P \geq 2J + K - 1$. ■

The above proposition implies that in SFBC MC-CDMA systems that employ blind channel estimation and have a limited number of available spreading codes, the user capacity can be increased by switching to a real modulation scheme at the expense of bandwidth efficiency.

We note that since $e^{j\phi}\mathbf{h}$, $\phi \in [0, 2\pi)$ is also an eigenvector of $\mathbf{\Omega}'_{ss}$ the channel can only be identified within a complex scalar ambiguity. This ambiguity is inherent to any second-order statistics-based approach for blind channel identification and can be resolved either by choosing Differential ST modulation schemes, e.g., [48]- [49], or by transmitting a very short training sequence. For the rest of this chapter, we assume that the complex scalar ambiguity is compensated by multiplying the estimates by the appropriate scaling factor.

3.4.2 SFBC vs. STBC

In STBC MC-CDMA systems (as in [36]), after overlap-adding (or CP removal) and applying the L -point Fast Fourier Transform (FFT), the discrete-time frequency-domain $L \times 1$ received vectors over two information symbol periods can be written as

$$\tilde{\mathbf{r}}[1] = \sum_{k=1}^K (b_k[1] \tilde{\mathbf{S}}_k \tilde{\mathbf{F}} \mathbf{h}_1 + b_k[2] \tilde{\mathbf{S}}_k \tilde{\mathbf{F}} \mathbf{h}_2) + \mathbf{n}_1, \quad (3.56)$$

$$\tilde{\mathbf{r}}[2] = \sum_{k=1}^K (b_k^*[1] \tilde{\mathbf{S}}_k \tilde{\mathbf{F}} \mathbf{h}_2 - b_k^*[2] \tilde{\mathbf{S}}_k \tilde{\mathbf{F}} \mathbf{h}_1) + \mathbf{n}_2, \quad (3.57)$$

where $b_k[1]$ and $b_k[2]$ are the k th user data symbols over a STBC block, $\tilde{\mathbf{F}}$ denotes the matrix formed by the first J columns of $\sqrt{L}\mathbf{F}$, $\mathbf{n}_1, \mathbf{n}_2 \sim \mathcal{CN}(0, \sigma^2 \mathbf{I}_L)$ are the noise vectors for the two symbol periods, $\tilde{\mathbf{S}}_k = \text{diag}\{\tilde{\mathbf{s}}_k\}$ and $\tilde{\mathbf{S}}_k = \text{diag}\{\tilde{\mathbf{s}}_k\}$ with $\tilde{\mathbf{s}}_k$ and $\tilde{\mathbf{s}}_k$ denoting the $L \times 1$ spreading codes assigned to the k th user.

Then, the orthogonality between the noise and signal subspace implies that

$$\tilde{\mathbf{Q}}_n^H \tilde{\mathbf{S}}_k \tilde{\mathbf{F}} \mathbf{h}_1 = 0 \quad (3.58)$$

$$\tilde{\mathbf{Q}}_n^H \tilde{\mathbf{S}}_k \tilde{\mathbf{F}} \mathbf{h}_2 = 0 \quad (3.59)$$

where $\tilde{\mathbf{Q}}_n$ spans the noise subspace of $\tilde{\mathbf{R}} \triangleq \mathbb{E}\{\tilde{\mathbf{r}}\tilde{\mathbf{r}}^H\}$.

The channel vector \mathbf{h} can now be identified as the zero eigenvector of a block diagonal matrix $\tilde{\mathbf{\Omega}}$ which can be written as

$$\tilde{\mathbf{\Omega}} \triangleq \begin{bmatrix} \tilde{\mathbf{\Omega}}_1 & \mathbf{0} \\ \mathbf{0} & \tilde{\mathbf{\Omega}}_2 \end{bmatrix}, \quad (3.60)$$

where $\tilde{\mathbf{\Omega}}_1$ and $\tilde{\mathbf{\Omega}}_2$ are square matrices of identical dimensions given by

$$\tilde{\mathbf{\Omega}}_1 = \tilde{\mathbf{F}}^H \tilde{\mathbf{S}}_k \tilde{\mathbf{Q}}_n \tilde{\mathbf{Q}}_n^H \tilde{\mathbf{S}}_k \tilde{\mathbf{F}}, \quad (3.61)$$

and

$$\tilde{\mathbf{\Omega}}_2 = \tilde{\mathbf{F}}^H \tilde{\mathbf{S}}_k \tilde{\mathbf{Q}}_n \tilde{\mathbf{Q}}_n^H \tilde{\mathbf{S}}_k \tilde{\mathbf{F}}. \quad (3.62)$$

As can be seen from (3.61) and (3.62), the values of $\tilde{\mathbf{\Omega}}_1, \tilde{\mathbf{\Omega}}_2$ depend on the users' spreading codes but, most importantly, they are equal if the user of interest transmits from each

antenna using the same code. Clearly, if $\tilde{\Omega}_1 = \tilde{\Omega}_2$ then the vector $[\mathbf{h}_2^T, \mathbf{h}_1^T]^T$ is also a zero eigenvector of $\tilde{\Omega}$ (in addition to $\mathbf{h} = [\mathbf{h}_1^T, \mathbf{h}_2^T]^T$). Therefore, the uniqueness of the solution can only be guaranteed if $\tilde{\Omega}_1 \neq \tilde{\Omega}_2$ which, in turn, necessitates that two different spreading codes be assigned to the desired user for each transmitter antenna. This requirement severely limits the number of users that can be accommodated in a STBC MC-CDMA system that employs blind channel estimation.

3.4.3 Finite Data Record Performance Analysis

As we pointed out, in practice, the ensemble average of the received signal autocorrelation matrix \mathbf{R} is not known and is sample-average estimated using N received vectors as in (3.29). Then, the channel vector estimate $\hat{\mathbf{h}}_{\text{ss}}$ is obtained as the eigenvector that corresponds to the smallest eigenvalue of the matrix $\hat{\Omega}_{\text{ss}}$ given by

$$\hat{\Omega}_{\text{ss}} \triangleq \mathbf{S}_{1,r}^H \hat{\mathbf{Q}}_n \hat{\mathbf{Q}}_n^H \mathbf{S}_{1,r} + \mathbf{S}_{1,i}^H \hat{\mathbf{Q}}_n \hat{\mathbf{Q}}_n^H \mathbf{S}_{1,i}, \quad (3.63)$$

where $\hat{\mathbf{Q}}_n$ is the $P \times (P - 2K)$ matrix whose columns are the eigenvectors that correspond to the $P - 2K$ smallest eigenvalues of $\hat{\mathbf{R}}$. In other words,

$$\hat{\mathbf{h}}_{\text{ss}} = \arg \min_{\mathbf{h}, \|\mathbf{h}\|=1} \mathbf{h}^H \hat{\Omega}_{\text{ss}} \mathbf{h}. \quad (3.64)$$

Clearly, for finite N , $\hat{\Omega}_{\text{ss}}$ will be a perturbed version of Ω_{ss} , i.e., $\hat{\Omega}_{\text{ss}} = \Omega_{\text{ss}} + \delta\Omega_{\text{ss}}$. The perturbation $\delta\Omega_{\text{ss}}$ will cause, in turn, an error in the estimated channel $\hat{\mathbf{h}}_{\text{ss}}$. In the rest of this section, we study the behaviour of the estimator in (3.64) for a finite data record size N . Specifically, by applying the small perturbation analysis technique, we show that the estimator is unbiased and we derive a closed form expression for its mean-square-error (MSE) performance.

Mean-Square-Error Performance

The MSE for subspace-based channel estimation algorithms under a general framework has been investigated in [40], [41]. The derivations, however, are based on the Singular Value Decomposition (SVD) of \mathbf{R} . In this work, we base our analysis in the context of SFBC MC-CDMA systems on the EVD of \mathbf{R} . This approach is not only consistent with the EVD-based channel estimation algorithms presented at the beginning of this section but also provides an analytical expression for the MSE that is closer approximation to its

corresponding actual MSE in low SNR than expression based on the SVD as is demonstrated in our simulation studies. The following theorem investigates the channel estimator bias and provides an analytical expression for its MSE under a small perturbation assumption.

Theorem 3 *Let $\delta\mathbf{h}_{ss} = \mathbf{h} - \hat{\mathbf{h}}_{ss}$ be the estimation error of the estimator in (3.64). Then, we have*

(i) $\mathbb{E}\{\delta\mathbf{h}_{ss}\} = \mathbf{0}$, i.e., the estimator is unbiased.

(ii) The mean-square-error (MSE) $\mathbb{E}\{\|\delta\mathbf{h}_{ss}\|^2\}$ is

$$\mathbb{E}\{\|\delta\mathbf{h}_{ss}\|^2\} \simeq \frac{\sigma^2}{N} (\rho_{r,r} \text{tr}\{\Sigma_r \Sigma_r^H\} + \rho_{r,i} \text{tr}\{\Sigma_r \Sigma_i^H\} + \rho_{i,r} \text{tr}\{\Sigma_i \Sigma_r^H\} + \rho_{i,i} \text{tr}\{\Sigma_i \Sigma_i^H\}),$$

where $\Sigma_r \triangleq \Omega_{ss}^\dagger \mathbf{S}_{1,r}^H \mathbf{Q}_n$, $\Sigma_i \triangleq \Omega_{ss}^\dagger \mathbf{S}_{1,i}^H \mathbf{Q}_n$ and the scalars $\rho_{r,r}, \rho_{r,i}, \rho_{i,r}$, and $\rho_{i,i}$ are, respectively, given by

$$\begin{aligned} \rho_{r,r} &= \mathbf{h}^H \mathbf{S}_{1,r}^H \Upsilon^\dagger \mathbf{R} \Upsilon \mathbf{S}_{1,r} \mathbf{h}, & \rho_{r,i} &= \mathbf{h}^H \mathbf{S}_{1,r}^H \Upsilon^\dagger \mathbf{R} \Upsilon \mathbf{S}_{1,i} \mathbf{h}, \\ \rho_{i,r} &= \mathbf{h}^H \mathbf{S}_{1,i}^H \Upsilon^\dagger \mathbf{R} \Upsilon \mathbf{S}_{1,r} \mathbf{h}, & \rho_{i,i} &= \mathbf{h}^H \mathbf{S}_{1,i}^H \Upsilon^\dagger \mathbf{R} \Upsilon \mathbf{S}_{1,i} \mathbf{h}. \end{aligned} \quad (3.65)$$

with $\Upsilon \triangleq \mathbf{Q}_s (\Lambda_s - \sigma^2 \mathbf{I}) \mathbf{Q}_s^H$.

Proof: Due to finite data samples, the imperfect estimation of \mathbf{R} introduces an estimation error $\delta\mathbf{R}$ in $\hat{\mathbf{R}}$, i.e., $\hat{\mathbf{R}} \triangleq \mathbf{R} + \delta\mathbf{R}$. This, in turn, results in perturbations of the estimated subspace \mathbf{Q}_n and the channel vector. In [50], it is shown that the first-order perturbation expansion can be used to get a linear approximation to the perturbations in the noise subspace and channel estimate, respectively, as

$$\delta\mathbf{Q}_n \simeq -\Upsilon^\dagger \delta\mathbf{R} \mathbf{Q}_n, \quad (3.66)$$

$$\delta\mathbf{h}_{ss} \triangleq \hat{\mathbf{h}}_{ss} - \mathbf{h} \simeq -\Omega_{ss}^\dagger \delta\Omega_{ss} \mathbf{h}, \quad (3.67)$$

where

$$\Upsilon \triangleq \mathbf{Q}_s (\Lambda_s - \sigma^2 \mathbf{I}) \mathbf{Q}_s^H.$$

According to (3.36), a perturbation in estimating \mathbf{Q}_n results in perturbation of Ω_{ss} equal to

$$\delta\Omega_{ss} \simeq \mathbf{S}_{1,r}^H (\delta\mathbf{Q}_n \mathbf{Q}_n^H + \mathbf{Q}_n \delta\mathbf{Q}_n^H) \mathbf{S}_{1,r} + \mathbf{S}_{1,i}^H (\delta\mathbf{Q}_n \mathbf{Q}_n^H + \mathbf{Q}_n \delta\mathbf{Q}_n^H) \mathbf{S}_{1,i}. \quad (3.68)$$

Substituting (3.66) into (3.68), and (3.68) into (3.67), and noticing that

$$\mathbf{Q}_n^H \mathbf{S}_{1,r} \mathbf{h} = \mathbf{Q}_n^H \mathbf{S}_{1,i} \mathbf{h} = 0,$$

we obtain

$$\delta \mathbf{h}_{\text{SS}} \simeq \Omega_{\text{SS}}^\dagger \mathbf{S}_{1,r}^H \mathbf{Q}_n \mathbf{Q}_n^H \delta \mathbf{R} \Upsilon^\dagger \mathbf{S}_{1,r} \mathbf{h} + \Omega_{\text{SS}}^\dagger \mathbf{S}_{1,i}^H \mathbf{Q}_n \mathbf{Q}_n^H \delta \mathbf{R} \Upsilon^\dagger \mathbf{S}_{1,i} \mathbf{h}. \quad (3.69)$$

From (3.69), we can see that $\delta \mathbf{h}_{\text{SS}}$ is linearly related to $\delta \mathbf{R}$. Considering the fact that $\hat{\mathbf{R}}$ is an unbiased estimate of \mathbf{R} , i.e., $\mathbb{E}\{\delta \mathbf{R}\} = 0$, (3.69) implies that the bias of the estimated channel vector is zero: $\mathbb{E}\{\delta \mathbf{h}_{\text{SS}}\} = 0$. This proves part (i) of the Theorem.

To prove part (ii), we first evaluate the covariance of $\delta \mathbf{h}_{\text{SS}}$. To keep the notation brief, we will define two matrices:

$$\Sigma_r = \Omega_{\text{SS}}^\dagger \mathbf{S}_{1,r}^H \mathbf{Q}_n \quad (3.70)$$

$$\Sigma_i = \Omega_{\text{SS}}^\dagger \mathbf{S}_{1,i}^H \mathbf{Q}_n. \quad (3.71)$$

Then, the covariance of $\delta \mathbf{h}_{\text{SS}}$ can be written as

$$\begin{aligned} \mathbb{E}\{\delta \mathbf{h}_{\text{SS}} \delta \mathbf{h}_{\text{SS}}^H\} &\simeq \Sigma_r \mathbf{Q}_n^H \mathbb{E}\{\delta \mathbf{R} \Upsilon^\dagger \mathbf{S}_{1,r} \mathbf{h} \mathbf{h}^H \mathbf{S}_{1,r}^H \Upsilon \delta \mathbf{R}\} \mathbf{Q}_n \Sigma_r^H \\ &\quad + \Sigma_r \mathbf{Q}_n^H \mathbb{E}\{\delta \mathbf{R} \Upsilon^\dagger \mathbf{S}_{1,r} \mathbf{h} \mathbf{h}^H \mathbf{S}_{1,i}^H \Upsilon \delta \mathbf{R}\} \mathbf{Q}_n \Sigma_i^H \\ &\quad + \Sigma_i \mathbf{Q}_n^H \mathbb{E}\{\delta \mathbf{R} \Upsilon^\dagger \mathbf{S}_{1,i} \mathbf{h} \mathbf{h}^H \mathbf{S}_{1,r}^H \Upsilon \delta \mathbf{R}\} \mathbf{Q}_n \Sigma_r^H \\ &\quad + \Sigma_i \mathbf{Q}_n^H \mathbb{E}\{\delta \mathbf{R} \Upsilon^\dagger \mathbf{S}_{1,i} \mathbf{h} \mathbf{h}^H \mathbf{S}_{1,i}^H \Upsilon \delta \mathbf{R}\} \mathbf{Q}_n \Sigma_i^H. \end{aligned} \quad (3.72)$$

For a multirate CDMA system, it is shown in [51] that the expectation of the quantity $\delta \mathbf{R} \mathbf{Z} \delta \mathbf{R}$ for an arbitrary matrix \mathbf{Z} can be evaluated. Applying the results in [51] to (3.72), we obtain the following closed form expression for the MSE:

$$\mathbb{E}\{\|\delta \mathbf{h}_{\text{SS}}\|^2\} \simeq \frac{\sigma^2}{N} (\rho_{r,r} \text{tr}\{\Sigma_r \Sigma_r^H\} + \rho_{r,i} \text{tr}\{\Sigma_r \Sigma_i^H\} + \rho_{i,r} \text{tr}\{\Sigma_i \Sigma_r^H\} + \rho_{i,i} \text{tr}\{\Sigma_i \Sigma_i^H\}), \quad (3.73)$$

where $\rho_{r,r}$, $\rho_{r,i}$, $\rho_{i,r}$, and $\rho_{i,i}$ are scalars defined in (3.65). ■

The unbiasedness of the estimator implies that the MSE given by (3.65) will be lower bounded by the CRB [52] that we derive next.

3.4.4 Cramer-Rao Bound

Most existing literature on the CRB for channel estimation in CDMA systems relies on the knowledge of all the users' spreading codes [42], [43]. Obviously, this assumption is not valid in the downlink where the receiver has no knowledge of any other active user's signature in the system but his own. In this subsection, we are interested in deriving a CRB for the channel estimation error which makes no assumption on the spreading codes and treats them as deterministic unknown quantities. This approach is especially useful for the downlink transmissions and provides a tighter bound than the CRB derived under the assumption of known spreading codes. In fact, the Cramer-Rao Bound (CRB) can be viewed as a measure of how difficult the corresponding estimation problem is. For example, in the problem of blind and supervised (i.e., under the assumption of known transmitted symbols) channel estimation one would expect the CRB in the first case to be higher than in the second case. This is due to the fact that the use of the training sequence results in an "easier" problem since a channel estimation algorithm would not have to deal with the uncertainty on the transmitted symbols but instead could incorporate the knowledge of their exact values to improve the estimation performance. Similarly, the knowledge of all the spreading sequences results in an "easier" estimation problem in the sense that it can lead to improved performance compared to the case when only a single spreading sequence is known. Therefore, we would expect that knowledge of all the spreading sequences should yield a lower CRB which would be a looser bound for algorithms that assume knowledge of only one spreading sequence compared to a CRB derived under the same assumption. Finally, we note that our derivation is based on a deterministic model for the transmitted symbols. This latter assumption leads to a CRB that is less tight than that obtained under a stochastic assumption on the transmitted symbols. However, the difference between the deterministic model versus the stochastic model is not considerable [53].

Treating the transmitted symbols as nuisance parameters, the likelihood and log-likelihood functions for N consecutive received blocks are, respectively, given by

$$L(\mathbf{r}(1), \dots, \mathbf{r}(N); \boldsymbol{\theta}) = (\pi\sigma^2)^{-PN} \exp \left\{ -\frac{1}{\sigma^2} \sum_{n=1}^N \left\| \mathbf{r}(n) - \sum_{k=1}^K (\mathbf{S}_{k,r} \mathbf{h} \Re(b_k(n)) + \mathbf{S}_{k,i} \mathbf{h} \Im(b_k(n))) \right\|^2 \right\}, \quad (3.74)$$

and

$$\mathcal{L} \triangleq \ln L(\mathbf{r}(1), \dots, \mathbf{r}(N); \boldsymbol{\theta}) = -PN \ln(\pi\sigma^2) - \frac{1}{\sigma^2} \sum_{n=1}^N \left\| \mathbf{r}(n) - \sum_{k=1}^K \left(\mathbf{S}_{k,r} \mathbf{h} \Re(b_k(n)) + \mathbf{S}_{k,i} \mathbf{h} \Im(b_k(n)) \right) \right\|^2. \quad (3.75)$$

where $\boldsymbol{\theta} \triangleq [\boldsymbol{\theta}_b^T, \boldsymbol{\theta}_s^T, \boldsymbol{\theta}_h^T]^T$, is a real vector of length $2KN + 4J + (K-1)L$ and denotes the set of unknown deterministic parameters with

$$\begin{aligned} \mathbf{b}(n) &\triangleq [b_1(n), b_2(n), \dots, b_K(n)]^T, n = 1, 2, \dots, N; \\ \boldsymbol{\theta}_h &\triangleq [\Re(\mathbf{h}_1)^T, \Im(\mathbf{h}_1)^T, \Re(\mathbf{h}_2)^T, \Im(\mathbf{h}_2)^T]^T; \\ \boldsymbol{\theta}_b &\triangleq [\Re(\mathbf{b}(1))^T, \Im(\mathbf{b}(1))^T, \dots, \Re(\mathbf{b}(N))^T, \Im(\mathbf{b}(N))^T]^T; \\ \boldsymbol{\theta}_s &\triangleq [\mathbf{s}_2^T, \dots, \mathbf{s}_K^T]^T. \end{aligned} \quad (3.76)$$

Denoting by $\hat{\boldsymbol{\theta}}$ any unbiased estimator of the vector $\boldsymbol{\theta}$, the CRB provides a lower bound on the variance of the unbiased $\boldsymbol{\theta}$ estimate, i.e.,

$$\mathbb{E} \left\{ (\hat{\boldsymbol{\theta}} - \boldsymbol{\theta})(\hat{\boldsymbol{\theta}} - \boldsymbol{\theta})^T \right\} \geq \text{CRB}(\boldsymbol{\theta}) = \text{diag}(\mathbf{J}_{\boldsymbol{\theta}\boldsymbol{\theta}})^{-1}, \quad (3.77)$$

where $\mathbf{J}_{\boldsymbol{\theta}\boldsymbol{\theta}}$ is the Fisher information matrix (FIM) for the parameter vector $\boldsymbol{\theta}$ given by

$$\mathbf{J}_{\boldsymbol{\theta}\boldsymbol{\theta}} \triangleq \mathbb{E} \left\{ \left(\frac{\partial \mathcal{L}}{\partial \boldsymbol{\theta}} \right) \left(\frac{\partial \mathcal{L}}{\partial \boldsymbol{\theta}} \right)^T \right\} = \begin{bmatrix} \mathbf{J}_{bb} & \mathbf{J}_{bs} & \mathbf{J}_{bh} \\ \mathbf{J}_{bs}^T & \mathbf{J}_{ss} & \mathbf{J}_{sh} \\ \mathbf{J}_{bh}^T & \mathbf{J}_{sh}^T & \mathbf{J}_{hh} \end{bmatrix}. \quad (3.78)$$

In order to evaluate the elements of the FIM in (3.78), we first compute the partial derivatives of log-likelihood function in (3.75) with respect to $\boldsymbol{\theta}$ to obtain

$$\frac{\partial \mathcal{L}(\mathbf{r})}{\partial \boldsymbol{\theta}} = \left[\left(\frac{\partial \mathcal{L}(\mathbf{r})}{\partial \Re(\mathbf{b}(p))} \right)^T, \left(\frac{\partial \mathcal{L}(\mathbf{r})}{\partial \Im(\mathbf{b}(p))} \right)^T, \left(\frac{\partial \mathcal{L}(\mathbf{r})}{\partial \Re(\mathbf{h})} \right)^T, \left(\frac{\partial \mathcal{L}(\mathbf{r})}{\partial \Im(\mathbf{h})} \right)^T, \left(\frac{\partial \mathcal{L}(\mathbf{r})}{\partial \tilde{\mathbf{S}}} \right)^T \right]^T,$$

where

$$\frac{\partial \mathcal{L}(\mathbf{r})}{\partial \Re(\mathbf{b}(p))} = \frac{2}{\sigma^2} \Re(\mathbf{G}_r^H \mathbf{n}(p)), \quad (3.79)$$

$$\frac{\partial \mathcal{L}(\mathbf{r})}{\partial \Im(\mathbf{b}(p))} = \frac{2}{\sigma^2} \Re(\mathbf{G}_i^H \mathbf{n}(p)), \quad (3.80)$$

$$\frac{\partial \mathcal{L}(\mathbf{r})}{\partial \Re(\mathbf{h})} = \frac{2}{\sigma^2} \sum_{p=1}^N \sum_{k=1}^K \Re(\mathcal{G}_k(p)^H \mathbf{n}(p)), \quad (3.81)$$

$$\frac{\partial \mathcal{L}(\mathbf{r})}{\partial \Im(\mathbf{h})} = \frac{2}{\sigma^2} \sum_{p=1}^N \sum_{k=1}^K \Re(-j \mathcal{G}_k(p)^H \mathbf{n}(p)), \quad (3.82)$$

$$\frac{\partial \mathcal{L}(\mathbf{r})}{\partial \mathbf{s}_k} = \frac{2}{\sigma^2} \sum_{p=1}^N \Re(\mathcal{T}_k(p)^H \mathbf{n}(p)) \quad k = 2, \dots, K, \quad (3.83)$$

with

$$\mathcal{T}_k(p) \triangleq (\mathbf{H}_1 \mathbf{F}^H \mathbf{D}_1 + \mathbf{H}_2 \mathbf{F}^H \mathbf{D}_3) \Re(b_k(p)) + (\mathbf{H}_1 \mathbf{F}^H \mathbf{D}_2 + \mathbf{H}_2 \mathbf{F}^H \mathbf{D}_4) \Im(b_k(p)),$$

$$\mathcal{G}_k(p) \triangleq \mathbf{S}_{k,r} \Re(b_k(p)) + \mathbf{S}_{k,i} \Im(b_k(p)),$$

$$\mathbf{G}_r \triangleq [\mathbf{g}_{1,r} \ \mathbf{g}_{2,r} \ \dots \ \mathbf{g}_{K,r}],$$

$$\mathbf{G}_i \triangleq [\mathbf{g}_{1,i} \ \mathbf{g}_{2,i} \ \dots \ \mathbf{g}_{K,i}],$$

$$\tilde{\mathbf{S}} = [\mathbf{s}_2, \dots, \mathbf{s}_K].$$

The elements of the FIM can then be calculated as

$$\mathbb{E} \left\{ \frac{\partial \mathcal{L}(\mathbf{r})}{\partial \Re(\mathbf{b}(p))} \left(\frac{\partial \mathcal{L}(\mathbf{r})}{\partial \Re(\mathbf{b}(q))} \right)^T \right\} = \frac{2}{\sigma^2} \Re(\mathbf{G}_r^H \mathbf{G}_r) \triangleq \tilde{\pi}_r \delta_{p,q} \quad (3.84)$$

$$\mathbb{E} \left\{ \frac{\partial \mathcal{L}(\mathbf{r})}{\partial \Re(\mathbf{b}(p))} \left(\frac{\partial \mathcal{L}(\mathbf{r})}{\partial \Im(\mathbf{b}(q))} \right)^T \right\} = \frac{2}{\sigma^2} \Re(\mathbf{G}_r^H \mathbf{G}_i) \triangleq \tilde{\pi}_r \delta_{p,q} \quad (3.85)$$

$$\mathbb{E} \left\{ \frac{\partial \mathcal{L}(\mathbf{r})}{\partial \Im(\mathbf{b}(p))} \left(\frac{\partial \mathcal{L}(\mathbf{r})}{\partial \Re(\mathbf{b}(q))} \right)^T \right\} = \frac{2}{\sigma^2} \Re(\mathbf{G}_i^H \mathbf{G}_r) \triangleq \tilde{\pi}_i \delta_{p,q} \quad (3.86)$$

$$\mathbb{E} \left\{ \frac{\partial \mathcal{L}(\mathbf{r})}{\partial \Im(\mathbf{b}(p))} \left(\frac{\partial \mathcal{L}(\mathbf{r})}{\partial \Im(\mathbf{b}(q))} \right)^T \right\} = \frac{2}{\sigma^2} \Re(\mathbf{G}_i^H \mathbf{G}_i) \triangleq \tilde{\pi}_i \delta_{p,q} \quad (3.87)$$

$$\mathbb{E} \left\{ \frac{\partial \mathcal{L}(\mathbf{r})}{\partial \Re(\mathbf{b}(p))} \left(\frac{\partial \mathcal{L}(\mathbf{r})}{\partial \mathbf{s}_k} \right)^T \right\} = \frac{2}{\sigma^2} \Re(\mathbf{G}_r^H \mathbf{T}_k(p)) \triangleq \mathcal{D}_{k,r}(p) \quad (3.88)$$

$$\mathbb{E} \left\{ \frac{\partial \mathcal{L}(\mathbf{r})}{\partial \Im(\mathbf{b}(p))} \left(\frac{\partial \mathcal{L}(\mathbf{r})}{\partial \mathbf{s}_k} \right)^T \right\} = \frac{2}{\sigma^2} \Re(\mathbf{G}_i^H \mathbf{T}_k(p)) \triangleq \mathcal{D}_{k,i}(p) \quad (3.89)$$

$$\mathbb{E} \left\{ \frac{\partial \mathcal{L}(\mathbf{r})}{\partial \Re(\mathbf{b}(p))} \left(\frac{\partial \mathcal{L}(\mathbf{r})}{\partial \Re(\mathbf{h})} \right)^T \right\} = \frac{2}{\sigma^2} \sum_{k=1}^K \Re(\mathbf{G}_r^H \mathcal{G}_k(p)) \triangleq \bar{\xi}_r(p) \quad (3.90)$$

$$\mathbb{E} \left\{ \frac{\partial \mathcal{L}(\mathbf{r})}{\partial \Re(\mathbf{b}(p))} \left(\frac{\partial \mathcal{L}(\mathbf{r})}{\partial \Im(\mathbf{h})} \right)^T \right\} = \frac{2}{\sigma^2} \sum_{k=1}^K \Re(j \mathbf{G}_r^H \mathcal{G}_k(p)) \triangleq \tilde{\xi}_r(p) \quad (3.91)$$

$$\mathbb{E} \left\{ \frac{\partial \mathcal{L}(\mathbf{r})}{\partial \Im(\mathbf{b}(p))} \left(\frac{\partial \mathcal{L}(\mathbf{r})}{\partial \Re(\mathbf{h})} \right)^T \right\} = \frac{2}{\sigma^2} \sum_{k=1}^K \Re(\mathbf{G}_i^H \mathcal{G}_k(p)) \triangleq \bar{\xi}_i(p) \quad (3.92)$$

$$\mathbb{E} \left\{ \frac{\partial \mathcal{L}(\mathbf{r})}{\partial \Im(\mathbf{b}(p))} \left(\frac{\partial \mathcal{L}(\mathbf{r})}{\partial \Im(\mathbf{h})} \right)^T \right\} = \frac{2}{\sigma^2} \sum_{k=1}^K \Re(j \mathbf{G}_i^H \mathcal{G}_k(p)) \triangleq \tilde{\xi}_i(p) \quad (3.93)$$

$$\mathbb{E} \left\{ \frac{\partial \mathcal{L}(\mathbf{r})}{\partial \mathbf{s}_k} \left(\frac{\partial \mathcal{L}(\mathbf{r})}{\partial \mathbf{s}_{k'}} \right)^T \right\} = \frac{2}{\sigma^2} \sum_{p=1}^N \Re(\mathbf{T}_k(p)^H \mathbf{T}_{k'}(p)) \triangleq \mathcal{S}_{k,k'} \quad (3.94)$$

$$\mathbb{E} \left\{ \frac{\partial \mathcal{L}(\mathbf{r})}{\partial \mathbf{s}_k} \left(\frac{\partial \mathcal{L}(\mathbf{r})}{\partial \Re(\mathbf{h})} \right)^T \right\} = \frac{2}{\sigma^2} \sum_{p=1}^N \Re(\mathbf{T}_k(p)^H \mathcal{G}_k(p)) \triangleq \psi_{k,r} \quad (3.95)$$

$$\mathbb{E} \left\{ \frac{\partial \mathcal{L}(\mathbf{r})}{\partial \mathbf{s}_k} \left(\frac{\partial \mathcal{L}(\mathbf{r})}{\partial \Im(\mathbf{h})} \right)^T \right\} = \frac{2}{\sigma^2} \sum_{p=1}^N \Re(j \mathbf{T}_k(p)^H \mathcal{G}_k(p)) \triangleq \psi_{k,i} \quad (3.96)$$

$$\mathbb{E} \left\{ \frac{\partial \mathcal{L}(\mathbf{r})}{\partial \Re(\mathbf{h})} \left(\frac{\partial \mathcal{L}(\mathbf{r})}{\partial \Re(\mathbf{h})} \right)^T \right\} = \frac{2}{\sigma^2} \sum_{p=1}^N \sum_{k=1}^K \Re(\mathcal{G}_k(p)^H \mathcal{G}_k(p)) \triangleq \bar{\phi} \quad (3.97)$$

$$\mathbb{E} \left\{ \frac{\partial \mathcal{L}(\mathbf{r})}{\partial \Re(\mathbf{h})} \left(\frac{\partial \mathcal{L}(\mathbf{r})}{\partial \Im(\mathbf{h})} \right)^T \right\} = \frac{2}{\sigma^2} \sum_{p=1}^N \sum_{k=1}^K \Re(j \mathcal{G}_k(p)^H \mathcal{G}_k(p)) \triangleq \tilde{\phi} \quad (3.98)$$

$$\mathbb{E} \left\{ \frac{\partial \mathcal{L}(\mathbf{r})}{\partial \Im(\mathbf{h})} \left(\frac{\partial \mathcal{L}(\mathbf{r})}{\partial \Re(\mathbf{h})} \right)^T \right\} = \frac{2}{\sigma^2} \sum_{p=1}^N \sum_{k=1}^K \Re(-j \mathcal{G}_k(p)^H \mathcal{G}_k(p)) \triangleq -\tilde{\phi} \quad (3.99)$$

$$\mathbb{E} \left\{ \frac{\partial \mathcal{L}(\mathbf{r})}{\partial \Im(\mathbf{h})} \left(\frac{\partial \mathcal{L}(\mathbf{r})}{\partial \Im(\mathbf{h})} \right)^T \right\} = \frac{2}{\sigma^2} \sum_{p=1}^N \sum_{k=1}^K \Re(\mathcal{G}_k(p)^H \mathcal{G}_k(p)) \triangleq \bar{\phi} \quad (3.100)$$

Let us define the following block matrices:

$$\begin{aligned} \mathbf{\Pi} &\triangleq \begin{bmatrix} \bar{\pi}_r & \tilde{\pi}_r \\ \bar{\pi}_i & \tilde{\pi}_i \end{bmatrix}, \mathbf{D}(p) \triangleq \begin{bmatrix} \mathcal{D}_{2,r}(p) & \dots & \mathcal{D}_{K,r}(p) \\ \mathcal{D}_{2,i}(p) & \dots & \mathcal{D}_{K,i}(p) \end{bmatrix}, \mathbf{\Xi}(n) \triangleq \begin{bmatrix} \bar{\xi}_r(n) & \tilde{\xi}_r(n) \\ \bar{\xi}_i(n) & \tilde{\xi}_i(n) \end{bmatrix}, \\ \mathbf{\Psi} &\triangleq \begin{bmatrix} \psi_{2,r}^T & \dots & \psi_{K,r}^T \\ \psi_{2,i}^T & \dots & \psi_{K,i}^T \end{bmatrix}^T, \mathbf{\Phi} \triangleq \begin{bmatrix} \bar{\phi} & \tilde{\phi} \\ -\tilde{\phi} & \bar{\phi} \end{bmatrix}, \mathbf{S} \triangleq \begin{bmatrix} \mathcal{S}_{2,2} & \dots & \mathcal{S}_{2,K} \\ \vdots & \dots & \vdots \\ \mathcal{S}_{K,2} & \dots & \mathcal{S}_{K,K} \end{bmatrix}. \end{aligned} \quad (3.101)$$

Assembling the equations (3.84)-(3.101) results in the following FIM:

$$\mathbf{J}_{\theta\theta} \triangleq \begin{array}{c|ccc|cc} \mathbf{\Pi} & \mathbf{0} & \dots & \mathbf{0} & \mathbf{D}(1) & \mathbf{\Xi}(1) \\ \mathbf{0} & \mathbf{\Pi} & \dots & \mathbf{0} & \mathbf{D}(2) & \mathbf{\Xi}(2) \\ \vdots & \vdots & \ddots & \vdots & \vdots & \vdots \\ \mathbf{0} & \mathbf{0} & \dots & \mathbf{\Pi} & \mathbf{D}(N) & \mathbf{\Xi}(N) \\ \hline \mathbf{D}^T(1) & \mathbf{D}^T(2) & \dots & \mathbf{D}^T(N) & \mathbf{S} & \mathbf{\Psi} \\ \hline \mathbf{\Xi}^T(1) & \mathbf{\Xi}^T(2) & \dots & \mathbf{\Xi}^T(N) & \mathbf{\Psi}^T & \mathbf{\Phi} \end{array}. \quad (3.102)$$

Finally, the submatrices \mathbf{J}_{bb} , \mathbf{J}_{bs} , \mathbf{J}_{bh} , \mathbf{J}_{ss} , \mathbf{J}_{sh} , and \mathbf{J}_{hh} in (3.78) have dimensions $2KN \times 2KN$, $2KN \times (K-1)L$, $2KN \times 4J$, $(K-1)L \times (K-1)L$, $(K-1)L \times 4J$, $4J \times 4J$, respectively, and are defined as

$$\begin{aligned} \mathbf{J}_{\text{bs}} &\triangleq [\mathbf{D}(1)^T, \dots, \mathbf{D}(N)^T]^T, & \mathbf{J}_{\text{bb}} &\triangleq \mathbf{I}_N \otimes \mathbf{\Pi}, & \mathbf{J}_{\text{ss}} &\triangleq \mathbf{S}, \\ \mathbf{J}_{\text{bh}} &\triangleq [\mathbf{\Xi}(1)^T, \dots, \mathbf{\Xi}(N)^T]^T, & \mathbf{J}_{\text{sh}} &\triangleq \mathbf{\Psi}, & \mathbf{J}_{\text{hh}} &\triangleq \mathbf{\Phi}, \end{aligned} \quad (3.103)$$

Using the block matrix inversion formula and forming the Schur complement of matrix \mathbf{J}_{hh} in (3.78), we obtain the following expression for the inverse CRB matrix of channel estimation:

$$\mathbf{J}(\mathbf{h}) \triangleq \mathbf{J}_{\text{hh}} - [\mathbf{J}_{\text{bh}}^T \ \mathbf{J}_{\text{sh}}^T] \begin{bmatrix} \mathbf{J}_{\text{bb}} & \mathbf{J}_{\text{bs}} \\ \mathbf{J}_{\text{bs}}^T & \mathbf{J}_{\text{ss}} \end{bmatrix}^{-1} \begin{bmatrix} \mathbf{J}_{\text{bh}} \\ \mathbf{J}_{\text{sh}} \end{bmatrix} = \text{CRB}^{-1}(\mathbf{h}). \quad (3.104)$$

In general, since the blind channel estimation is only possible up to a scalar factor, it is expected that the matrix in the RHS of (3.104) to be singular. To regularize the channel estimation problem, a set of constraints should be imposed on the channel. In this work, instead of applying constraints on the channel, we choose to form the CRB by taking

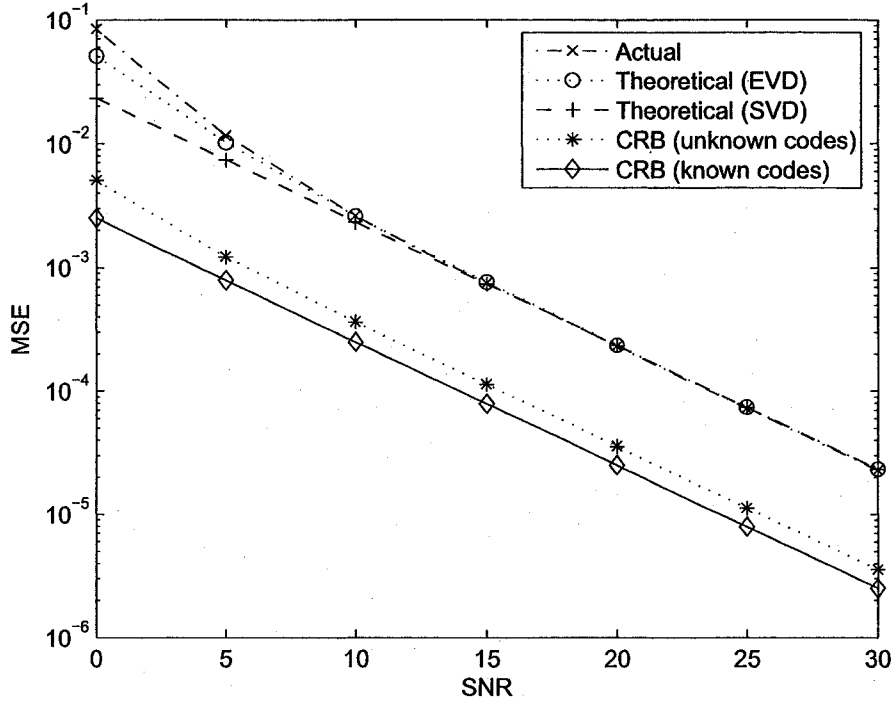


Fig. 3.7 The MSE as a function of the SNR.

the Moore-Penrose-inverse of the FIM. The latter corresponds to the application of the minimum number of independent constraints [54]. Then, we have

$$\text{CRB}(\mathbf{h}) = \left(\mathbf{J}_{\text{hh}} - [\mathbf{J}_{\text{bh}}^T \ \mathbf{J}_{\text{sh}}^T] \begin{bmatrix} \mathbf{J}_{\text{bb}} & \mathbf{J}_{\text{bs}} \\ \mathbf{J}_{\text{bs}}^T & \mathbf{J}_{\text{ss}} \end{bmatrix}^{-1} \begin{bmatrix} \mathbf{J}_{\text{bh}} \\ \mathbf{J}_{\text{sh}} \end{bmatrix} \right)^\dagger \quad (3.105)$$

3.4.5 Simulations Studies

We consider a MC-CDMA system with 6 users utilizing code sequences of length⁷ 32 which is also the number of subcarriers. We use zero padding of length 8 which is 1/4th of the FFT size. A data record of $N = 200$ samples is used for estimating the autocorrelation matrix. The transmitter and the receiver are equipped with 2 and 1 antennas, respectively, while the SFBC employed is the orthogonal block code of [3]. Each subchannel has 3 paths each with a variance of $\sigma_c^2 = 1$. In what follows, the presented results are averages over

⁷Constructed from Gold sequences of length 31 by appending a +1.

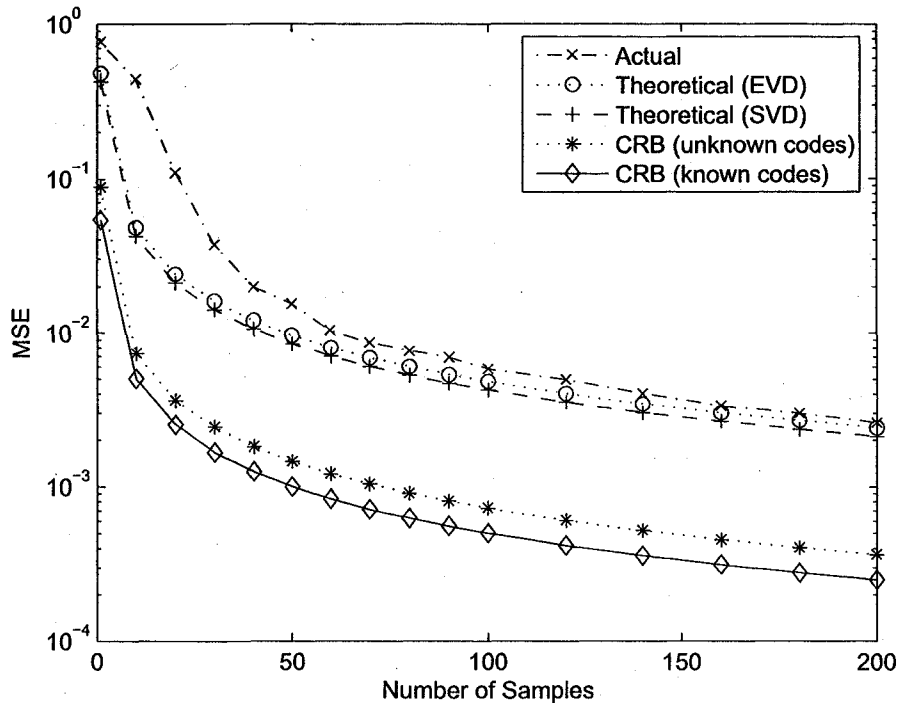


Fig. 3.8 The MSE as a function of the number of samples used for estimating the autocorrelation matrix.

100 independent channel realizations.

Fig. 3.7 depicts the MSE performance versus the SNR of all users (assumed to be the same). From Fig. 3.7, we infer that for high SNR values the analytical expressions provide good approximations to the actual MSE's obtained from simulation. Also in Fig. 3.7, we included the theoretical MSE performance based on the SVD (see [40], [41]). It can be seen that in low SNRs our MSE expression based on the EVD provides a closer approximation to the actual MSE than SVD-based expressions. In Fig. 3.8, we examine the effect of the data record size used to form the autocorrelation matrix estimate in (3.29) on the performance of the subspace-based method. The SNRs of all users in the system are fixed at 10dB. In both Figs. 3.7 and 3.8, we also plot the CRB along with the analytical and experimental MSE curves. As can be seen from Fig. 3.8, by increasing the data record size, there is a considerable improvement in estimation error. This was expected because the subspace algorithms rely heavily on the good estimate of the autocorrelation matrix.

In order to examine whether the subspace algorithm is able to approach the CRB in

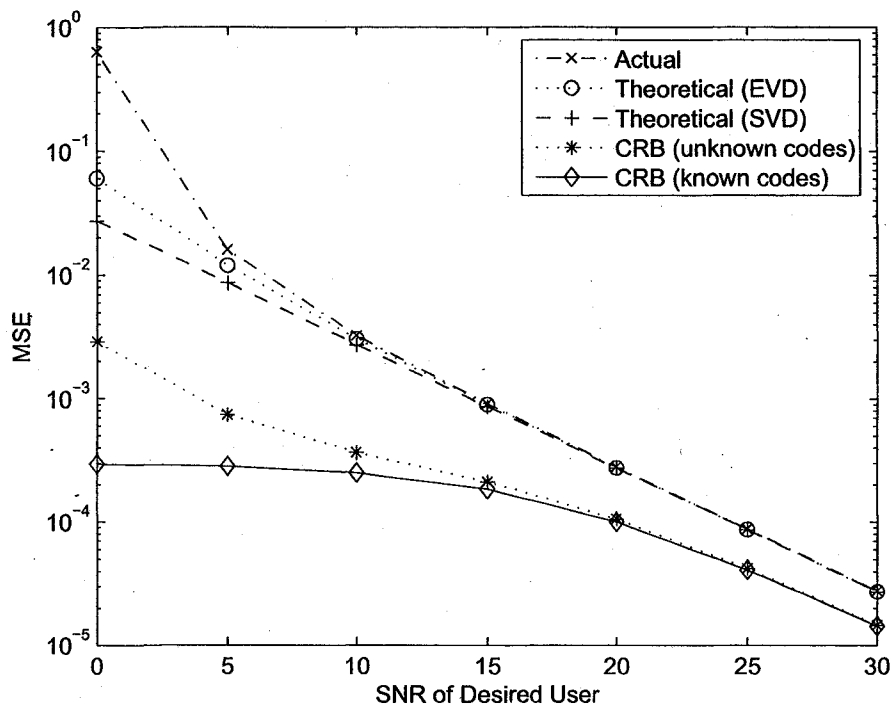


Fig. 3.9 The MSE as a function of the SNR of the desired user.

large SNRs, we plot in Fig. 3.9 the MSE performance versus the SNR of the desired user. For this experiment, all other users in the system are assumed to have a SNR of 10 dB. As can be seen from Figs. 3.7, 3.8, 3.9, the CRB which incorporates the knowledge of spreading codes of all users in the system always provides a looser bound than the CRB which assumes no knowledge of the interfering users' signatures. However, as it is shown in Fig. 3.9, in high SNRs both CRBs are almost identical. This can be attributed principally to the fact that as the SNR of the desired user increases the effect of the MAI and in turn the assumption of the knowledge of the interfering users' signatures becomes less significant.

Finally, to demonstrate the appropriateness of the use of the CRB with unknown signatures (i.e., providing a tighter bound on the MSE) in high interference situations, the MSE versus the number of active users is shown in Fig. 3.10, while in Fig. 3.11 the MSE performance is studied in near-far situations. The near-far situation arises when the signals from the interfering users arrive at the receiver with higher power than that of the desired one. For Fig. 3.11, the near-far ratio is defined as the ratio of the power of interfering users to the power of the desired user. The SNR of the desired user is fixed at 10dB. Figs. 3.10 and

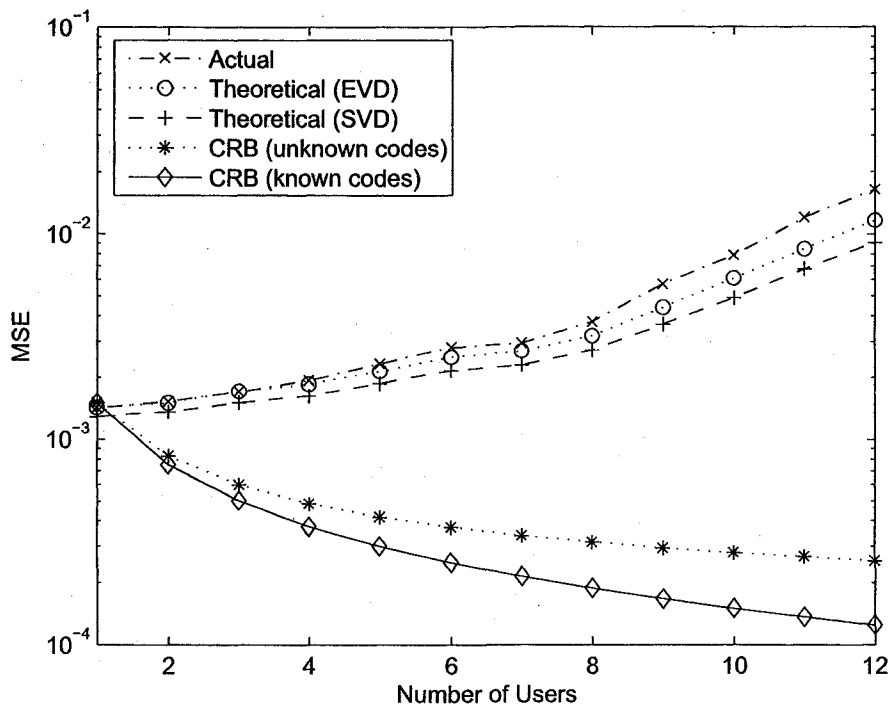


Fig. 3.10 The MSE as a function of the number of users in the system.

3.11 show that the CRB which assumes the knowledge of all signatures is a monotonically decreasing function of interference. The decreasing behaviour also illustrates that this CRB is not a meaningful benchmark for the downlink channel estimation performance. This is expected since the other users' signals are not treated as interference and are assumed to be explicitly utilized for channel estimation. On the other hand, the CRB that treats the interfering users' spreading codes as unknown deterministic quantities becomes flat for high interference levels. Also from Fig. 3.11, we see that the MSE performance of the channel estimation algorithm is insensitive to the near-far ratio. In other words, subspace-based channel estimation algorithms are near-far resistant.

3.5 MVDR-type Blind Channel Estimation

In the previous section, we studied subspace-based algorithms for blind channel identification in SFBC MC-CDMA systems. Unfortunately, the application of subspace methods is limited to the favorable communication systems such as those with light loading or mild

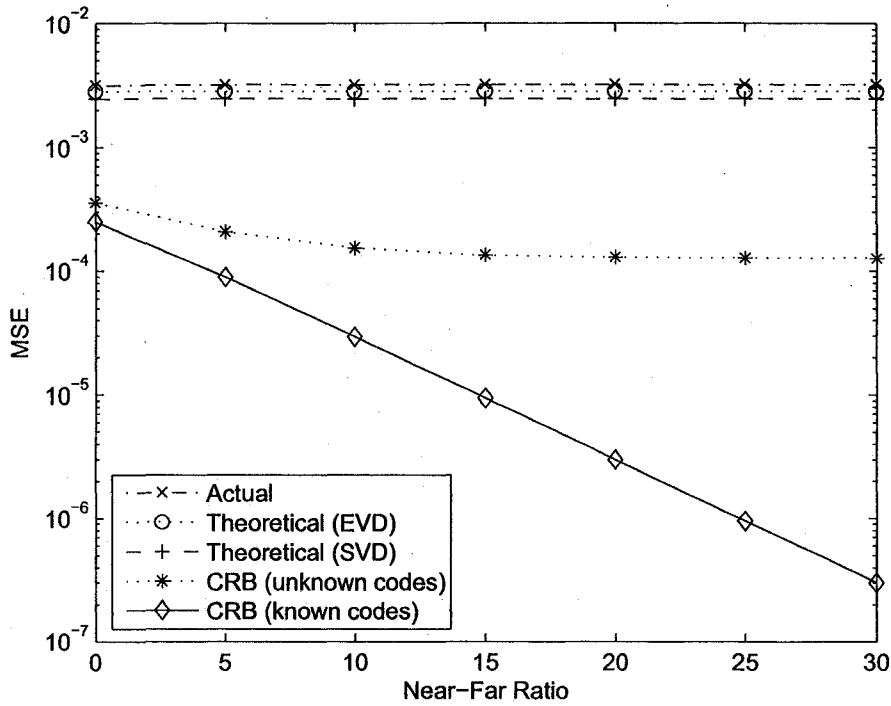


Fig. 3.11 The MSE as a function of the Near-Far Ratio.

multipath distortion. In this section, as a closely related method, we present MVDR-type channel estimation algorithms which are built on MVDR beamforming principles. As we will show, the technique significantly outperforms the subspace method in the case of medium to heavy system loading. This stems from the fact that unlike subspace approaches which rely on subspace decomposition, the MVDR algorithms are based on subspace approximation. Therefore, they avoid rank estimation and show robustness to system loading and other imperfectness such as channel order mismatch [55].

Consider a filterbank $\mathbf{W} \triangleq [\mathbf{w}_{mv,r} \ \mathbf{w}_{mv,i}]$ whose design is based on the MVDR approach, i.e., it is designed to minimize the sum of the variance at the output of each filter while at the same time imposes a constraint of unit-response to $\mathbf{g}_{1,r}$ and $\mathbf{g}_{1,i}$ [24], i.e.,

$$\begin{aligned} \mathbf{W}_{\min} = \arg \min_{\mathbf{W} \in \mathbb{C}^{P \times 2}} \text{tr}(\mathbf{W}^H \mathbf{R} \mathbf{W}), \quad \text{subject to} \\ \mathbf{w}_{mv,r}^H \mathbf{g}_{1,r} = 1 \quad \text{and} \quad \mathbf{w}_{mv,i}^H \mathbf{g}_{1,i} = 1 \end{aligned} \quad (3.106)$$

It can be shown that the minimum overall output power of the filterbank as a function of

the channel vector \mathbf{h} is given by

$$\mathcal{V}(\mathbf{h}) = (\mathbf{h}^H \mathbf{S}_{1,r}^H \mathbf{R}^{-1} \mathbf{S}_{1,r} \mathbf{h})^{-1} + (\mathbf{h}^H \mathbf{S}_{1,i}^H \mathbf{R}^{-1} \mathbf{S}_{1,i} \mathbf{h})^{-1}. \quad (3.107)$$

In the MVDR method we estimate the channel vector \mathbf{h} by maximizing the overall output variance in (3.107). Note that $\mathcal{V}(\mathbf{h})$ in (3.107) is a nonlinear function of \mathbf{h} . Therefore, rather than maximizing (3.107), we follow the common approach of solving the following minimization problem [16]:

$$\mathbf{h}_{\text{mv}} = \arg \min_{\mathbf{h}, \|\mathbf{h}\|=1} \mathbf{h}^H (\mathbf{S}_{1,r}^H \mathbf{R}^{-1} \mathbf{S}_{1,r} + \mathbf{S}_{1,i}^H \mathbf{R}^{-1} \mathbf{S}_{1,i}) \mathbf{h}. \quad (3.108)$$

In particular, the estimated channel vector is identified as the eigenvector that corresponds to the minimum eigenvalue of the $2J \times 2J$ matrix $\mathbf{\Omega}_{\text{mv}}$ given by

$$\mathbf{\Omega}_{\text{mv}} \triangleq \mathbf{S}_{1,r}^H \mathbf{R}^{-1} \mathbf{S}_{1,r} + \mathbf{S}_{1,i}^H \mathbf{R}^{-1} \mathbf{S}_{1,i}. \quad (3.109)$$

The issue of existence and uniqueness of the MVDR-type channel estimate has been addressed in [24], [16]. The following theorem states a sufficient condition for the problem under consideration which guarantees the channel vector to be identifiable up to a complex scalar. The proof is similar to that of Theorem 2.

Theorem 4 *A sufficient condition for the channel vector \mathbf{h}_{mv} in (3.108) to be uniquely identifiable up to an unknown complex scalar is that the following matrix has full column rank:*

$$\mathbf{\Gamma} \triangleq \begin{bmatrix} \mathbf{S}_{1,r} & \tilde{\mathbf{G}} & \mathbf{0} \\ \mathbf{S}_{1,i} & \mathbf{0} & \bar{\mathbf{G}} \end{bmatrix} \quad (3.110)$$

where

$$\tilde{\mathbf{G}} \triangleq [\mathbf{g}_{2,r} \ \cdots \ \mathbf{g}_{K,r} \ \mathbf{g}_{1,i} \ \mathbf{g}_{2,i} \ \cdots \ \mathbf{g}_{K,i}], \quad (3.111)$$

$$\bar{\mathbf{G}} \triangleq [\mathbf{g}_{1,r} \ \mathbf{g}_{2,r} \ \cdots \ \mathbf{g}_{K,r} \ \mathbf{g}_{2,i} \ \cdots \ \mathbf{g}_{K,i}]. \quad (3.112)$$

■

The above theorem implies that since $\mathbf{\Gamma}$ in (3.110) is a $2P \times 2(J + K - 1)$ matrix, for the sufficient condition to be satisfied, we should have $K \leq (P - J + 1)/2$. However, Theorem 4 does not imply that the channel is not identifiable for $K > (P - J + 1)/2$. In

fact, simulation studies presented later show that the MVDR estimator can provide reliable channel estimates even for $K > (P - J + 1)/2$. This is in contrast to the subspace approach in which for $K > (P - J + 1)/2$ the noise subspace does not exist at all and the subspace algorithm is not applicable. Another advantage of the MVDR algorithm is that unlike subspace methods, there is no need for the number of users to be estimated.

As we mentioned, in practice, the ensemble average of the received signal autocorrelation matrix \mathbf{R} is not known and is replaced by $\hat{\mathbf{R}}$. Then, the channel vector estimate $\hat{\mathbf{h}}$ is obtained as the eigenvector that corresponds to the smallest eigenvalue of the matrix $\hat{\Omega}_{mv}$ given by

$$\hat{\Omega}_{mv} \triangleq \mathbf{S}_{1,r}^H \hat{\mathbf{R}}^{-1} \mathbf{S}_{1,r} + \mathbf{S}_{1,i}^H \hat{\mathbf{R}}^{-1} \mathbf{S}_{1,i}. \quad (3.113)$$

In other words,

$$\hat{\mathbf{h}}_{mv} = \arg \min_{\mathbf{h}, \|\mathbf{h}\|=1} \mathbf{h}^H \hat{\Omega}_{mv} \mathbf{h}. \quad (3.114)$$

3.5.1 Performance Analysis

It is expected that in practical scenarios the performance of the MVDR channel estimator, as for many other blind channel estimation techniques, to be subject to various sources of degradation such as background noise, finite data samples, unknown channel order, etc. Thus, performance prediction under those errors is necessary to better evaluate the robustness of the method. In this subsection, we study the performance of the MVDR-based channel estimation techniques under sufficiently large data record size and small noise assumptions which result in small perturbations to \mathbf{R} . More specifically, we first evaluate the bias of the estimator due to the noise assuming that perfect knowledge of \mathbf{R} is available. Then, we study the variance of the estimator caused by replacing \mathbf{R} with its sample average estimate $\hat{\mathbf{R}}$.

The following theorem presents a closed form expression for the channel estimation error due to noise only. The proof is an extension of the perturbation analysis presented in [24] and is thus omitted.

Theorem 5 *Let $\mathbf{S}_{1,r}$ and $\mathbf{S}_{1,i}$ be defined by (3.7) with $k = 1$. Then, under small noise assumptions, the channel estimation bias $\Delta \mathbf{h}$ is given by*

$$\Delta \mathbf{h}_{mv} = \mathbf{h}_{mv} - \mathbf{h} \simeq -\sigma^2 \mathbf{A}_0^\dagger \mathbf{A}_1 \mathbf{h}, \quad (3.115)$$

where

$$\mathbf{A}_0 = \mathbf{S}_{1,r}^H \mathbf{Q}_n \mathbf{Q}_n^H \mathbf{S}_{1,r} + \mathbf{S}_{1,i}^H \mathbf{Q}_n \mathbf{Q}_n^H \mathbf{S}_{1,i}, \quad (3.116)$$

$$\mathbf{A}_1 = \mathbf{S}_{1,r}^H \mathbf{Q}_s \mathbf{\Lambda}_s^{-1} \mathbf{Q}_s^H \mathbf{S}_{1,r} + \mathbf{S}_{1,i}^H \mathbf{Q}_s \mathbf{\Lambda}_s^{-1} \mathbf{Q}_s^H \mathbf{S}_{1,i}. \quad (3.117)$$

■

Next, we study the behaviour of the estimator in (3.114) for a finite data record size N . Clearly, for finite N , $\widehat{\boldsymbol{\Omega}}_{mv}$ in (3.113) will be a perturbed version of $\boldsymbol{\Omega}_{mv}$, i.e., $\widehat{\boldsymbol{\Omega}}_{mv} = \boldsymbol{\Omega}_{mv} + \delta\boldsymbol{\Omega}_{mv}$. The perturbation $\delta\boldsymbol{\Omega}_{mv}$ will cause, in turn, an error in the estimated channel, i.e., $\widehat{\mathbf{h}}_{mv} = \mathbf{h}_{mv} + \delta\mathbf{h}_{mv}$. The following theorem investigates the channel estimation error between $\widehat{\mathbf{h}}_{mv}$ and \mathbf{h}_{mv} due to finite data record size and provides an analytical expression for its variance under a small perturbation assumption.

Theorem 6 *Let $\delta\mathbf{h}_{mv} = \widehat{\mathbf{h}}_{mv} - \mathbf{h}_{mv}$ and $\delta\mathbf{R} \triangleq \widehat{\mathbf{R}} - \mathbf{R}$ be the perturbation to the channel estimator $\widehat{\mathbf{h}}_{mv}$ in (3.114) and the sample-average estimate $\widehat{\mathbf{R}}$ in (3.29) due to finite data samples assumption, respectively. Then, we have*

(i)

$$\mathbb{E}\{\delta\mathbf{h}_{mv}\} = \mathbb{E}\{\boldsymbol{\Omega}_{mv}^\dagger \delta\boldsymbol{\Omega}_{mv} \mathbf{h}_{mv}\} = \mathbf{0}, \quad (3.118)$$

where $\delta\boldsymbol{\Omega}_{mv} = \mathbf{S}_{1,r}^H \mathbf{R}^{-1} \delta\mathbf{R} \mathbf{R}^{-1} \mathbf{S}_{1,r} + \mathbf{S}_{1,i}^H \mathbf{R}^{-1} \delta\mathbf{R} \mathbf{R}^{-1} \mathbf{S}_{1,i}$.

(ii) *The variance of an estimate $\widehat{\mathbf{h}}_{mv}$ is given by*

$$\begin{aligned} \mathbb{E}\{\|\delta\mathbf{h}_{mv}\|^2\} &\simeq \text{tr}\{\widetilde{\boldsymbol{\Sigma}}_r^H \mathbb{E}\{\delta\mathbf{R} \boldsymbol{\Upsilon}_{rr} \delta\mathbf{R}\} \widetilde{\boldsymbol{\Sigma}}_r\} + \text{tr}\{\widetilde{\boldsymbol{\Sigma}}_r^H \mathbb{E}\{\delta\mathbf{R} \boldsymbol{\Upsilon}_{ri} \delta\mathbf{R}\} \widetilde{\boldsymbol{\Sigma}}_i\} \\ &+ \text{tr}\{\widetilde{\boldsymbol{\Sigma}}_i^H \mathbb{E}\{\delta\mathbf{R} \boldsymbol{\Upsilon}_{ir} \delta\mathbf{R}\} \widetilde{\boldsymbol{\Sigma}}_r\} + \text{tr}\{\widetilde{\boldsymbol{\Sigma}}_i^H \mathbb{E}\{\delta\mathbf{R} \boldsymbol{\Upsilon}_{ii} \delta\mathbf{R}\} \widetilde{\boldsymbol{\Sigma}}_i\}, \end{aligned} \quad (3.119)$$

where for an arbitrary matrix \mathbf{Z} , $\mathbb{E}\{\delta\mathbf{R} \mathbf{Z} \delta\mathbf{R}\} = (\text{tr}\{\mathbf{R} \mathbf{Z}\} \mathbf{R} - \mathbf{G}(\mathbf{I} \odot \mathbf{G}^H \mathbf{Z} \mathbf{G}) \mathbf{G}^H) / N$, $\widetilde{\boldsymbol{\Sigma}}_r \triangleq \mathbf{R}^{-1} \mathbf{S}_{1,r} \boldsymbol{\Omega}_{mv}^\dagger$, $\widetilde{\boldsymbol{\Sigma}}_i \triangleq \mathbf{R}^{-1} \mathbf{S}_{1,i} \boldsymbol{\Omega}_{mv}^\dagger$, and the matrices $\boldsymbol{\Upsilon}_{rr}$, $\boldsymbol{\Upsilon}_{ri}$, $\boldsymbol{\Upsilon}_{ir}$, and $\boldsymbol{\Upsilon}_{ii}$ are, respectively, given by

$$\begin{aligned} \boldsymbol{\Upsilon}_{rr} &= \mathbf{R}^{-1} \mathbf{S}_{1,r} \mathbf{h}_{mv} \mathbf{h}_{mv}^H \mathbf{S}_{1,r}^H \mathbf{R}^{-1}, \\ \boldsymbol{\Upsilon}_{ri} &= \mathbf{R}^{-1} \mathbf{S}_{1,r} \mathbf{h}_{mv} \mathbf{h}_{mv}^H \mathbf{S}_{1,i}^H \mathbf{R}^{-1}, \\ \boldsymbol{\Upsilon}_{ir} &= \mathbf{R}^{-1} \mathbf{S}_{1,i} \mathbf{h}_{mv} \mathbf{h}_{mv}^H \mathbf{S}_{1,r}^H \mathbf{R}^{-1}, \\ \boldsymbol{\Upsilon}_{ii} &= \mathbf{R}^{-1} \mathbf{S}_{1,i} \mathbf{h}_{mv} \mathbf{h}_{mv}^H \mathbf{S}_{1,i}^H \mathbf{R}^{-1}. \end{aligned} \quad (3.120)$$

Proof: According to (3.109), the matrix Ω_{mv} is a function of \mathbf{R}^{-1} , therefore, the imperfect estimation of \mathbf{R} due to finite data samples introduces a perturbation on Ω_{mv} . This, in turn, results in perturbation of the estimated channel vector \mathbf{h}_{mv} .

Using the first-order Taylor expansion, we have

$$(\mathbf{R} + \delta\mathbf{R})^{-1} \simeq \mathbf{R}^{-1} - \mathbf{R}^{-1}\delta\mathbf{R}\mathbf{R}^{-1}. \quad (3.121)$$

Substituting (3.121) into (3.109), we obtain the following expression for the perturbation of Ω_{mv}

$$\delta\Omega_{\text{mv}} = -(\mathbf{S}_{1,r}^H \mathbf{R}^{-1} \delta\mathbf{R} \mathbf{R}^{-1} \mathbf{S}_{1,r} + \mathbf{S}_{1,i}^H \mathbf{R}^{-1} \delta\mathbf{R} \mathbf{R}^{-1} \mathbf{S}_{1,i}). \quad (3.122)$$

In [50], it is shown that the first-order perturbation expansion can be used to get a linear approximation to the perturbation in the channel estimate as

$$\delta\mathbf{h}_{\text{mv}} \triangleq \hat{\mathbf{h}}_{\text{mv}} - \mathbf{h}_{\text{mv}} \simeq -\Omega_{\text{mv}}^\dagger \delta\Omega_{\text{mv}} \mathbf{h}_{\text{mv}}, \quad (3.123)$$

Substituting (3.122) into (3.123), and noticing the fact that both $\Omega_{\text{mv}}^\dagger$ and \mathbf{R}^{-1} are Hermitian matrices, we obtain

$$\delta\mathbf{h}_{\text{mv}} = (\tilde{\Sigma}_r^H \delta\mathbf{R} \mathbf{R}^{-1} \mathbf{S}_{1,r} + \tilde{\Sigma}_i^H \delta\mathbf{R} \mathbf{R}^{-1} \mathbf{S}_{1,i}) \mathbf{h}_{\text{mv}}, \quad (3.124)$$

where $\tilde{\Sigma}_r \triangleq \mathbf{R}^{-1} \mathbf{S}_{1,r} \Omega_{\text{mv}}^\dagger$, and $\tilde{\Sigma}_i \triangleq \mathbf{R}^{-1} \mathbf{S}_{1,i} \Omega_{\text{mv}}^\dagger$.

From (3.124), we can see that $\delta\mathbf{h}_{\text{mv}}$ is linearly related to $\delta\mathbf{R}$. Considering the fact that $\hat{\mathbf{R}}$ is an unbiased estimate of \mathbf{R} , i.e., $\mathbf{E}\{\delta\mathbf{R}\} = 0$, (3.124) implies that: $\mathbf{E}\{\delta\mathbf{h}_{\text{mv}}\} = 0$. This proves part (i) of the Theorem.

To prove part (ii), we first evaluate the covariance of $\delta\mathbf{h}_{\text{mv}}$ given by

$$\begin{aligned} \mathbf{E}\{\delta\mathbf{h}\delta\mathbf{h}^H\} &\simeq \tilde{\Sigma}_r^H \mathbf{E}\{\delta\mathbf{R} \Upsilon_{rr} \delta\mathbf{R}\} \tilde{\Sigma}_r + \tilde{\Sigma}_r^H \mathbf{E}\{\delta\mathbf{R} \Upsilon_{ri} \delta\mathbf{R}\} \tilde{\Sigma}_i \\ &\quad + \tilde{\Sigma}_i^H \mathbf{E}\{\delta\mathbf{R} \Upsilon_{ir} \delta\mathbf{R}\} \tilde{\Sigma}_r + \tilde{\Sigma}_i^H \mathbf{E}\{\delta\mathbf{R} \Upsilon_{ii} \delta\mathbf{R}\} \tilde{\Sigma}_i, \end{aligned} \quad (3.125)$$

where the matrices Υ_{rr} , Υ_{ri} , Υ_{ir} , and Υ_{ii} are, respectively, given by

$$\begin{aligned}\Upsilon_{rr} &= \mathbf{R}^{-1} \mathbf{S}_{1,r} \mathbf{h}_{\text{mv}} \mathbf{h}_{\text{mv}}^H \mathbf{S}_{1,r}^H \mathbf{R}^{-1}, \\ \Upsilon_{ri} &= \mathbf{R}^{-1} \mathbf{S}_{1,r} \mathbf{h}_{\text{mv}} \mathbf{h}_{\text{mv}}^H \mathbf{S}_{1,i}^H \mathbf{R}^{-1}, \\ \Upsilon_{ir} &= \mathbf{R}^{-1} \mathbf{S}_{1,i} \mathbf{h}_{\text{mv}} \mathbf{h}_{\text{mv}}^H \mathbf{S}_{1,r}^H \mathbf{R}^{-1}, \\ \Upsilon_{ii} &= \mathbf{R}^{-1} \mathbf{S}_{1,i} \mathbf{h}_{\text{mv}} \mathbf{h}_{\text{mv}}^H \mathbf{S}_{1,i}^H \mathbf{R}^{-1}.\end{aligned}\tag{3.126}$$

Finally, taking the trace of the covariance matrix in (3.125), we get the expression for $\mathbb{E}\{\|\delta \mathbf{h}_{\text{mv}}\|^2\}$ given by (3.119). \blacksquare

Combining the results from Theorem 5 and 6, the MSE for the MVDR channel estimator is given by

$$\begin{aligned}\mathbb{E}\{\|\hat{\mathbf{h}}_{\text{mv}} - \mathbf{h}\|^2\} &= \mathbb{E}\{\|(\mathbf{h}_{\text{mv}} - \mathbf{h}) + (\hat{\mathbf{h}}_{\text{mv}} - \mathbf{h}_{\text{mv}})\|^2\} \\ &= \mathbb{E}\{(\Delta \mathbf{h}_{\text{mv}} + \delta \mathbf{h}_{\text{mv}})^H (\Delta \mathbf{h}_{\text{mv}} + \delta \mathbf{h}_{\text{mv}})\} \\ &= \|\Delta \mathbf{h}_{\text{mv}}\|^2 + \mathbb{E}\{\|\delta \mathbf{h}_{\text{mv}}\|^2\}.\end{aligned}\tag{3.127}$$

In the derivation of (3.127), we have used the fact that $\Delta \mathbf{h}_{\text{mv}}$ is deterministic which in conjunction with the result from the part (i) of Theorem 6 implies $\Delta \mathbf{h}_{\text{mv}}^H \mathbb{E}\{\delta \mathbf{h}_{\text{mv}}\} = \mathbb{E}\{\delta \mathbf{h}_{\text{mv}}^H\} \Delta \mathbf{h}_{\text{mv}} = 0$. The first term in the RHS of (3.127) represents the contribution to the MSE of the bias of the estimate $\hat{\mathbf{h}}_{\text{mv}}$. This is in contrast to the subspace approach which provides unbiased estimates. It is worth noting that at sufficiently high SNR, since the squared norm of the bias is proportional to σ^4 , the first term in (3.127) can be considered negligible and as $\sigma \rightarrow 0$, the MSE converges to $\mathbb{E}\{\|\delta \mathbf{h}_{\text{mv}}\|^2\}$.

3.5.2 Cramer-Rao Bound

From (3.127), we see that the MVDR method is a biased estimator, therefore, the corresponding MSE cannot be compared to the traditional CRB which is valid only for unbiased estimators [52]. In the following, we will derive the CRB for biased SFBC MC-CDMA channel estimators under the assumption that transmitted symbols, channel and spreading codes are all unknown deterministic quantities.

The CRB on the covariance of a biased estimator is given by [56]

$$\mathbb{E}\left\{(\hat{\boldsymbol{\theta}} - \mathbb{E}\{\hat{\boldsymbol{\theta}}\})(\hat{\boldsymbol{\theta}} - \mathbb{E}\{\hat{\boldsymbol{\theta}}\})^T\right\} \geq \frac{\partial \mathbb{E}\{\hat{\boldsymbol{\theta}}\}}{\partial \boldsymbol{\theta}} \mathbf{J}_{\boldsymbol{\theta}\boldsymbol{\theta}}^{-1} \frac{\partial \mathbb{E}\{\hat{\boldsymbol{\theta}}\}^T}{\partial \boldsymbol{\theta}},\tag{3.128}$$

where

$$\frac{\partial \mathbb{E}\{\hat{\boldsymbol{\theta}}\}}{\partial \boldsymbol{\theta}} = \begin{bmatrix} \frac{\partial \mathbb{E}\{\hat{\boldsymbol{\theta}}_b\}}{\partial \boldsymbol{\theta}_b} & \frac{\partial \mathbb{E}\{\hat{\boldsymbol{\theta}}_b\}}{\partial \boldsymbol{\theta}_s} & \frac{\partial \mathbb{E}\{\hat{\boldsymbol{\theta}}_b\}}{\partial \boldsymbol{\theta}_h} \\ \frac{\partial \mathbb{E}\{\hat{\boldsymbol{\theta}}_s\}}{\partial \boldsymbol{\theta}_b} & \frac{\partial \mathbb{E}\{\hat{\boldsymbol{\theta}}_s\}}{\partial \boldsymbol{\theta}_s} & \frac{\partial \mathbb{E}\{\hat{\boldsymbol{\theta}}_s\}}{\partial \boldsymbol{\theta}_h} \\ \frac{\partial \mathbb{E}\{\hat{\boldsymbol{\theta}}_h\}}{\partial \boldsymbol{\theta}_b} & \frac{\partial \mathbb{E}\{\hat{\boldsymbol{\theta}}_h\}}{\partial \boldsymbol{\theta}_s} & \frac{\partial \mathbb{E}\{\hat{\boldsymbol{\theta}}_h\}}{\partial \boldsymbol{\theta}_h} \end{bmatrix}. \quad (3.129)$$

Recognizing the fact that the channel bias expression in (3.115) is not a function of the transmitted data symbols $\boldsymbol{\theta}_b$, we may readily conclude that $\frac{\partial \mathbb{E}\{\hat{\boldsymbol{\theta}}_b\}}{\partial \boldsymbol{\theta}_b} = 0$. Moreover, since our channel estimator is not tied up to a code signature estimator, we may make the assumption that the code signature vectors are estimated by an unbiased estimator, i.e., $\frac{\partial \mathbb{E}\{\hat{\boldsymbol{\theta}}_s\}}{\partial \boldsymbol{\theta}_h} = 0$. Therefore, the CRB on the covariance of the MVDR channel estimator is given by

$$\begin{aligned} & \mathbb{E} \left\{ (\hat{\mathbf{h}}_{\text{mv}} - \mathbb{E}\{\hat{\mathbf{h}}_{\text{mv}}\})(\hat{\mathbf{h}}_{\text{mv}} - \mathbb{E}\{\hat{\mathbf{h}}_{\text{mv}}\})^T \right\} \\ & \geq \left(\frac{\partial \mathbb{E}\{\hat{\mathbf{h}}_{\text{mv}}\}}{\partial \boldsymbol{\theta}_h} \right)^T \mathbf{J}^\dagger(\mathbf{h}) \frac{\partial \mathbb{E}\{\hat{\mathbf{h}}_{\text{mv}}\}}{\partial \boldsymbol{\theta}_h} = \text{BCRB}(\mathbf{h}), \end{aligned} \quad (3.130)$$

where $\mathbf{J}(\mathbf{h})$ is the Schur complement of matrix \mathbf{J}_{hh} in (3.78) defined by (3.104).

In (3.130), $\mathbb{E}\{\hat{\mathbf{h}}_{\text{mv}}\} = \mathbf{h} + \Delta \mathbf{h}_{\text{mv}} = (\mathbf{I}_{2J} - \sigma^2 \mathbf{A}_0^\dagger \mathbf{A}_1) \mathbf{h}$, and

$$\frac{\partial \mathbb{E}\{\hat{\mathbf{h}}_{\text{mv}}\}}{\partial \boldsymbol{\theta}_h} = \left[\left(\frac{\partial \mathbb{E}\{\hat{\mathbf{h}}_{\text{mv}}\}}{\partial \Re(\mathbf{h})} \right)^T, \left(\frac{\partial \mathbb{E}\{\hat{\mathbf{h}}_{\text{mv}}\}}{\partial \Im(\mathbf{h})} \right)^T \right]^T, \quad (3.131)$$

with

$$\begin{aligned} \frac{\partial \mathbb{E}\{\hat{\mathbf{h}}_{\text{mv}}\}}{\partial \Re(\mathbf{h})} &= 2\Re \left(\mathbf{I}_{2J} - \sigma^2 \mathbf{A}_0^\dagger \mathbf{A}_1 \right), \\ \frac{\partial \mathbb{E}\{\hat{\mathbf{h}}_{\text{mv}}\}}{\partial \Im(\mathbf{h})} &= 2\Im \left(\mathbf{I}_{2J} - \sigma^2 \mathbf{A}_0^\dagger \mathbf{A}_1 \right). \end{aligned}$$

Finally, the lower bound on the overall mean-squared channel estimation error can be obtained as

$$\mathbb{E}\{\|\hat{\mathbf{h}}_{\text{mv}} - \mathbf{h}\|^2\} \geq \text{tr}\{\text{BCRB}(\mathbf{h})\} + \|\Delta \mathbf{h}_{\text{mv}}\|^2. \quad (3.132)$$

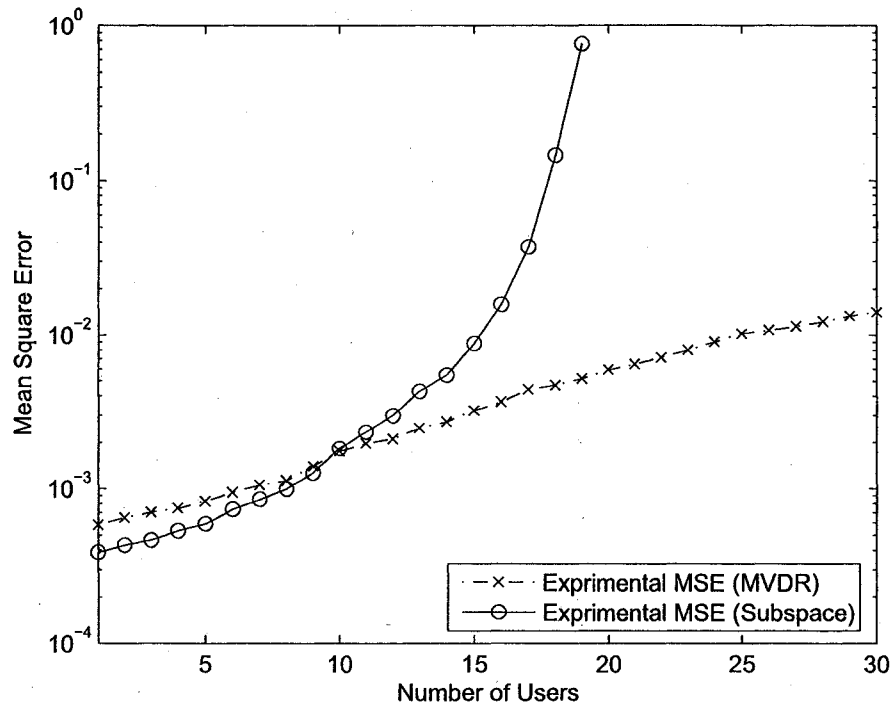


Fig. 3.12 The MSE as a function of the number of users in the system.

3.5.3 Simulations Studies

We consider a MC-CDMA system with 6 users utilizing code sequences of length⁸ 32 which is also the number of subcarriers. We use cyclic prefix of length 8 which is 1/4th of the FFT size. Unless otherwise specified, a data record of $N = 100$ samples is used for estimating the autocorrelation matrix. The transmitter and the receiver are equipped with 2 and 1 antennas, respectively, while the SFBC employed is the orthogonal block code of [3]. Each subchannel has 4 paths with a variance equal to $\sigma_c^2 = 1$. In what follows, the presented results are averages over 100 independent channel realizations.

To show the merit of the MVDR channel estimator versus its subspace counterpart for an overloaded system we show in Fig. 3.12 the experimental MSEs for both algorithms versus the number of active users. For this experiment, all interfering users are assumed to have a SNR of 10 dB while the SNR of the desired user is fixed at 20 dB. As can be seen from Fig. 3.12, for $10 < K < 20$ the MVDR method substantially outperforms the

⁸Constructed from Gold sequences of length 31 by appending a +1.

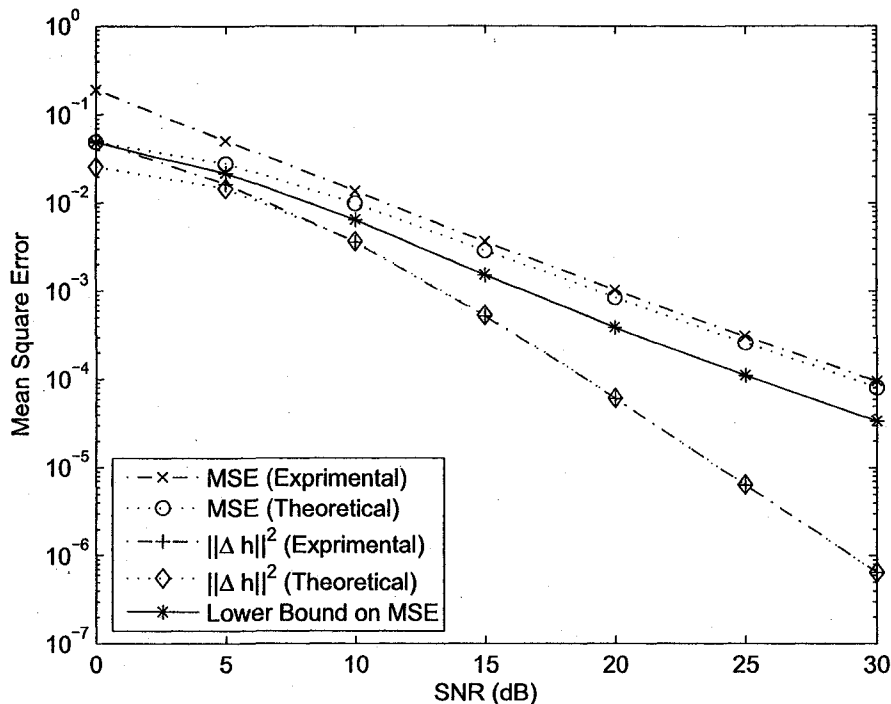


Fig. 3.13 The MSE as a function of the SNR.

subspace approach while for $K > 20$ the latter is not applicable anymore.

In the following studies, we examine the accuracy of the MSE expression in (3.127) and we compare the MSE performance of the MVDR algorithm to the lower bound in (3.132). We also examine the accuracy of the bias expression in (3.115). Fig. 3.13 shows the MSE performance of the MVDR channel estimator as a function of the input SNR. From Fig. 3.13, we infer that for the relatively high SNRs the analytical expressions of the bias and the MSE provide good approximations to their corresponding actual values obtained from simulations. In Fig. 3.14, we examine the effect of the data record size used to form the sample estimate $\hat{\mathbf{R}}$ on the performance of the MVDR algorithm. The SNRs of all users in the system are fixed at 10 dB. As can be seen from this experiment, by increasing the data record size, there is a considerable improvement in the MSE. This was expected because the MVDR algorithm, as any other second-order statistics-based method, relies heavily on a good estimate of the autocorrelation matrix.

Finally, in Fig. 3.15, the MSE performance is studied in near-far situations. The near-far situation arises when the signals from the interfering users arrive at the receiver with

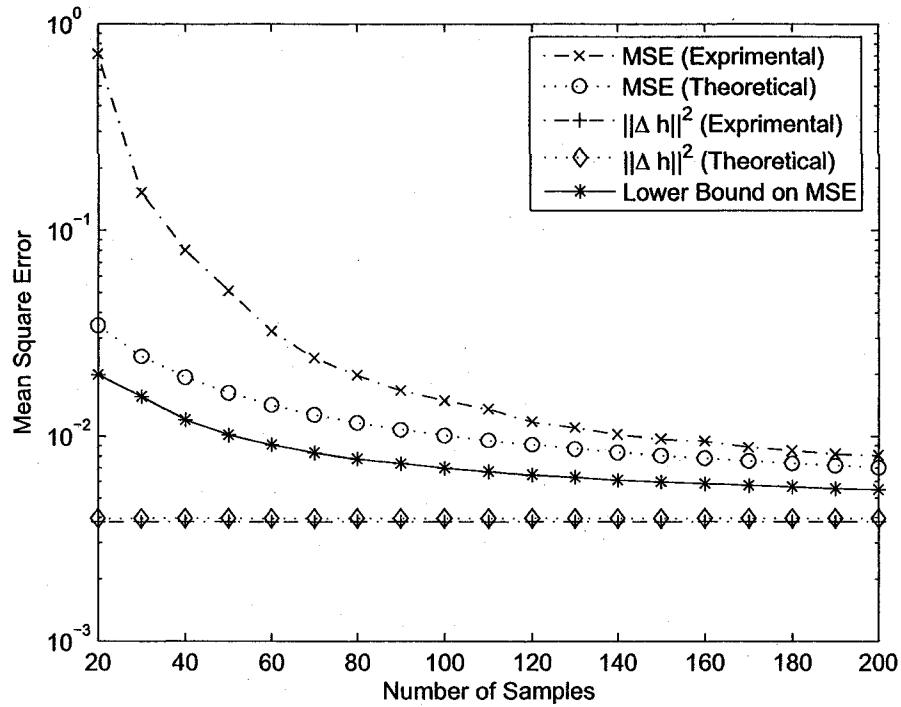


Fig. 3.14 The MSE as a function of the data record size.

higher power than that of the desired one. For this experiment, the near-far ratio is defined as the ratio of the power of interfering users to the power of the desired user. The SNR of the desired user is fixed at 20 dB. From Fig. 3.15, we see that the MVDR channel estimation algorithms are near-far resistant.

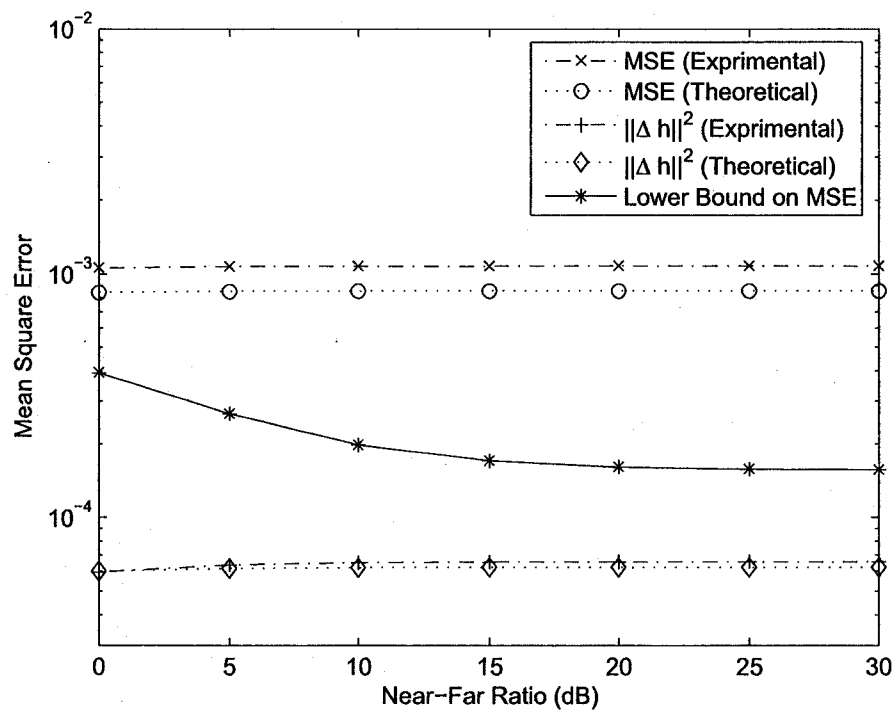


Fig. 3.15 The MSE as a function of the Near-Far Ratio.

Chapter 4

Space-Frequency Block Coded MC-CDMA: A Post-FFT Approach

4.1 Introduction

In the previous chapter, we introduced blind channel estimation and detection schemes for SFBC MC-CDMA systems that combine the advantages of SFBC with those of MC-CDMA to alleviate some of the shortcomings of SFBC-OFDM or those of STBC MC-CDMA systems. Our approach, however, was to exploit the covariance matrix of the time-domain received vector (i.e., before overlap-adding (or CP removal) and FFT operation). In this chapter, we extend our scope of interest and expose yet another very interesting property of the SFBC MC-CDMA systems which is a structured covariance matrix at the output of the Fast Fourier Transform (FFT). In fact, as will be illustrated, for the post-FFT approach the entries of covariance matrix which form alternating subdiagonals of the corresponding matrix are zero. Our study reveals that, as opposed to their pre-FFT counterparts presented in the previous chapter, the channel estimation and detection schemes obtained using the post-FFT approach have the advantage of fully exploiting the inherent structure imposed by SFBC on the covariance matrix to yield improved performance at lower computation complexity. The price to be paid for these achievements is some loss in the degrees of freedom of the estimators (i.e., fewer users can be supported by the channel estimator) for an overloaded system, where the number of active users is relatively large compared to the FFT size and the length of the channel.

In general, there exist different strategies in designing blind channel estimators for dif-

ferent communication scenarios. Many of these blind schemes are designed using either the sample data covariance matrix directly or its eigencomponents. However, there are two major design considerations associated with such blind algorithms. First, they require the collection of sample records that are sufficiently long to ensure the accurate estimation of the sample covariance matrix. Second, they tend to have a computational complexity that is normally cubic in the length of the received vector. All these issues become even more problematic when multiple antennas are involved on either or both sides of the transmission ends. This stems from the fact that the length of the received vector of the resulting multiple-antenna implementation increases as the number of antennas is increased. A longer received vector in turn implies the collection of longer sample records and higher computational complexity. Those provide the motivation for computationally efficient methods requiring relatively short data records such as those presented in this work. Particularly, as in Chapter 3, we formulate two methods that rely on the second-order properties of the frequency-domain FFT-processed received blocks, namely: (i) a Minimum Variance Distortionless Response (MVDR)-type channel estimator, and (ii) a subspace-based channel estimator. For these methods, we address the issue of channel identifiability and we investigate the necessary and sufficient conditions under which the channel estimates are unique (within a complex scalar). Our studies reveal that unlike subspace methods the MVDR algorithms can be employed in medium to highly loaded systems; besides, they are more advantageous in systems with severe multipath distortion, small FFT size, or small processing gain.

In practice, the channel is estimated from the received signals, and those estimates coincide with the true channel only when the number of received samples becomes infinitely large. Therefore, channel estimators show performance degradation when there is insufficient number of data samples. In this chapter, with the aid of the analytical studies in [51] and [55], we investigate the performance of the aforementioned algorithms under finite sample size. More specifically, we derive the analytical closed-form expressions for the bias and the MSE of each estimator under small perturbations assumptions, and we show that, unlike their subspace counterparts, the MVDR algorithms are asymptotically biased. In the derivation of the asymptotic bias expression (i.e., the bias due to the noise) for the MVDR methods, we suggest a new approach based on the Newton-Raphson criterion that is robust to the number of active users in the system. It should be noted that the bias expressions presented in [24] for the MVDR-type channel estimators are based on the noise components of the received signal covariance matrix and are not applicable to the system

under consideration for which the noise subspace may not exist at all in the medium to heavy loaded systems. Finally, to benchmark the accuracy of our estimation algorithms we also derive the Cramer-Rao bounds (CRBs) for both biased and unbiased estimators which are exclusively designed for the downlink transmissions.

The rest of this chapter is organized as follows. In Section 4.2, we describe the combined SFBC MC-CDMA system model. The second-order statistics (SOS)-based blind channel estimation algorithms are presented in Section 4.3. In Section 4.4, we provide some modifications of the presented algorithms to enhance their performance and lower their computational complexity. The issue of channel identifiability is also addressed in 4.4. In Section 4.5, we analyze the performance of the derived algorithms by providing the channel estimators' MSE. The analytical expressions of the CRB for both biased and unbiased estimators are derived in Section 4.6. The MVDR-based linear joint SF block decoding and detection algorithms are investigated in Section 4.7, followed by simulation studies in Section 4.8.

4.2 System Model

We consider a wireless system where downlink transmissions take place using the combined SFBC and MC-CDMA scheme described in Chapter 3. However, in this chapter, we take a different approach for representing the received vector, namely, we define the discrete-time frequency-domain $L \times 1$ received vector after removing the CP and applying the L -point Fast Fourier Transform (FFT). In this case, the received vector \mathbf{r} is given by

$$\mathbf{r} = \mathbf{F}\tilde{\mathbf{H}}_1\mathbf{F}^H\mathbf{x}_1 + \mathbf{F}\tilde{\mathbf{H}}_2\mathbf{F}^H\mathbf{x}_2 + \mathbf{n}, \quad (4.1)$$

where $\tilde{\mathbf{H}}_1$ and $\tilde{\mathbf{H}}_2$ are $L \times L$ circulant channel matrices defined in (3.14) and (3.15), respectively; \mathbf{F} is the $L \times L$ FFT matrix whose (m, n) th entry is equal to $\exp\{-j2\pi(m-1)(n-1)/L\}/\sqrt{L}$; and $\mathbf{n} \sim \mathcal{CN}(\mathbf{0}, \sigma^2\mathbf{I}_L)$ is additive white complex Gaussian noise.

4.2.1 Equivalent Single-Input-Single-Output Representation

To explicitly express the received vector in terms of the unknown channel vector \mathbf{h} that we wish to estimate, we rewrite \mathbf{r} in (4.1) by separating the real and imaginary components

of the transmitted symbols to obtain

$$\mathbf{r} = \sum_{k=1}^K (\Re(b_k) \mathbf{S}_{k,r} \mathbf{h} + \Im(b_k) \mathbf{S}_{k,i} \mathbf{h}) + \mathbf{n}, \quad (4.2)$$

where $\Re(b_k)$ and $\Im(b_k)$ indicate the real and imaginary parts of b_k , respectively, and $\mathbf{S}_{k,r}$ and $\mathbf{S}_{k,i}$ are $L \times 2J$ matrices given by

$$\mathbf{S}_{k,r} \triangleq [\mathbf{D}_1 \quad \mathbf{D}_3] \tilde{\mathbf{S}}_k \tilde{\mathbf{F}} \quad \text{and} \quad \mathbf{S}_{k,i} \triangleq [\mathbf{D}_2 \quad \mathbf{D}_4] \tilde{\mathbf{S}}_k \tilde{\mathbf{F}}, \quad (4.3)$$

respectively. In (4.3), $\tilde{\mathbf{S}}_k = \text{diag}(\mathbf{s}_k)$, $\tilde{\mathbf{F}}$ is the matrix formed by the first $2J$ columns of $\sqrt{L}\mathbf{F}$, and $\mathbf{D}_1, \mathbf{D}_2, \mathbf{D}_3, \mathbf{D}_4$ are $L \times L$ precoding matrices defined by

$$\begin{aligned} \mathbf{D}_1 &\triangleq \mathbf{I}_{L/2} \otimes \begin{bmatrix} 1 & 0 \\ 0 & -1 \end{bmatrix}, & \mathbf{D}_2 &\triangleq j\mathbf{I}_L, \\ \mathbf{D}_3 &\triangleq \mathbf{I}_{L/2} \otimes \begin{bmatrix} 0 & 1 \\ 1 & 0 \end{bmatrix}, & \mathbf{D}_4 &\triangleq \mathbf{I}_{L/2} \otimes \begin{bmatrix} 0 & j \\ -j & 0 \end{bmatrix}. \end{aligned} \quad (4.4)$$

As we can see from (4.2), the real and imaginary parts of b_k , $k = 1, \dots, K$, modulate two different effective signatures $\mathbf{g}_{k,r} \triangleq \mathbf{S}_{k,r} \mathbf{h}$ and $\mathbf{g}_{k,i} \triangleq \mathbf{S}_{k,i} \mathbf{h}$, respectively. However, due to the SF block coding performed at the receiver the vectors $\mathbf{g}_{k,r}$ and $\mathbf{g}_{k,i}$ exhibit a special structure and relationship as identified in the following lemma.

Lemma 3 *Let $\mathbf{g}_{k,r}$ and $\mathbf{g}_{k,i}$ be the effective signatures corresponding to the real and imaginary parts, respectively, of the k th user transmitted symbol, $k = 1, \dots, K$. Then*

$$i) \quad \mathbf{g}_{k,i} = j\mathbf{D}_1 \mathbf{g}_{k,r}, \quad \text{where } \mathbf{D}_1 = \mathbf{I}_{L/2} \otimes \begin{bmatrix} 1 & 0 \\ 0 & -1 \end{bmatrix}.$$

$$ii) \quad \Re(\mathbf{g}_{k,i}^H \mathbf{g}_{k,r}) = 0$$

Proof: In view of (4.2)-(4.4), we first express the effective signatures as

$$\mathbf{g}_{k,r} = \mathbf{D}_1 \tilde{\mathbf{S}}_k \tilde{\mathbf{F}} \mathbf{h}_1 + \mathbf{D}_3 \tilde{\mathbf{S}}_k \tilde{\mathbf{F}} \mathbf{h}_2, \quad (4.5)$$

$$\mathbf{g}_{k,i} = \mathbf{D}_2 \tilde{\mathbf{S}}_k \tilde{\mathbf{F}} \mathbf{h}_1 + \mathbf{D}_4 \tilde{\mathbf{S}}_k \tilde{\mathbf{F}} \mathbf{h}_2. \quad (4.6)$$

Then, by noticing that $\mathbf{D}_2 = j\mathbf{D}_1\mathbf{D}_1$ and $\mathbf{D}_4 = j\mathbf{D}_1\mathbf{D}_3$, we conclude that $\mathbf{g}_{k,i} = j\mathbf{D}_1\mathbf{g}_{k,r}$. Now, we may use this relationship to write

$$\mathbf{g}_{k,i}^H\mathbf{g}_{k,r} = -j\mathbf{g}_{k,r}^H\mathbf{D}_1\mathbf{g}_{k,r} = -\mathbf{g}_{k,r}^H\mathbf{g}_{k,i} = -(\mathbf{g}_{k,i}^H\mathbf{g}_{k,r})^H$$

which implies that $\Re(\mathbf{g}_{k,i}^H\mathbf{g}_{k,r}) = 0$. ■

4.3 Second-Order-Statistics-based Channel Estimation Methods: Background and Simplifications

In this section, we present two SOS-based channel estimation algorithms for SFBC MC-CDMA systems, namely MVDR and subspace. The quantity assumed known for the implementation of both channel identification methods is the signature of the user of interest (assumed to be user 1). Furthermore, for the subspace method, we make the additional assumption that the total number of users K is known. We note that the knowledge of K allows accurate signal and noise subspace separation and, in practice, can be obtained through the use of information theoretic criteria as in [46].

The first step in developing such blind algorithms is to identify the special structure of the covariance matrix of the received signal which is summarized in the following Lemma.

Lemma 4 *Under the assumption that each user's information symbols are independent and identically distributed (i.i.d) with zero mean and unit variance, and that the symbol streams of the users are independent, the $L \times L$ covariance matrix $\mathbf{R} \triangleq \mathbb{E}\{\mathbf{r}\mathbf{r}^H\}$ of the received vector \mathbf{r} in (4.2) has the following form:*

$$\mathbf{R} = [R_{p,q} \cdot \delta(p \bmod 2, q \bmod 2)]_{1 \leq p, q \leq L}, \quad (4.7)$$

where $\delta(m, n)$ denotes the Kronecker delta function¹.

Proof: By expressing the matrix \mathbf{R} in terms of the effective signatures $\mathbf{g}_{k,r}$ and $\mathbf{g}_{k,i}$, $k = 1, \dots, K$, we obtain

$$\mathbf{R} = \sum_{k=1}^K (\mathbf{g}_{k,r}\mathbf{g}_{k,r}^H + \mathbf{g}_{k,i}\mathbf{g}_{k,i}^H) + \sigma^2\mathbf{I}_L. \quad (4.8)$$

¹ $\delta(p, q)$ is equal to one if $p = q$, and zero if $p \neq q$.

We proceed by using the result from Lemma 3 to rewrite \mathbf{R} in (4.8) as

$$\mathbf{R} = \sum_{k=1}^K (\mathbf{g}_{k,r} \mathbf{g}_{k,r}^H + \mathbf{D}_1 \mathbf{g}_{k,r} \mathbf{g}_{k,r}^H \mathbf{D}_1) + \sigma^2 \mathbf{I}_L. \quad (4.9)$$

It can be verified² that owing to the structure of the matrix \mathbf{D}_1 , as defined in (4.4), from (4.9) the matrix \mathbf{R} has the form in (4.7). ■

An interesting observation from Lemma 4 is that the elements of \mathbf{R} which form alternating subdiagonals of the corresponding matrix are zeros (i.e., the main diagonal is nonzero and the subdiagonals on either side of the main diagonal are alternatively zero). For example, for $L = 4$ the matrix \mathbf{R} has the following form:

$$\mathbf{R} = \begin{bmatrix} R_{1,1} & 0 & R_{1,3} & 0 \\ 0 & R_{2,2} & 0 & R_{2,4} \\ R_{1,3}^* & 0 & R_{3,3} & 0 \\ 0 & R_{2,4}^* & 0 & R_{4,4} \end{bmatrix}, \quad \text{with } R_{1,1}, \dots, R_{4,4} \neq 0. \quad (4.10)$$

The covariance matrix \mathbf{R} can also be expressed in terms of the noise and signal subspaces derived from an eigenvalue decomposition (EVD) of \mathbf{R} [44], i.e.,

$$\mathbf{R} = \mathbf{Q} \mathbf{\Lambda} \mathbf{Q}^H = [\mathbf{Q}_s \ \mathbf{Q}_n] \begin{bmatrix} \mathbf{\Lambda}_s & \mathbf{0} \\ \mathbf{0} & \mathbf{\Lambda}_n \end{bmatrix} \begin{bmatrix} \mathbf{Q}_s^H \\ \mathbf{Q}_n^H \end{bmatrix}, \quad (4.11)$$

where $\mathbf{\Lambda} \triangleq \text{diag}[\mathbf{\Lambda}_s \ \mathbf{\Lambda}_n] = \text{diag}(\lambda_1, \lambda_2, \dots, \lambda_L)$, $\lambda_1 \geq \dots \geq \lambda_{2K} > \lambda_{2K+1} = \dots = \lambda_L = \sigma^2$ contains in its diagonal the eigenvalues of \mathbf{R} in descending order, and $\mathbf{Q} \triangleq [\mathbf{Q}_s \ \mathbf{Q}_n]$ is the matrix of the corresponding eigenvectors. In (4.11), the columns of $\mathbf{Q}_s \triangleq [\mathbf{q}_1, \dots, \mathbf{q}_{2K}]$ span the signal subspace, whereas the columns of $\mathbf{Q}_n \triangleq [\mathbf{q}_{2K+1}, \dots, \mathbf{q}_L]$ span the noise subspace.

Lemma 4 allows us to establish the following lemma.

²As a representative example, for $L = 2$ we have $\mathbf{g}_{k,r} \mathbf{g}_{k,r}^H \triangleq \begin{bmatrix} x_{1,1} & x_{1,2} \\ x_{1,2}^* & x_{2,2} \end{bmatrix}$ and $\mathbf{D}_1 \mathbf{g}_{k,r} \mathbf{g}_{k,r}^H \mathbf{D}_1 = \begin{bmatrix} x_{1,1} & -x_{1,2} \\ -x_{1,2}^* & x_{2,2} \end{bmatrix}$.

Lemma 5 Let \mathbf{D}_1 and \mathbf{R} be defined as in (4.4) and (4.7), respectively. Then, we have

$$(i) \quad \mathbf{R} = \mathbf{D}_1 \mathbf{R} \mathbf{D}_1, \quad (4.12)$$

$$(ii) \quad \mathbf{R}^{-1} = \mathbf{D}_1 \mathbf{R}^{-1} \mathbf{D}_1, \quad (4.13)$$

$$(iii) \quad \mathbf{Q}_n \mathbf{Q}_n^H = \mathbf{D}_1 \mathbf{Q}_n \mathbf{Q}_n^H \mathbf{D}_1, \quad (4.14)$$

where $\mathbf{Q}_n = [\mathbf{q}_{2K+1}, \dots, \mathbf{q}_L]$ span the noise subspace.

Proof: Part (i) follows easily from (4.9) after premultiplication and postmultiplication by the unitary matrix \mathbf{D}_1 i.e., $\mathbf{D}_1 \mathbf{D}_1^T = \mathbf{I}$). Part (ii) follows from part (i) by taking the inverse of both sides of part (i) and noticing that \mathbf{D}_1 is an orthonormal matrix (i.e., $\mathbf{D}_1 \mathbf{D}_1^{-1} = \mathbf{I}$). Finally, to prove part (iii) we first note that the matrix $\mathbf{Q} \triangleq \mathbf{Q}_n \mathbf{Q}_n^H$ has a similar structure as that of \mathbf{R} indicated in (4.7) (i.e., the subdiagonals on either side of the main diagonal are alternatively zero). Then, noticing that due to the special structure of \mathbf{D}_1 the premultiplication and postmultiplication by \mathbf{D}_1 do not affect the nonzero elements of \mathbf{Q} , we arrive at the third identity in (4.14). \blacksquare

4.3.1 MVDR Channel Estimator

As it was shown in Chapter 3, in MVDR-based channel estimation methods, the channel vector \mathbf{h} is estimated by solving the following minimization problem:

$$\mathbf{h}_{\text{mv}} = \arg \min_{\mathbf{h}, \|\mathbf{h}\|=1} \mathbf{h}^H (\mathbf{S}_{1,r}^H \mathbf{R}^{-1} \mathbf{S}_{1,r} + \mathbf{S}_{1,i}^H \mathbf{R}^{-1} \mathbf{S}_{1,i}) \mathbf{h}, \quad (4.15)$$

More specifically, we estimate the channel vector as the eigenvector that corresponds to the minimum eigenvalue of the $2J \times 2J$ matrix $\mathbf{\Omega}_{\text{mv}}$ given by

$$\mathbf{\Omega}_{\text{mv}} \triangleq \mathbf{S}_{1,r}^H \mathbf{R}^{-1} \mathbf{S}_{1,r} + \mathbf{S}_{1,i}^H \mathbf{R}^{-1} \mathbf{S}_{1,i}. \quad (4.16)$$

But from Lemmas 3 and 5 we can see that

$$\mathbf{S}_{1,i}^H \mathbf{R}^{-1} \mathbf{S}_{1,i} = j(-j) \mathbf{S}_{1,r}^H \mathbf{D}_1 \mathbf{R}^{-1} \mathbf{D}_1 \mathbf{S}_{1,r} = \mathbf{S}_{1,r}^H \mathbf{R}^{-1} \mathbf{S}_{1,r}, \quad (4.17)$$

which implies that (4.16) reduces to $2\mathbf{S}_{1,r}^H \mathbf{R}^{-1} \mathbf{S}_{1,r}$. Thus, we proved the following proposition.

Proposition 4 Let $\mathbf{S}_{1,r}$ and \mathbf{R} be defined by (4.3) and (4.7), respectively, with $k = 1$.

Then, the matrix Ω_{mv} in (4.16) reduces to

$$\Omega_{mv} \triangleq 2\mathbf{S}_{1,r}^H \mathbf{R}^{-1} \mathbf{S}_{1,r}. \quad (4.18)$$

■

In practice, the ensemble average of the received signal covariance matrix \mathbf{R} is not known and is replaced by its sample-average estimate $\hat{\mathbf{R}}$ using N received vectors $\mathbf{r}(i)$, $i = 1, \dots, N$, given by

$$\hat{\mathbf{R}} \triangleq \frac{1}{N} \sum_{i=1}^N \mathbf{r}(i) \mathbf{r}(i)^H. \quad (4.19)$$

We note that, in general, if \mathbf{R} in (4.18) is replaced by $\hat{\mathbf{R}}$, the expressions in (4.16) and (4.18) are not equivalent anymore. This stems from the fact that the estimation error in $\hat{\mathbf{R}}$ is likely to be propagated differently in the first and second terms of (4.16) (i.e., $\mathbf{S}_{1,r}^H \hat{\mathbf{R}}^{-1} \mathbf{S}_{1,r} \neq \mathbf{S}_{1,i}^H \hat{\mathbf{R}}^{-1} \mathbf{S}_{1,i}$). In this case, we obtain the channel vector estimate $\hat{\mathbf{h}}_{mv}$ as the eigenvector that corresponds to the smallest eigenvalue of the matrix $\hat{\Omega}_{mv}$ given by

$$\hat{\Omega}_{mv} \triangleq \mathbf{S}_{1,r}^H \hat{\mathbf{R}}^{-1} \mathbf{S}_{1,r} + \mathbf{S}_{1,i}^H \hat{\mathbf{R}}^{-1} \mathbf{S}_{1,i}. \quad (4.20)$$

4.3.2 Subspace Channel Estimator

The starting point in the development of the subspace algorithms is to use the orthogonality between the noise subspace and the signal subspace which gives rise to the following statement:

$$\| \mathbf{Q}_n^H \mathbf{g}_{1,r} \|^2 = \| \mathbf{Q}_n^H \mathbf{g}_{1,i} \|^2 = 0. \quad (4.21)$$

Since both real and imaginary parts of the complex transmitted symbol are passing through the same channel filter, the equation (4.21) is equivalent to

$$\mathbf{g}_{1,r}^H \mathbf{Q}_n \mathbf{Q}_n^H \mathbf{g}_{1,r} + \mathbf{g}_{1,i}^H \mathbf{Q}_n \mathbf{Q}_n^H \mathbf{g}_{1,i} = 0. \quad (4.22)$$

From (4.3), we can see that the channel vector \mathbf{h} satisfies

$$\mathbf{h}^H \Omega_{ss} \mathbf{h} = 0, \quad (4.23)$$

where Ω_{ss} is the $2J \times 2J$ matrix given by

$$\Omega_{ss} \triangleq \mathbf{S}_{1,r}^H \mathbf{Q}_n \mathbf{Q}_n^H \mathbf{S}_{1,r} + \mathbf{S}_{1,i}^H \mathbf{Q}_n \mathbf{Q}_n^H \mathbf{S}_{1,i}. \quad (4.24)$$

Similar to the MVDR algorithms, the special structure inherent to SFBC MC-CDMA systems allows a simplification of the expression of Ω_{ss} in (4.24). The result is expressed in the following proposition.

Proposition 5 *Let $\mathbf{S}_{1,r}$ be defined by (4.3) with $k = 1$. Then, the matrix Ω_{ss} in (4.24) reduces to*

$$\Omega_{ss} = 2\mathbf{S}_{1,r}^H \mathbf{Q}_n \mathbf{Q}_n^H \mathbf{S}_{1,r}, \quad (4.25)$$

where \mathbf{Q}_n span the noise subspace.

Proof: To show (4.25), it suffices to show that

$$\mathbf{S}_{1,i}^H \mathbf{Q}_n \mathbf{Q}_n^H \mathbf{S}_{1,i} = \mathbf{S}_{1,r}^H \mathbf{Q}_n \mathbf{Q}_n^H \mathbf{S}_{1,r}. \quad (4.26)$$

Using Lemma 3, we first write the expression of Ω_{ss} in (4.24) as

$$\Omega_{ss} = \mathbf{S}_{1,r}^H \mathbf{Q}_n \mathbf{Q}_n^H \mathbf{S}_{1,r} + \mathbf{S}_{1,r}^H \mathbf{D}_1 \mathbf{Q}_n \mathbf{Q}_n^H \mathbf{D}_1 \mathbf{S}_{1,r}. \quad (4.27)$$

Then, the expression in (4.25) easily follows using Lemma 5. ■

It should be noted that, similar to the MVDR algorithms, the above result is not valid when \mathbf{Q}_n in (4.24) is replaced by an estimate. In this case, it is preferable to estimate the channel as the eigenvector that corresponds to the smallest eigenvalue of the matrix $\hat{\Omega}_{ss}$ given by

$$\hat{\Omega}_{ss} \triangleq \mathbf{S}_{1,r}^H \hat{\mathbf{Q}}_n \hat{\mathbf{Q}}_n^H \mathbf{S}_{1,r} + \mathbf{S}_{1,i}^H \hat{\mathbf{Q}}_n \hat{\mathbf{Q}}_n^H \mathbf{S}_{1,i}, \quad (4.28)$$

where $\hat{\mathbf{Q}}_n$ is the $L \times (L - 2K)$ matrix whose columns are the eigenvectors that correspond to the $L - 2K$ smallest eigenvalues of $\hat{\mathbf{R}}$. In other words,

$$\hat{\mathbf{h}}_{ss} = \arg \min_{\mathbf{h}, \|\mathbf{h}\|=1} \mathbf{h}^H \hat{\Omega}_{ss} \mathbf{h}. \quad (4.29)$$

4.4 Improved Blind Channel Estimation Algorithms

The performance of blind channel estimation methods employing the received signal covariance matrix depends heavily on the accuracy of the covariance matrix estimate. A

common approach for increasing the accuracy of the covariance matrix estimate is to collect longer data records. The purpose of this section is to take advantage of the special structure imposed by SFBC on the true covariance matrix \mathbf{R} to improve the corresponding sample average estimate $\widehat{\mathbf{R}}$ and, at the same time, reduce the computational complexity. The idea, as expressed in the following proposition, is to enforce the matrix $\widehat{\mathbf{R}}$ to have the same structure as that of \mathbf{R} .

Proposition 6 *Let $\widetilde{\mathbf{R}} \triangleq \frac{1}{2}(\widehat{\mathbf{R}} + \mathbf{D}_1\widehat{\mathbf{R}}\mathbf{D}_1)$ where \mathbf{D}_1 and $\widehat{\mathbf{R}}$ are defined as in (4.4) and (4.19), respectively. Then, $\widetilde{\mathbf{R}}$ is a more accurate estimate of \mathbf{R} compared to that of $\widehat{\mathbf{R}}$, in the sense that*

$$\|\mathbf{R} - \widetilde{\mathbf{R}}\|_F \leq \|\mathbf{R} - \widehat{\mathbf{R}}\|_F, \quad (4.30)$$

where $\|\cdot\|_F$ denotes the Frobenius norm.

Proof: Let $\delta\widetilde{\mathbf{R}} \triangleq \mathbf{R} - \widetilde{\mathbf{R}}$, $\delta\widehat{\mathbf{R}} \triangleq \mathbf{R} - \widehat{\mathbf{R}}$, and \mathbf{P} be the $N \times N$ permutation matrix representing a single right cyclic shift given by

$$\mathbf{P} = \begin{bmatrix} 0 & \dots & 0 & 1 \\ 1 & 0 & \ddots & 0 \\ & \ddots & \ddots & \vdots \\ \mathbf{0} & & 1 & 0 \end{bmatrix}. \quad (4.31)$$

Without loss of generality, we express $\|\delta\widetilde{\mathbf{R}}\|_F^2$ as the sum of the 2-norm squared of the main diagonal of the shifted versions of the matrix $\delta\widetilde{\mathbf{R}}$ to obtain

$$\begin{aligned} \|\delta\widetilde{\mathbf{R}}\|_F^2 &= \sum_{i=0}^{N/2} \|\text{diag}(\delta\widetilde{\mathbf{R}}P^i)\|_2^2 \\ &= \sum_{i=0}^{N/2} \|\text{diag}(\delta\widetilde{\mathbf{R}}P^{2i})\|_2^2 + \sum_{i=0}^{N/2} \|\text{diag}(\delta\widetilde{\mathbf{R}}P^{2i+1})\|_2^2 \end{aligned} \quad (4.32)$$

where $\|\cdot\|_2$ denotes the 2-norm.

Obviously, the second term in (4.32) is zero, since it corresponds to the sum of the 2-norm squared of the main diagonal of those shifted versions of $\widetilde{\mathbf{R}}$ which have zero entries on their main diagonal. Now, using $\delta\widetilde{\mathbf{R}} = \frac{1}{2}(\delta\widehat{\mathbf{R}} + \mathbf{D}_1\delta\widehat{\mathbf{R}}\mathbf{D}_1)$ and noticing that

$\|\text{diag}(\delta\widehat{\mathbf{R}}P^{2i})\|_2^2 = \|\text{diag}(\mathbf{D}_1\delta\widehat{\mathbf{R}}\mathbf{D}_1P^{2i})\|_2^2$, we may express the first term in (4.32) as

$$\sum_{i=0}^{N/2} \|\text{diag}(\delta\widehat{\mathbf{R}}P^{2i})\|_2^2 \leq \sum_{i=0}^{N/2} \|\text{diag}(\delta\widehat{\mathbf{R}}P^{2i})\|_2^2 + \sum_{i=0}^{N/2} \|\text{diag}(\delta\widehat{\mathbf{R}}P^{2i+1})\|_2^2 = \|\delta\widehat{\mathbf{R}}\|_F^2,$$

thereby completing the proof of the proposition. \blacksquare

The purpose of the above modification on the sample average estimate is to annihilate all the entries of the matrix $\widehat{\mathbf{R}}$ which correspond to the zero elements of \mathbf{R} .

We now turn our attention on using the structure of $\widetilde{\mathbf{R}}$ to simplify the computations involved in estimating the channel through the simplification of the cost functions to be minimized. As we mentioned before, since $\mathbf{S}_{1,r}^H\widehat{\mathbf{R}}^{-1}\mathbf{S}_{1,r} \neq \mathbf{S}_{1,i}^H\widehat{\mathbf{R}}^{-1}\mathbf{S}_{1,i}$ for MVDR estimators, in general, the channel vector estimate $\widehat{\mathbf{h}}_{\text{mv}}$ is obtained as the eigenvector that corresponds to the smallest eigenvalue of the matrix $\widehat{\mathbf{\Omega}}_{\text{mv}}$ in (4.20). On the other hand, when $\widehat{\mathbf{R}}$ is replaced by $\widetilde{\mathbf{R}}$ in (4.20), it can be verified that

$$\mathbf{S}_{1,r}^H\widetilde{\mathbf{R}}^{-1}\mathbf{S}_{1,r} = \mathbf{S}_{1,i}^H\widetilde{\mathbf{R}}^{-1}\mathbf{S}_{1,i}. \quad (4.33)$$

Thus, the result presented in Proposition 4 is now applicable and the channel vector estimate $\widetilde{\mathbf{h}}_{\text{mv}}$ is obtained as the eigenvector that corresponds to the smallest eigenvalue of the matrix $\widetilde{\mathbf{\Omega}}_{\text{mv}} = \mathbf{S}_{1,r}^H\widetilde{\mathbf{R}}^{-1}\mathbf{S}_{1,r}$, i.e.,

$$\widetilde{\mathbf{h}}_{\text{mv}} = \arg \min_{h, \|h\|=1} h^H\widetilde{\mathbf{\Omega}}_{\text{mv}}h. \quad (4.34)$$

Following a similar approach, it can be shown that for subspace algorithms, we have

$$\mathbf{S}_{1,r}^H\widetilde{\mathbf{Q}}_n\widetilde{\mathbf{Q}}_n^H\mathbf{S}_{1,r} = \mathbf{S}_{1,i}^H\widetilde{\mathbf{Q}}_n\widetilde{\mathbf{Q}}_n^H\mathbf{S}_{1,i}, \quad (4.35)$$

where $\widetilde{\mathbf{Q}}_n$ is the $L \times (L - 2K)$ matrix whose columns are the eigenvectors that correspond to the $L - 2K$ smallest eigenvalues of $\widetilde{\mathbf{R}}$.

In this case, the channel vector estimate $\widetilde{\mathbf{h}}_{\text{ss}}$ is obtained as the eigenvector that corresponds to the smallest eigenvalue of the matrix $\widetilde{\mathbf{\Omega}}_{\text{ss}}$ given by

$$\widetilde{\mathbf{\Omega}}_{\text{ss}} \triangleq \mathbf{S}_{1,r}^H\widetilde{\mathbf{Q}}_n\widetilde{\mathbf{Q}}_n^H\mathbf{S}_{1,r}. \quad (4.36)$$

The use of matrix $\tilde{\mathbf{R}}$ has yet another important practical implication which leads to further reduction of the computational complexity. First, let us express the objective function in the MVDR method to be minimized as

$$2\mathbf{g}_{1,r}^H \tilde{\mathbf{R}}^{-1} \mathbf{g}_{1,r} = 2\bar{\mathbf{g}}_{1,r}^H \begin{bmatrix} \mathbf{A} & \mathbf{0} \\ \mathbf{0} & \mathbf{B} \end{bmatrix}^{-1} \bar{\mathbf{g}}_{1,r}, \quad (4.37)$$

where $\mathbf{A} \triangleq [\tilde{R}_{(2p-1),(2q-1)}]_{1 \leq p,q \leq L/2}$ and $\mathbf{B} \triangleq [\tilde{R}_{2p,2q}]_{1 \leq p,q \leq L/2}$ are the $L/2 \times L/2$ matrices associated with the *odd* and *even* rows and columns of $\tilde{\mathbf{R}}$, respectively, and $\bar{\mathbf{g}}_{1,r}$ is the $L \times 1$ vector formed by augmenting the odd elements of $\mathbf{g}_{1,r}$ by their even counterparts. Then, using the inversion property of a block diagonal matrix, we rewrite (4.37) as

$$2\mathbf{g}_{1,r}^H \tilde{\mathbf{R}}^{-1} \mathbf{g}_{1,r} = 2\bar{\mathbf{g}}_{1,r}^H \begin{bmatrix} \mathbf{A}^{-1} & \mathbf{0} \\ \mathbf{0} & \mathbf{B}^{-1} \end{bmatrix} \bar{\mathbf{g}}_{1,r}. \quad (4.38)$$

Note that $\tilde{\mathbf{R}}$ is twice the size of \mathbf{A} or \mathbf{B} ; therefore, by calculating the inverse of the matrices \mathbf{A} and \mathbf{B} in (4.38) which involves $O((L/2)^3)$ flops each, compared to that of $\tilde{\mathbf{R}}$ that requires $O(L^3)$ flops, we significantly reduce the computational complexity of the MVDR estimator. Similarly, the complexity of subspace-based methods which mainly comes from the eigendecomposition can be reduced by applying EVD on smaller size matrices.

4.4.1 Identifiability

Inherent to all MISO blind channel identification problems without side information are permutation and scalar ambiguities [57]. The former, also known as antenna order ambiguity, arises when a system employing multiple antennas cannot distinguish between the subchannels, while the scalar ambiguity corresponds to the complex scale factor indeterminacy associated with the channel estimates. Generally, in an OFDM system these two ambiguities are resolved by sending known symbols from all transmitting antennas [10], but at the expense of a loss in bandwidth efficiency. In a CDMA system, on the other hand, the permutation ambiguity can be resolved by assigning distinct spreading codes to each user at each antenna [36], [15], [16]. However, such an approach again comes at the expense of extra resources, namely, the prohibitive penalty of requiring more than one spreading code per user. It is notable that in any CDMA-based system, the total number of active users that can be supported at any time is limited by the number of available spreading codes

(the length of the spreading factor). As can be seen from our system model, a significant advantage of the SFBC MC-CDMA systems compared to the above mentioned schemes is its ability to transform the spreading code \mathbf{s}_k for a given k to a set of linearly independent vectors. This can be interpreted as assigning each user different spreading codes (one for each transmit antenna). In other words, due to the signal structure imposed by SFBC, the SFBC MC-CDMA systems do not exhibit antenna order ambiguity.

In order to guarantee the unique identifiability of the channel estimates the conditions described by the following theorems have to hold.

Theorem 7 *The sufficient condition for the channel vectors \mathbf{h}_{mv} in (4.15) or \mathbf{h} in (4.23) to be uniquely identifiable up to an unknown complex scalar is that the matrix $\mathbf{\Gamma} \triangleq [\mathbf{S}_{1,r} \ \mathbf{g}_{2,r} \ \dots \ \mathbf{g}_{K,r} \ \mathbf{g}_{1,i} \ \mathbf{g}_{2,i} \ \dots \ \mathbf{g}_{K,i}]$ be full column rank.*

Proof: See Theorem 2 in Chapter 3 for a similar proof. ■

Theorem 8 *The necessary condition for the channel vector \mathbf{h} in (4.23) to be uniquely identifiable up to an unknown complex scalar is that $L \geq 2J + 2K - 1$.*

Proof: Using the fact that the channel is identifiable only if the $2J \times 2J$ matrix $\mathbf{\Omega}_{ss}$ in (4.25) is rank deficient by one, i.e., $\text{Rank}(\mathbf{\Omega}_{ss}) = 2J - 1$, it follows that there exists only one eigenvector that corresponds to the one zero eigenvalue. Moreover, since $\text{Rank}(\mathbf{\Omega}_{ss}) = \text{Rank}(\mathbf{S}_{1,r}^H \mathbf{Q}_n)$, we must have $2J - 1 \leq \min(2J, L - 2K)$, or equivalently, $L \geq 2J + 2K - 1$. ■

Theorem 7 implies that since $\mathbf{\Gamma}$ is a $L \times (2J + 2K - 1)$ matrix, for the sufficient condition to be satisfied, we should have $K \leq (L - 2J + 1)/2 \triangleq K'$. However, this does not imply that the channel is not identifiable for $K > K'$. In fact, as the simulation studies presented later show, the MVDR estimator is capable to provide reliable channel estimates even for $K > K'$. This is in contrast to the subspace approach in which the necessary condition imposes a hard upper limit, K' , on the number of users. More specifically, in the case of $K > K'$, the noise subspace does not exist at all and the subspace algorithm is therefore not applicable.

Another interesting observation from Theorem 7 is that compared to the pre-FFT subspace channel estimator presented in Chapter 3 where the necessary condition imposes the upper bound $(L + 1)/2$ on the number of active users, the post-FFT approach suffers from some loss in the degrees of freedom. In other words, the former would be able to support J users more than the post-FFT approach in the same system.

4.5 Performance Analysis

In this section, we provide a theoretical performance analysis of the modified channel estimation methods described above under small perturbations assumptions. More specifically, we first evaluate the bias of each estimator followed by the derivation of closed form expressions for the corresponding mean-square-error (MSE) performance. In the next section, we develop the Cramer-Rao bounds (CRBs) on the error variance of any unbiased or biased channel estimator for SFBC MC-CDMA systems.

4.5.1 MVDR Algorithm Mean-Squared Error Performance

In [24] under a small noise assumption, an analytical expression for the asymptotic bias of the MVDR estimators is derived which involves the noise subspace \mathbf{Q}_n and is given by

$$\Delta \mathbf{h}_{mv} = \mathbf{h}_{mv} - \mathbf{h} \simeq -\sigma^2 \mathbf{A}_0^\dagger \mathbf{A}_1 \mathbf{h}, \quad (4.39)$$

where

$$\mathbf{A}_0 = 2\mathbf{S}_{1,r}^H \mathbf{Q}_n \mathbf{Q}_n^H \mathbf{S}_{1,r}, \quad (4.40)$$

$$\mathbf{A}_1 = 2\mathbf{S}_{1,r}^H \mathbf{Q}_s \Lambda_s^{-1} \mathbf{Q}_s^H \mathbf{S}_{1,r}. \quad (4.41)$$

The major shortcoming of this approach lies on the fact that in SFBC MC-CDMA systems for medium to highly loaded cases where $L < 2J + 2K - 1$ (see Theorem 8) the noise subspace does not exist. In this subsection, we will present an alternative approach to derive a closed form expression for the asymptotic bias of the MVDR channel estimator that does not suffer from the shortcomings of the traditional approach. The presented analysis is particularly attractive in situations where the size of noise subspace is small, namely, systems with medium to heavy loading, severe multipath distortion, small FFT size, or small processing gain. In essence, the expression in (4.39) typically requires a sufficiently large noise subspace in order to accurately estimate the asymptotic bias. The proposed approach is based on the multivariate first-order Taylor series expansion of the Lagrangian function corresponding to the constraint optimization problem in (4.15).

Theorem 9 *Let \mathbf{h}_{mv} be the solution to the minimization problem in (4.15). Then, the*

asymptotic channel estimation bias $\Delta \mathbf{h}_{mv} = \mathbf{h}_{mv} - \mathbf{h}$ is given by

$$\Delta \mathbf{h}_{mv} \simeq \left((\mathbf{h}^H \boldsymbol{\Omega}_{mv}^{-1} \mathbf{h})^{-1} \boldsymbol{\Omega}_{mv}^{-1} - \mathbf{I}_{2J} \right) \mathbf{h}, \quad (4.42)$$

where $\boldsymbol{\Omega}_{mv} \triangleq 2\mathbf{S}_{1,r}^H \mathbf{R}^{-1} \mathbf{S}_{1,r}$.

Proof: Let $f(\mathbf{h}) = 2\mathbf{h}^H \mathbf{S}_{1,r}^H \mathbf{R}^{-1} \mathbf{S}_{1,r} \mathbf{h}$ be the function to be minimized subject to the constraint $c(\mathbf{h}) = \mathbf{h}^H \mathbf{h} - 1$. The asymptotic biased channel estimate \mathbf{h}_{mv} satisfies

$$\nabla F(\mathbf{h}_{mv}, \tilde{\lambda}) = 0, \quad (4.43)$$

where

$$F(\mathbf{h}, \lambda) = 2\mathbf{h}^H \mathbf{S}_{1,r}^H \mathbf{R}^{-1} \mathbf{S}_{1,r} \mathbf{h} - \lambda(\mathbf{h}^H \mathbf{h} - 1), \quad (4.44)$$

is the augmented Lagrangian function with λ as the Lagrange multiplier. Thus, by considering the multivariate first-order Taylor series expansion of $\nabla F(\mathbf{h}, \lambda)$ around $[\mathbf{h}^T, 0]^T$ and retaining terms up to the second order, we can write

$$\nabla F(\mathbf{h}, \lambda) \simeq \nabla F(\mathbf{h}, 0) + \nabla^2 F(\mathbf{h}, 0) \begin{bmatrix} \mathbf{h} - \mathbf{h} \\ \lambda \end{bmatrix}, \quad (4.45)$$

where

$$\begin{aligned} \nabla^2 F(\mathbf{h}, 0) &= \begin{bmatrix} \mathcal{H} & \mathcal{M} \\ \mathcal{M}^H & \mathbf{0} \end{bmatrix}, \\ \nabla F(\mathbf{h}, 0) &= \begin{bmatrix} \mathcal{N} \\ c(\mathbf{h}) \end{bmatrix}. \end{aligned} \quad (4.46)$$

In (4.46),

$$\mathcal{N} \triangleq 2 \left. \frac{\partial F(\mathbf{h}, \lambda)}{\partial \mathbf{h}^*} \right|_{\mathbf{h}=\mathbf{h}, \lambda=0} = 4\mathbf{S}_{1,r}^H \mathbf{R}^{-1} \mathbf{S}_{1,r} \mathbf{h} = 2\boldsymbol{\Omega}_{mv} \mathbf{h} \in \mathbb{C}^{2J \times 1} \quad (4.47)$$

and

$$\mathcal{H} \triangleq \left. \frac{\partial^2 F(\mathbf{h}, \lambda)}{\partial \mathbf{h} \partial \mathbf{h}^H} \right|_{\mathbf{h}=\mathbf{h}, \lambda=0} = 4\mathbf{S}_{1,r}^H \mathbf{R}^{-1} \mathbf{S}_{1,r} = 2\boldsymbol{\Omega}_{mv} \in \mathbb{C}^{2J \times 2J} \quad (4.48)$$

are the gradient and the Hessian, respectively, of $\nabla F(\mathbf{h}, \lambda)$ evaluated at $\mathbf{h} = \mathbf{h}$ and $\lambda = 0$ and

$$\mathcal{M} \triangleq 2 \frac{\partial c(\mathbf{h})}{\partial \mathbf{h}^*} \Big|_{\mathbf{h}=\mathbf{h}} = 2\mathbf{h} \in \mathbb{C}^{2J \times 1} \quad (4.49)$$

is the gradient of the constraint $c(\mathbf{h})$ evaluated at $\mathbf{h} = \mathbf{h}$. For $\mathbf{h} = \mathbf{h}_{mv}$ and $\lambda = \tilde{\lambda}$, we can write

$$\nabla F(\mathbf{h}_{mv}, \tilde{\lambda}) \simeq \nabla F(\mathbf{h}, 0) + \nabla^2 F(\mathbf{h}, 0) \begin{bmatrix} \Delta \mathbf{h}_{mv} \\ \tilde{\lambda} \end{bmatrix}, \quad (4.50)$$

from which we obtain the following system

$$\mathcal{H} \Delta \mathbf{h}_{mv} + \mathcal{M} \tilde{\lambda} \simeq -\mathcal{N}, \quad (4.51)$$

$$\mathcal{M}^H \Delta \mathbf{h}_{mv} \simeq -c(\mathbf{h}). \quad (4.52)$$

Solving for $\Delta \mathbf{h}_{mv}$ we obtain

$$\Delta \mathbf{h}_{mv} \simeq -\mathcal{H}^{-1} (\mathcal{N} + \mathcal{M} (\mathcal{M}^H \mathcal{H}^{-1} \mathcal{M})^{-1} (c(\mathbf{h}) - \mathcal{M}^H \mathcal{H}^{-1} \mathcal{N})), \quad (4.53)$$

which using (4.47)-(4.49) and the constraint expression results in (4.42). We note that since \mathbf{R}^{-1} is positive definite and both matrices \mathbf{S}_k and $\tilde{\mathbf{F}}$ have full rank, Ω_{mv} is positive definite and, therefore, invertible. ■

Since $\Delta \mathbf{h}_{mv} = \mathbf{h}_{mv} - \mathbf{h}$, the theorem above immediately implies the following corollary.

Corollary 1 *The channel estimate \mathbf{h}_{mv} can be approximated by*

$$\mathbf{h}_{mv} \simeq \frac{\Omega_{mv}^{-1} \mathbf{h}}{\mathbf{h}^H \Omega_{mv}^{-1} \mathbf{h}}. \quad (4.54)$$

■

The above theorem presents the channel estimation error due to the noise only, however, the performance of the MVDR estimator is also affected by finite received data samples. By adapting the results presented in [55] to the system under consideration and assuming that the size of collected data samples is sufficiently large such that perturbation technique is applicable, we obtain the following theorem which provides an analytical expression for the MSE between $\tilde{\mathbf{h}}_{mv}$ and \mathbf{h}_{mv} .

Theorem 10 *Let $\delta \mathbf{h}_{mv} = \tilde{\mathbf{h}}_{mv} - \mathbf{h}_{mv}$ be the estimation error of the MVDR estimator in*

(4.34). We have

$$(i) \delta \mathbf{h}_{mv} = \Sigma_{mv}^H \delta \mathbf{R} \mathbf{R}^{-1} \mathbf{S}_{1,r} \mathbf{h}_{mv}, \text{ where } \Sigma_{mv} \triangleq \mathbf{R}^{-1} \mathbf{S}_{1,r} \Omega_{mv}^\dagger \text{ and } \delta \mathbf{R} \triangleq \tilde{\mathbf{R}} - \mathbf{R}.$$

$$(ii) \mathbb{E}\{\|\delta \mathbf{h}_{mv}\|^2\} \simeq \text{tr}(\Sigma_{mv}^H \mathbb{E}\{\delta \mathbf{R} \mathbf{Z} \delta \mathbf{R}\} \Sigma_{mv}), \text{ where } \mathbf{Z} \triangleq \mathbf{R}^{-1} \mathbf{S}_{1,r} \mathbf{h}_{mv} \mathbf{h}_{mv}^H \mathbf{S}_{1,r}^H \mathbf{R}^{-1}, \text{ and}$$

$$\mathbb{E}\{\delta \mathbf{R} \mathbf{Z} \delta \mathbf{R}\} = (\text{tr}(\mathbf{R} \mathbf{Z}) \mathbf{R} - \mathbf{G}(\mathbf{I} \odot \mathbf{G}^H \mathbf{Z} \mathbf{G}) \mathbf{G}^H) / N. \quad (4.55)$$

Proof: See Theorem 5 in Chapter 3 for a similar proof. ■

Combining the results from Theorems 9 and 10, we obtain the following Corollary.

Corollary 2 *The overall mean-squared channel estimation error of the MVDR estimator is given by*

$$\begin{aligned} \mathbb{E}\{\|\tilde{\mathbf{h}}_{mv} - \mathbf{h}\|^2\} &= \mathbb{E}\{\|(\mathbf{h}_{mv} - \mathbf{h}) + (\tilde{\mathbf{h}}_{mv} - \mathbf{h}_{mv})\|^2\} \\ &= \|\Delta \mathbf{h}_{mv}\|^2 + \mathbb{E}\{\|\delta \mathbf{h}_{mv}\|^2\}. \end{aligned} \quad (4.56)$$

In the derivation of (4.56), we have used the fact that $\Delta \mathbf{h}_{mv}$ is deterministic which in conjunction with the result from the part (i) of Theorem 10 (i.e. $\mathbb{E}\{\delta \mathbf{h}_{mv}\} = 0$) implies that $\Delta \mathbf{h}_{mv}^H \mathbb{E}\{\delta \mathbf{h}_{mv}\} = \mathbb{E}\{\delta \mathbf{h}_{mv}^H\} \Delta \mathbf{h}_{mv} = 0$. Note that the first term in the RHS of (4.56) represents the contribution to the MSE of the asymptotic bias of the estimate $\hat{\mathbf{h}}_{mv}$. ■

4.5.2 Subspace Algorithm Mean-Squared Error Performance

The statistical performance of the subspace-based channel estimation algorithms in terms of channel MSE has been investigated in [40], [41]. Those works, however, are based on the Singular Value Decomposition (SVD) of \mathbf{R} . In this subsection, using a method similar to that used in Chapter 3, in which the bias and MSE for conventional subspace are found in terms of the eigenvalue decomposition (EVD) of \mathbf{R} , we have the following results.

Theorem 11 *Let $\delta \mathbf{h}_{ss} = \mathbf{h} - \tilde{\mathbf{h}}_{ss}$ be the estimation error of the subspace based estimator. Then, the bias and the MSE of the estimator are, respectively, given by*

$$(i) \delta \mathbf{h}_{ss} \simeq \boldsymbol{\Omega}_{ss}^\dagger \mathbf{S}_{1,r}^H \mathbf{Q}_n \mathbf{Q}_n^H \delta \mathbf{R} \boldsymbol{\Upsilon}^\dagger \mathbf{S}_{1,r} \mathbf{h},$$

where $\boldsymbol{\Upsilon} \triangleq \mathbf{Q}_s (\boldsymbol{\Lambda}_s - \sigma^2 \mathbf{I}) \mathbf{Q}_s^H$ and $\delta \mathbf{R} \triangleq \tilde{\mathbf{R}} - \mathbf{R}$.

$$(ii) \mathbb{E}\{|\delta \mathbf{h}_{ss}|^2\} \simeq \frac{2\sigma^2 \rho}{N} \text{tr}(\boldsymbol{\Sigma}_{ss}^H \boldsymbol{\Sigma}_{ss}),$$

where $\boldsymbol{\Sigma}_{ss} \triangleq \mathbf{Q}_n^H \mathbf{S}_{1,r} \boldsymbol{\Omega}_{ss}^\dagger$, and $\rho = \mathbf{h}^H \mathbf{S}_{1,r}^H \boldsymbol{\Upsilon}^\dagger \mathbf{R} \boldsymbol{\Upsilon}^\dagger \mathbf{S}_{1,r} \mathbf{h}$.

Proof: See Theorem 3 in Chapter 3 for a similar proof. ■

A direct implication of the above theorem is that unlike the MVDR estimator, the subspace estimator is asymptotically unbiased (i.e., $\mathbb{E}\{\delta \mathbf{h}_{ss}\} = 0$) even in the presence of noise. Therefore, the MSE given by the part (ii) of the above theorem will be lower bounded by the classical CRB [52] which is derived next.

4.6 Cramer-Rao Bounds

In this section, we derive the CRBs for both unbiased and biased estimators, wherein the spreading codes of the interfering users and the transmitted symbols are treated as unknown deterministic quantities. We start by deriving the bound for unbiased estimators.

Let us define the set of unknown deterministic parameters $\boldsymbol{\theta}$ as

$$\boldsymbol{\theta} \triangleq [\boldsymbol{\theta}_b^T, \boldsymbol{\theta}_s^T, \boldsymbol{\theta}_h^T]^T \in \mathbb{R}^{2KN+4J+(K-1)L}, \quad (4.57)$$

where

$$\begin{aligned} \boldsymbol{\theta}_h &\triangleq [\Re(\mathbf{h}_1)^T, \Re(\mathbf{h}_2)^T, \Im(\mathbf{h}_1)^T, \Im(\mathbf{h}_2)^T]^T, \\ \boldsymbol{\theta}_s &\triangleq [\mathbf{s}_2^T, \dots, \mathbf{s}_K^T]^T, \\ \boldsymbol{\theta}_b &\triangleq [\Re(\mathbf{b}(1))^T, \Im(\mathbf{b}(1))^T, \dots, \Re(\mathbf{b}(N))^T, \Im(\mathbf{b}(N))^T]^T, \end{aligned}$$

with $\mathbf{b}(n) \triangleq [b_1(n), b_2(n), \dots, b_K(n)]^T$, $n = 1, 2, \dots, N$. The CRB provides a lower bound on the covariance of any unbiased estimate $\hat{\boldsymbol{\theta}}$ of the parameter vector $\boldsymbol{\theta}$, i.e.,

$$\mathbb{E}\{(\hat{\boldsymbol{\theta}} - \boldsymbol{\theta})(\hat{\boldsymbol{\theta}} - \boldsymbol{\theta})^T\} \geq \text{Diag}(\mathbf{J}_{\boldsymbol{\theta}\boldsymbol{\theta}})^{-1} = \text{CRB}(\boldsymbol{\theta}), \quad (4.58)$$

where $\mathbf{J}_{\theta\theta}$ is the Fisher information matrix (FIM) given by

$$\mathbf{J}_{\theta\theta} \triangleq \mathbb{E} \left\{ \left(\frac{\partial \mathcal{L}}{\partial \boldsymbol{\theta}} \right) \left(\frac{\partial \mathcal{L}}{\partial \boldsymbol{\theta}} \right)^T \right\} = \begin{bmatrix} \mathbf{J}_{\mathbf{b}\mathbf{b}} & \mathbf{J}_{\mathbf{b}\mathbf{s}} & \mathbf{J}_{\mathbf{b}\mathbf{h}} \\ \mathbf{J}_{\mathbf{b}\mathbf{s}}^T & \mathbf{J}_{\mathbf{s}\mathbf{s}} & \mathbf{J}_{\mathbf{s}\mathbf{h}} \\ \mathbf{J}_{\mathbf{b}\mathbf{h}}^T & \mathbf{J}_{\mathbf{s}\mathbf{h}}^T & \mathbf{J}_{\mathbf{h}\mathbf{h}} \end{bmatrix}, \quad (4.59)$$

with \mathcal{L} denoting the log-likelihood function for N consecutive received blocks defined by

$$\mathcal{L} = -LN \ln(\pi\sigma^2) - \frac{1}{\sigma^2} \sum_{n=1}^N \left\| \mathbf{r}(n) - \sum_{k=1}^K \left(\mathbf{S}_{k,r} \mathbf{h} \Re(b_k(n)) + \mathbf{S}_{k,i} \mathbf{h} \Im(b_k(n)) \right) \right\|^2. \quad (4.60)$$

Applying the same approach as in Chapter 3, we compute the elements of the FIM in (4.59) by first taking partial derivatives of log-likelihood function in (4.60) with respect to $\boldsymbol{\theta}$ to obtain

$$\frac{\partial \mathcal{L}}{\partial \boldsymbol{\theta}} = \left[\left(\frac{\partial \mathcal{L}}{\partial \Re(\mathbf{b}(p))} \right)^T, \left(\frac{\partial \mathcal{L}}{\partial \Im(\mathbf{b}(p))} \right)^T, \left(\frac{\partial \mathcal{L}}{\partial \Re(\mathbf{h})} \right)^T, \left(\frac{\partial \mathcal{L}}{\partial \Im(\mathbf{h})} \right)^T, \left(\frac{\partial \mathcal{L}}{\partial \tilde{\mathbf{S}}} \right)^T \right]^T,$$

where

$$\frac{\partial \mathcal{L}}{\partial \Re(\mathbf{b}(p))} = \frac{2}{\sigma^2} \Re(\mathbf{G}_r^H \mathbf{n}(p)), \quad (4.61)$$

$$\frac{\partial \mathcal{L}}{\partial \Im(\mathbf{b}(p))} = \frac{2}{\sigma^2} \Im(\mathbf{G}_i^H \mathbf{n}(p)), \quad (4.62)$$

$$\frac{\partial \mathcal{L}}{\partial \Re(\mathbf{h})} = \frac{2}{\sigma^2} \sum_{p=1}^N \sum_{k=1}^K \Re(\mathcal{G}_k(p)^H \mathbf{n}(p)), \quad (4.63)$$

$$\frac{\partial \mathcal{L}}{\partial \Im(\mathbf{h})} = \frac{2}{\sigma^2} \sum_{p=1}^N \sum_{k=1}^K \Im(-j \mathcal{G}_k(p)^H \mathbf{n}(p)), \quad (4.64)$$

$$\frac{\partial \mathcal{L}}{\partial \mathbf{s}_k} = \frac{2}{\sigma^2} \sum_{p=1}^N \Re(\mathcal{T}_k(p)^H \mathbf{n}(p)) \quad k = 2, \dots, K, \quad (4.65)$$

with

$$\begin{aligned} \mathcal{T}_k(p) &\triangleq (\mathbf{F}\mathbf{H}_1\mathbf{F}^H\mathbf{D}_1 + \mathbf{F}\mathbf{H}_2\mathbf{F}^H\mathbf{D}_3) \Re(b_k(p)) + (\mathbf{F}\mathbf{H}_1\mathbf{F}^H\mathbf{D}_2 + \mathbf{F}\mathbf{H}_2\mathbf{F}^H\mathbf{D}_4) \Im(b_k(p)), \\ \mathcal{G}_k(p) &\triangleq \mathbf{S}_{k,r} \Re(b_k(p)) + \mathbf{S}_{k,i} \Im(b_k(p)), \end{aligned}$$

$$\begin{aligned}
\mathbf{G}_r &\triangleq [\mathbf{g}_{1,r} \ \mathbf{g}_{2,r} \ \dots \ \mathbf{g}_{K,r}], \\
\mathbf{G}_i &\triangleq [\mathbf{g}_{1,i} \ \mathbf{g}_{2,i} \ \dots \ \mathbf{g}_{K,i}], \\
\tilde{\mathbf{S}} &\triangleq [\mathbf{s}_2, \dots, \mathbf{s}_K],
\end{aligned}$$

The elements of the FIM can then be calculated as

$$\mathbb{E} \left\{ \frac{\partial \mathcal{L}}{\partial \Re(\mathbf{b}(p))} \left(\frac{\partial \mathcal{L}}{\partial \Re(\mathbf{b}(q))} \right)^T \right\} = \frac{2}{\sigma^2} \Re(\mathbf{G}_r^H \mathbf{G}_r) \triangleq \tilde{\pi} \delta_{p,q} \quad (4.66)$$

$$\mathbb{E} \left\{ \frac{\partial \mathcal{L}}{\partial \Re(\mathbf{b}(p))} \left(\frac{\partial \mathcal{L}}{\partial \Im(\mathbf{b}(q))} \right)^T \right\} = \frac{2}{\sigma^2} \Re(\mathbf{G}_r^H \mathbf{G}_i) \triangleq \tilde{\pi} \delta_{p,q} \quad (4.67)$$

$$\mathbb{E} \left\{ \frac{\partial \mathcal{L}}{\partial \Im(\mathbf{b}(p))} \left(\frac{\partial \mathcal{L}}{\partial \Re(\mathbf{b}(q))} \right)^T \right\} = \frac{2}{\sigma^2} \Re(\mathbf{G}_i^H \mathbf{G}_r) \triangleq -\tilde{\pi} \delta_{p,q} \quad (4.68)$$

$$\mathbb{E} \left\{ \frac{\partial \mathcal{L}}{\partial \Im(\mathbf{b}(p))} \left(\frac{\partial \mathcal{L}}{\partial \Im(\mathbf{b}(q))} \right)^T \right\} = \frac{2}{\sigma^2} \Re(\mathbf{G}_i^H \mathbf{G}_i) \triangleq \tilde{\pi} \delta_{p,q} \quad (4.69)$$

$$\mathbb{E} \left\{ \frac{\partial \mathcal{L}}{\partial \Re(\mathbf{b}(p))} \left(\frac{\partial \mathcal{L}}{\partial \mathbf{s}_k} \right)^T \right\} = \frac{2}{\sigma^2} \Re(\mathbf{G}_r^H \mathbf{T}_k(p)) \triangleq \mathcal{D}_{k,r}(p) \quad (4.70)$$

$$\mathbb{E} \left\{ \frac{\partial \mathcal{L}}{\partial \Im(\mathbf{b}(p))} \left(\frac{\partial \mathcal{L}}{\partial \mathbf{s}_k} \right)^T \right\} = \frac{2}{\sigma^2} \Re(\mathbf{G}_i^H \mathbf{T}_k(p)) \triangleq \mathcal{D}_{k,i}(p) \quad (4.71)$$

$$\mathbb{E} \left\{ \frac{\partial \mathcal{L}}{\partial \Re(\mathbf{b}(p))} \left(\frac{\partial \mathcal{L}}{\partial \Re(\mathbf{h})} \right)^T \right\} = \frac{2}{\sigma^2} \sum_{k=1}^K \Re(\mathbf{G}_r^H \mathcal{G}_k(p)) \triangleq \bar{\xi}_r(p) \quad (4.72)$$

$$\mathbb{E} \left\{ \frac{\partial \mathcal{L}}{\partial \Re(\mathbf{b}(p))} \left(\frac{\partial \mathcal{L}}{\partial \Im(\mathbf{h})} \right)^T \right\} = \frac{2}{\sigma^2} \sum_{k=1}^K \Re(j \mathbf{G}_r^H \mathcal{G}_k(p)) \triangleq \tilde{\xi}_r(p) \quad (4.73)$$

$$\mathbb{E} \left\{ \frac{\partial \mathcal{L}}{\partial \Im(\mathbf{b}(p))} \left(\frac{\partial \mathcal{L}}{\partial \Re(\mathbf{h})} \right)^T \right\} = \frac{2}{\sigma^2} \sum_{k=1}^K \Re(\mathbf{G}_i^H \mathcal{G}_k(p)) \triangleq \bar{\xi}_i(p) \quad (4.74)$$

$$\mathbb{E} \left\{ \frac{\partial \mathcal{L}}{\partial \Im(\mathbf{b}(p))} \left(\frac{\partial \mathcal{L}}{\partial \Im(\mathbf{h})} \right)^T \right\} = \frac{2}{\sigma^2} \sum_{k=1}^K \Re(j \mathbf{G}_i^H \mathcal{G}_k(p)) \triangleq \tilde{\xi}_i(p) \quad (4.75)$$

$$\mathbb{E} \left\{ \frac{\partial \mathcal{L}}{\partial \mathbf{s}_k} \left(\frac{\partial \mathcal{L}}{\partial \mathbf{s}_{k'}} \right)^T \right\} = \frac{2}{\sigma^2} \sum_{p=1}^N \Re(\mathbf{T}_k(p)^H \mathbf{T}_{k'}(p)) \triangleq \mathcal{S}_{k,k'} \quad (4.76)$$

$$\mathbb{E} \left\{ \frac{\partial \mathcal{L}}{\partial \mathbf{s}_k} \left(\frac{\partial \mathcal{L}}{\partial \Re(\mathbf{h})} \right)^T \right\} = \frac{2}{\sigma^2} \sum_{p=1}^N \Re(\mathbf{T}_k(p)^H \mathcal{G}_k(p)) \triangleq \psi_{k,r} \quad (4.77)$$

$$\mathbb{E} \left\{ \frac{\partial \mathcal{L}}{\partial \mathbf{s}_k} \left(\frac{\partial \mathcal{L}}{\partial \mathfrak{S}(\mathbf{h})} \right)^T \right\} = \frac{2}{\sigma^2} \sum_{p=1}^N \Re (j \mathbf{T}_k(p)^H \mathcal{G}_k(p)) \triangleq \psi_{k,i} \quad (4.78)$$

$$\mathbb{E} \left\{ \frac{\partial \mathcal{L}}{\partial \Re(\mathbf{h})} \left(\frac{\partial \mathcal{L}}{\partial \Re(\mathbf{h})} \right)^T \right\} = \frac{2}{\sigma^2} \sum_{p=1}^N \sum_{k=1}^K \Re (\mathcal{G}_k(p)^H \mathcal{G}_k(p)) \triangleq \bar{\phi} \quad (4.79)$$

$$\mathbb{E} \left\{ \frac{\partial \mathcal{L}}{\partial \Re(\mathbf{h})} \left(\frac{\partial \mathcal{L}}{\partial \Im(\mathbf{h})} \right)^T \right\} = \frac{2}{\sigma^2} \sum_{p=1}^N \sum_{k=1}^K \Re (j \mathcal{G}_k(p)^H \mathcal{G}_k(p)) \triangleq \tilde{\phi} \quad (4.80)$$

$$\mathbb{E} \left\{ \frac{\partial \mathcal{L}}{\partial \Im(\mathbf{h})} \left(\frac{\partial \mathcal{L}}{\partial \Re(\mathbf{h})} \right)^T \right\} = \frac{2}{\sigma^2} \sum_{p=1}^N \sum_{k=1}^K \Re (-j \mathcal{G}_k(p)^H \mathcal{G}_k(p)) \triangleq -\tilde{\phi} \quad (4.81)$$

$$\mathbb{E} \left\{ \frac{\partial \mathcal{L}}{\partial \Im(\mathbf{h})} \left(\frac{\partial \mathcal{L}}{\partial \Im(\mathbf{h})} \right)^T \right\} = \frac{2}{\sigma^2} \sum_{p=1}^N \sum_{k=1}^K \Re (\mathcal{G}_k(p)^H \mathcal{G}_k(p)) \triangleq \bar{\phi} \quad (4.82)$$

Let us define the following block matrices:

$$\begin{aligned} \mathbf{\Pi} &\triangleq \begin{bmatrix} \bar{\pi} & \tilde{\pi} \\ -\tilde{\pi} & \bar{\pi} \end{bmatrix}, \mathbf{D}(p) \triangleq \begin{bmatrix} \mathcal{D}_{2,r}(p) & \dots & \mathcal{D}_{K,r}(p) \\ \mathcal{D}_{2,i}(p) & \dots & \mathcal{D}_{K,i}(p) \end{bmatrix}, \mathbf{\Xi}(n) \triangleq \begin{bmatrix} \bar{\xi}_r(n) & \tilde{\xi}_r(n) \\ \bar{\xi}_i(n) & \tilde{\xi}_i(n) \end{bmatrix}, \\ \mathbf{\Psi} &\triangleq \begin{bmatrix} \psi_{2,r}^T & \dots & \psi_{K,r}^T \\ \psi_{2,i}^T & \dots & \psi_{K,i}^T \end{bmatrix}^T, \mathbf{\Phi} \triangleq \begin{bmatrix} \bar{\phi} & \tilde{\phi} \\ -\tilde{\phi} & \bar{\phi} \end{bmatrix}, \mathbf{S} \triangleq \begin{bmatrix} \mathcal{S}_{2,2} & \dots & \mathcal{S}_{2,K} \\ \vdots & \dots & \vdots \\ \mathcal{S}_{K,2} & \dots & \mathcal{S}_{K,K} \end{bmatrix}. \end{aligned} \quad (4.83)$$

Assembling the equations (4.66)-(4.83) results in the following FIM:

$$\mathbf{J}_{\theta\theta} \triangleq \begin{array}{c|cc} \begin{array}{cccc} \mathbf{\Pi} & \mathbf{0} & \dots & \mathbf{0} \\ \mathbf{0} & \mathbf{\Pi} & \dots & \mathbf{0} \\ \vdots & \vdots & \ddots & \vdots \\ \mathbf{0} & \mathbf{0} & \dots & \mathbf{\Pi} \end{array} & \begin{array}{c} \mathbf{D}(1) \\ \mathbf{D}(2) \\ \vdots \\ \mathbf{D}(N) \end{array} & \begin{array}{c} \mathbf{\Xi}(1) \\ \mathbf{\Xi}(2) \\ \vdots \\ \mathbf{\Xi}(N) \end{array} \\ \hline \begin{array}{cccc} \mathbf{D}^T(1) & \mathbf{D}^T(2) & \dots & \mathbf{D}^T(N) \end{array} & \mathbf{S} & \mathbf{\Psi} \\ \hline \begin{array}{cccc} \mathbf{\Xi}^T(1) & \mathbf{\Xi}^T(2) & \dots & \mathbf{\Xi}^T(N) \end{array} & \mathbf{\Psi}^T & \mathbf{\Phi} \end{array} \quad (4.84)$$

Finally, we have

$$\begin{aligned} \mathbf{J}_{\text{bs}} &\triangleq [\mathbf{D}(1)^T, \dots, \mathbf{D}(N)^T]^T, & \mathbf{J}_{\text{bb}} &\triangleq \mathbf{I}_N \otimes \mathbf{\Pi}, & \mathbf{J}_{\text{ss}} &\triangleq \mathbf{S}, \\ \mathbf{J}_{\text{bh}} &\triangleq [\mathbf{\Xi}(1)^T, \dots, \mathbf{\Xi}(N)^T]^T, & \mathbf{J}_{\text{sh}} &\triangleq \mathbf{\Psi}, & \mathbf{J}_{\text{hh}} &\triangleq \mathbf{\Phi}, \end{aligned} \quad (4.85)$$

Since we are interested in the covariance matrix of the channel estimate, we may use the

block inversion formula to form the Schur complement of matrix $\mathbf{J}_{\mathbf{h}\mathbf{h}}$ in (4.59) as

$$\mathbf{J}(\mathbf{h}) = \mathbf{J}_{\mathbf{h}\mathbf{h}} - [\mathbf{J}_{\mathbf{b}\mathbf{h}}^T \quad \mathbf{J}_{\mathbf{s}\mathbf{h}}^T] \begin{bmatrix} \mathbf{J}_{\mathbf{b}\mathbf{b}} & \mathbf{J}_{\mathbf{b}\mathbf{s}} \\ \mathbf{J}_{\mathbf{b}\mathbf{s}}^T & \mathbf{J}_{\mathbf{s}\mathbf{s}} \end{bmatrix}^{-1} \begin{bmatrix} \mathbf{J}_{\mathbf{b}\mathbf{h}} \\ \mathbf{J}_{\mathbf{s}\mathbf{h}} \end{bmatrix}. \quad (4.86)$$

Consequently, the CRB on the error covariance of any unbiased channel estimator is given by $\text{CRB}(\mathbf{h}) = \mathbf{J}(\mathbf{h})^\dagger$. We note that, for this problem, in order to regularize the channel estimation problem without imposing any additional constraint on the channel, we chose to form the CRB by taking the pseudo-inverse of $\mathbf{J}(\mathbf{h})$ in (4.86). This approach corresponds to the application of the minimum number of independent constraints [54]. Moreover, in the derivation of the CRB, due to the downlink application of the presented channel estimator, we assumed the knowledge of only the spreading code of the desired user. As is shown in Chapter 3, the latter results in a tighter bound than the CRB derived based on the knowledge of all users' spreading signatures including those presented in [42], [43]. More specifically, by treating the interfering users spreading codes as deterministic unknown quantities, the additional terms $\mathbf{J}_{\mathbf{b}\mathbf{s}}$, $\mathbf{J}_{\mathbf{s}\mathbf{s}}$ and $\mathbf{J}_{\mathbf{s}\mathbf{h}}$ have to be determined for evaluation of the FIM.

A bound of the form developed above is only valid for unbiased estimators. However for the biased estimators, such as the MVDR estimators, the variance of the estimates cannot be bounded by the classical CRB. In such cases, it is shown in [56] that the total variance of any estimator with a given bias is bounded by the biased CRB (BCRB), which is an extension of the CRB for unbiased estimators. In the following, we derive the BCRB for the MVDR channel estimator.

Following similar approach as in Chapter 3, the covariance of $\tilde{\mathbf{h}}_{\text{mv}}$ must satisfy

$$\begin{aligned} \mathbb{E} \left\{ (\tilde{\mathbf{h}}_{\text{mv}} - \mathbb{E}\{\tilde{\mathbf{h}}_{\text{mv}}\})(\tilde{\mathbf{h}}_{\text{mv}} - \mathbb{E}\{\tilde{\mathbf{h}}_{\text{mv}}\})^T \right\} \\ \geq \left(\frac{\partial \mathbb{E}\{\tilde{\mathbf{h}}_{\text{mv}}\}}{\partial \boldsymbol{\theta}_h} \right)^H \mathbf{J}^\dagger(\mathbf{h}) \frac{\partial \mathbb{E}\{\tilde{\mathbf{h}}_{\text{mv}}\}}{\partial \boldsymbol{\theta}_h} = \text{BCRB}(\mathbf{h}), \end{aligned} \quad (4.87)$$

where $\mathbb{E}\{\tilde{\mathbf{h}}_{\text{mv}}\} = \mathbf{h} + \Delta \mathbf{h}_{\text{mv}}$, and

$$\frac{\partial \mathbb{E}\{\tilde{\mathbf{h}}_{\text{mv}}\}}{\partial \boldsymbol{\theta}_h} = \left[\left(\frac{\partial \mathbb{E}\{\tilde{\mathbf{h}}_{\text{mv}}\}}{\partial \Re(\mathbf{h})} \right)^T, \left(\frac{\partial \mathbb{E}\{\tilde{\mathbf{h}}_{\text{mv}}\}}{\partial \Im(\mathbf{h})} \right)^T \right]^T. \quad (4.88)$$

Indeed, from (4.42) we obtain

$$\mathbb{E}\{\hat{\mathbf{h}}_{\text{mv}}\} = \frac{\boldsymbol{\Omega}_{\text{mv}}^{-1} \mathbf{h}}{\mathbf{h}^H \boldsymbol{\Omega}_{\text{mv}}^{-1} \mathbf{h}}. \quad (4.89)$$

After some algebraic manipulations, it can be shown that

$$\frac{\partial \mathbb{E}\{\hat{\mathbf{h}}_{\text{mv}}\}}{\partial \Re(\mathbf{h})} = \frac{(\mathbf{h}^H \boldsymbol{\Omega}_{\text{mv}}^{-1} \mathbf{h}) \boldsymbol{\Omega}_{\text{mv}}^{-1} - 2\Re(\boldsymbol{\Omega}_{\text{mv}}^{-1} \mathbf{h})^T \boldsymbol{\Omega}_{\text{mv}}^{-1} \mathbf{h} \mathbf{I}_{2J}}{(\mathbf{h}^H \boldsymbol{\Omega}_{\text{mv}}^{-1} \mathbf{h})^2} \in \mathbb{C}^{2J \times 2J}, \quad (4.90)$$

$$\frac{\partial \mathbb{E}\{\hat{\mathbf{h}}_{\text{mv}}\}}{\partial \Im(\mathbf{h})} = \frac{j(\mathbf{h}^H \boldsymbol{\Omega}_{\text{mv}}^{-1} \mathbf{h}) \boldsymbol{\Omega}_{\text{mv}}^{-1} - 2\Im(\boldsymbol{\Omega}_{\text{mv}}^{-1} \mathbf{h})^T \boldsymbol{\Omega}_{\text{mv}}^{-1} \mathbf{h} \mathbf{I}_{2J}}{(\mathbf{h}^H \boldsymbol{\Omega}_{\text{mv}}^{-1} \mathbf{h})^2} \in \mathbb{C}^{2J \times 2J}. \quad (4.91)$$

Finally, the lower bounds on the overall mean-squared channel estimation error of the subspace estimator and the MVDR estimator can, respectively, be obtained as

$$\mathbb{E}\{\|\tilde{\mathbf{h}}_{\text{ss}} - \mathbf{h}\|^2\} \geq \text{tr}(\text{CRB}(\mathbf{h})), \quad (4.92)$$

$$\mathbb{E}\{\|\tilde{\mathbf{h}}_{\text{mv}} - \mathbf{h}\|^2\} \geq \text{tr}(\text{BCRB}(\mathbf{h})) + \|\Delta \mathbf{h}_{\text{mv}}\|^2. \quad (4.93)$$

4.7 Detection Algorithms

In this section, we extend the results of the previous sections to develop a linear joint SF block decoding and detection scheme based on the MVDR approach which offers lower computational complexity and improved performance.

In the MVDR-based receiver, a filterbank $\mathbf{W} \triangleq [\mathbf{w}_r \ \mathbf{w}_i]$ is designed such that the variance at the output of each filter is minimized while at the same time multiple constraints in the direction of the desired signal are imposed [24], i.e.,

$$\mathbf{W}_{\min} = \arg \min_{\mathbf{W} \in \mathbb{C}^{L \times 2}} \text{tr}(\mathbf{W}^H \mathbf{R} \mathbf{W}),$$

subject to

$$\mathbf{w}_r^H \mathbf{g}_{1,r} = 1 \quad \text{and} \quad \mathbf{w}_i^H \mathbf{g}_{1,i} = 1. \quad (4.94)$$

Solving the optimization problem in (4.94) while enforcing the constraints yields

$$\mathbf{w}_r = (\mathbf{g}_{1,r}^H \mathbf{R}^{-1} \mathbf{g}_{1,r})^{-1} \mathbf{R}^{-1} \mathbf{g}_{1,r}, \quad (4.95)$$

$$\mathbf{w}_i = (\mathbf{g}_{1,i}^H \mathbf{R}^{-1} \mathbf{g}_{1,i})^{-1} \mathbf{R}^{-1} \mathbf{g}_{1,i}. \quad (4.96)$$

The estimate of the complex symbol b_1 of the user of interest can now be obtained from the received signal \mathbf{r} as follows

$$\hat{b}_1 = \text{sgn}[\Re(\mathbf{w}_r^H \mathbf{r})] + j \text{sgn}[\Re(\mathbf{w}_i^H \mathbf{r})]. \quad (4.97)$$

Thanks to the inherent signal structure imposed by SF coding, we may establish the following proposition which eventually leads to further simplification at the receiver.

Proposition 7 *Let the linear filters \mathbf{w}_r and \mathbf{w}_i be defined by (4.95) and (4.96), respectively. Then,*

$$(i) \quad \mathbf{w}_i = j \mathbf{D}_1 \mathbf{w}_r, \quad (4.98)$$

$$(ii) \quad \Re(\mathbf{W}^H [\mathbf{g}_{1,r} \quad \mathbf{g}_{1,i}]) = \mathbf{I}. \quad (4.99)$$

Proof: By substituting (4.95) into (4.98) we obtain

$$\mathbf{w}_i = \frac{j \mathbf{D}_1 \mathbf{R}^{-1} \mathbf{g}_{1,r}}{\mathbf{g}_{1,r}^H \mathbf{R}^{-1} \mathbf{g}_{1,r}}, \quad (4.100)$$

Meanwhile, from Lemmas 3 and 5 it is easy to verify that

$$\mathbf{g}_{1,i}^H \mathbf{R}^{-1} \mathbf{g}_{1,i} = j(-j) \mathbf{g}_{1,r}^H \mathbf{D}_1 \mathbf{R}^{-1} \mathbf{D}_1 \mathbf{g}_{1,r} = \mathbf{g}_{1,r}^H \mathbf{R}^{-1} \mathbf{g}_{1,r}.$$

Part (i) of the proposition then easily follows from part (i) of Lemma 3 by noticing that $\mathbf{D}_1 \mathbf{R}^{-1} = \mathbf{R}^{-1} \mathbf{D}_1$. Correspondingly, part (ii) follows from part (ii) of Lemma 3 and considering the facts that $\mathbf{w}_r^H \mathbf{g}_{1,r} = 1$ and $\mathbf{w}_i^H \mathbf{g}_{1,i} = 1$. ■

An immediate result following from part (i) of Proposition 7 is that we only need to evaluate one of the linear filters since the other filter can easily be constructed using the identity in (4.98). Furthermore, according to part (ii), the MVDR receiver is immune to self-interference, i.e., interference caused by signals of the same user. In fact, each one of

the linear filters \mathbf{w}_r or \mathbf{w}_i is distortionless in the direction of only one of the two signal components of the desired user while canceling the interference caused by the other signal component.

In practice, the estimate of the linear filters in (4.95) and (4.96) can be obtained by replacing the ensemble average of the received signal covariance matrix \mathbf{R} by its sample-average estimate $\hat{\mathbf{R}}$. However, using the same approach as described for channel estimation, one may use $\tilde{\mathbf{R}}$ instead of $\hat{\mathbf{R}}$ to achieve better performance, i.e.,

$$\tilde{\mathbf{w}}_r = (\mathbf{g}_{1,r}^H \tilde{\mathbf{R}}^{-1} \mathbf{g}_{1,r})^{-1} \tilde{\mathbf{R}}^{-1} \mathbf{g}_{1,r}, \quad (4.101)$$

$$\tilde{\mathbf{w}}_i = (\mathbf{g}_{1,i}^H \tilde{\mathbf{R}}^{-1} \mathbf{g}_{1,i})^{-1} \tilde{\mathbf{R}}^{-1} \mathbf{g}_{1,i}. \quad (4.102)$$

4.8 Simulations Studies

We consider a MC-CDMA system with 6 users utilizing code sequences of length³ 32 which is also the number of subcarriers. The cyclic prefix has length 4 samples which is 1/8th of the FFT size. The transmitter and the receiver are equipped with 2 and 1 antennas, respectively, while the SFBC employed is the orthogonal block code of [3] with a QPSK constellation. Each subchannel has 4 paths each randomly generated following a complex Gaussian distribution with zero-mean and unit-variance. Unless otherwise mentioned, the SNRs of all users in the system including the user of interest are fixed at 10 dB while a data record of $N = 40$ samples is used for estimating the covariance matrix. In what follows, the presented results are averages over 100 independent channel realizations.

We first verify the performance gains attained utilizing the proposed channel estimation methods compared to conventional methods by plotting the MSE performance versus the SNR of all users (assumed to be the same). In Fig. 4.1, the simulated performance of the MVDR algorithm is depicted while the performance of the subspace method is shown in Fig. 4.2. As expected, the proposed algorithms utilizing the improved sample matrix estimate offer better performance than the conventional methods wherein the actual sample estimate is employed. Also in Figs. 4.1 and 4.2, we include the analytical results obtained in Section 4.5. From these experiments, we infer that for sufficiently high SNR the actual MSEs of the proposed methods obtained from simulation provide good approximations to the analytical expressions even for the case of a short data record size $N = 40$. In order to examine whether the MSE of each channel estimator is able to approach the corresponding

³Constructed from Gold sequences of length 31 by appending a +1.

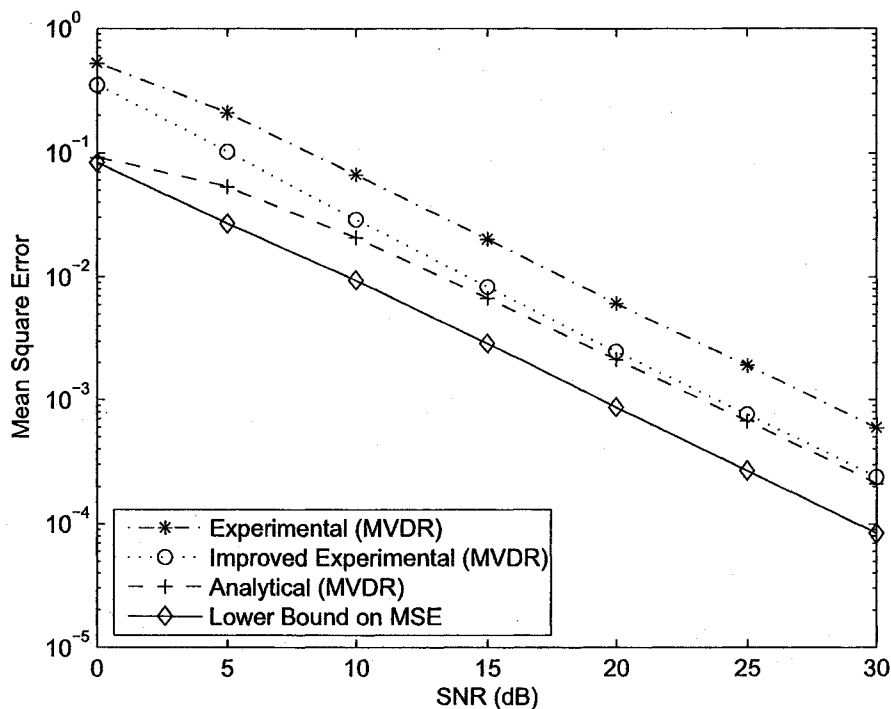


Fig. 4.1 The MVDR method MSE performance as a function of the SNR.

lower bound in large SNRs, the MSE performances of the MVDR and the subspace methods versus the SNR of the desired user are plotted in Figs. 4.3 and 4.4, respectively. These two figures further validate the accuracy of the performance lower bounds developed in this chapter.

We next examine the effect of the data record size used to form the sample matrix estimate on the performance of the channel identification methods. Fig. 4.5 shows the MSE performance as a function of the data length N for both MVDR and subspace algorithms. The proposed methods again exhibit their superior performance in the short data record sizes, whereas a severe performance loss is observed for conventional schemes due to insufficient observations. However, as can be seen from this experiment, by increasing the data record size, both approaches converge for each estimator.

The effect of the number of active users in the system is considered next. In Fig. 4.6, the MSE versus the number of active users is shown. The SNR of the desired user in the system is fixed at 20 dB. As can be seen from Fig. 4.6, the subspace method performance degrades dramatically for $K > 10$. However, for heavily loaded systems, the MVDR method still

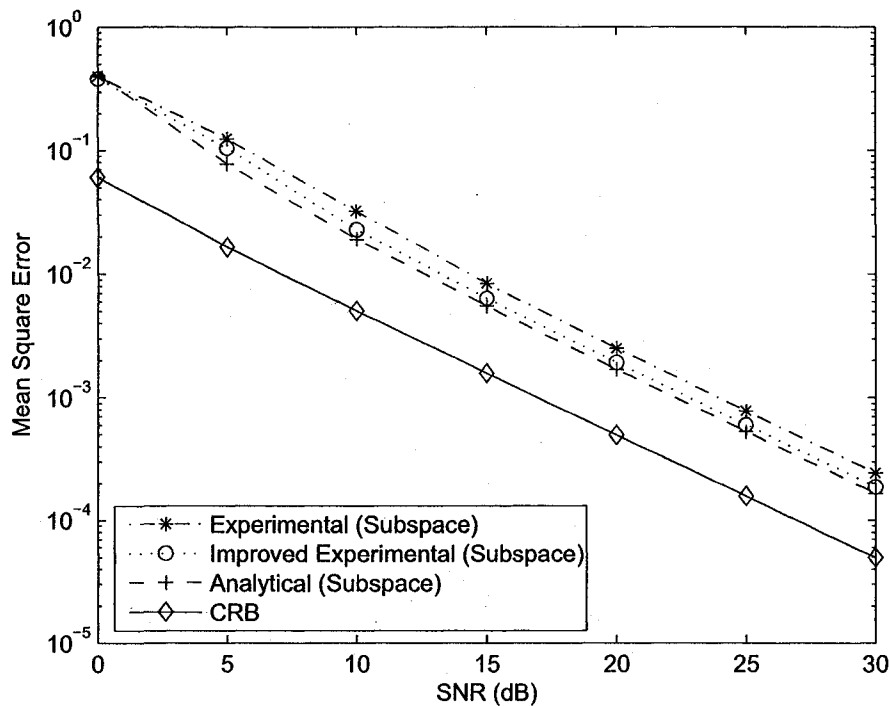


Fig. 4.2 The subspace method MSE performance as a function of the SNR.

is able to achieve satisfactory performance. This result can be justified by noticing that there is a theoretical limit on the number of users can be accommodated by the system when subspace methods are employed for channel parameter estimation as we mentioned in Section 4.4.1.

The next simulation experiment investigates the blind algorithms performance in near-far situations. The near-far problem arises when the signals from the interfering users arrive at the receiver with higher power than that of the desired one. Fig. 4.7 illustrates the MSE performance as a function of the near far ratio. The near-far ratio is defined as the ratio of the power of interfering users to the power of the desired user. The SNR of the desired user is fixed at 10dB. We see that the MSE performance of the channel estimation algorithms is insensitive to the near-far ratio. In other words, the presented channel estimation algorithms are near-far resistant.

Finally, the overall performance of the MVDR-based receiver is illustrated in Fig. 4.8. Fig. 4.8 illustrates the bit-error-rate (BER) performance as a function of the SNR. As was the case for the channel estimator, the proposed modification offers a considerable

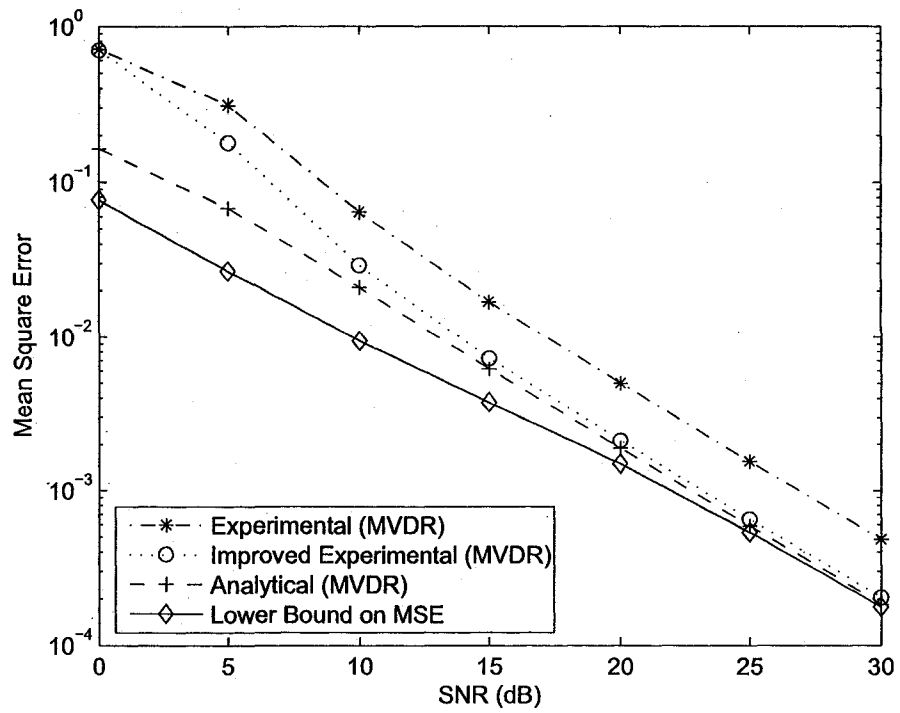


Fig. 4.3 The MVDR method MSE performance as a function of the SNR of the desired user.

performance improvement in the detection task.

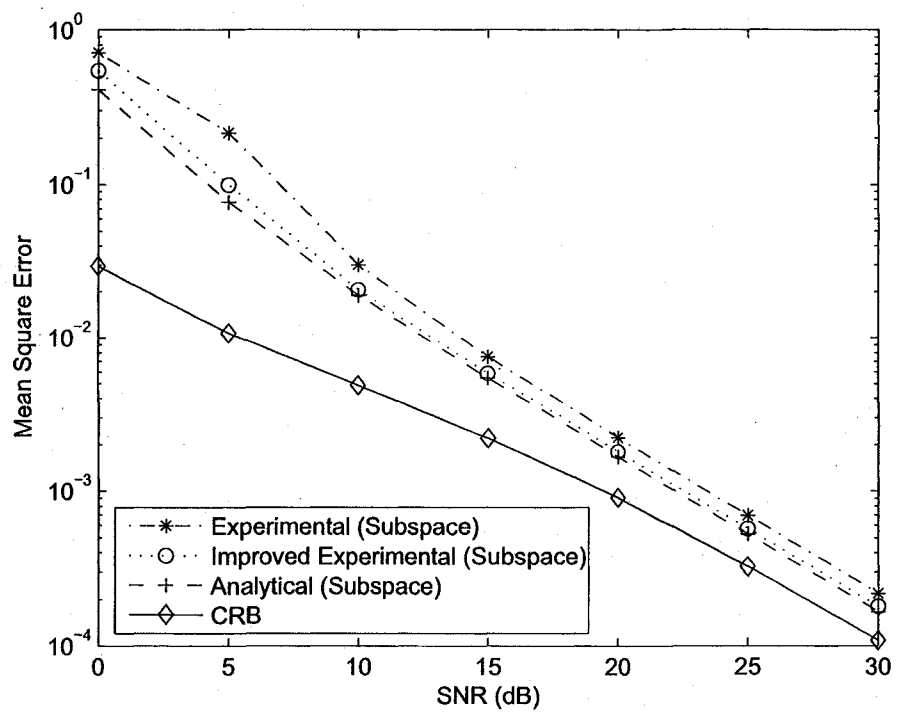


Fig. 4.4 The subspace method MSE performance as a function of the SNR of the desired user.

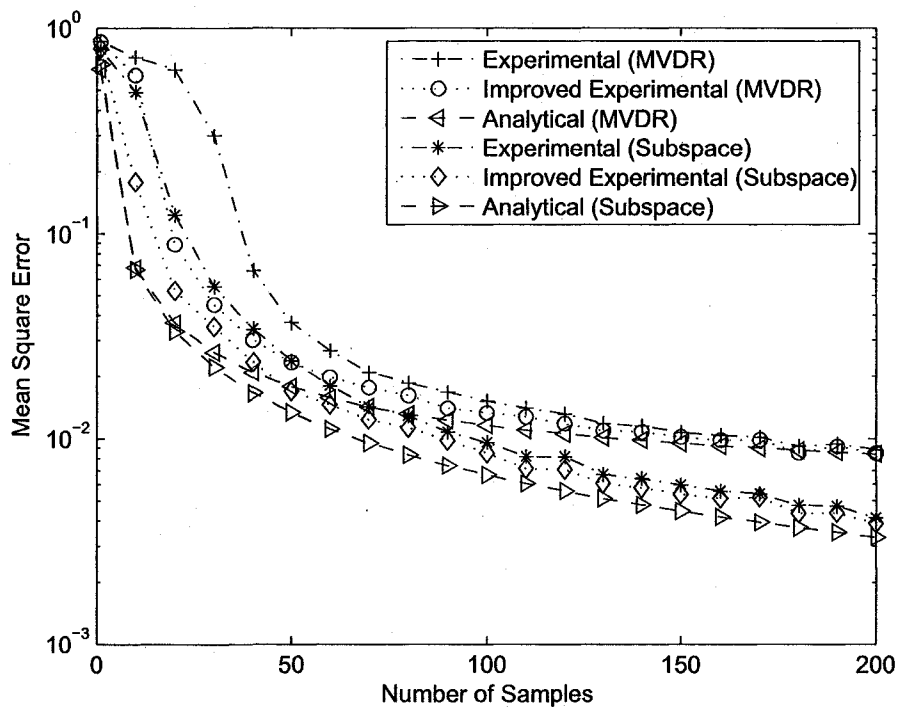


Fig. 4.5 The MSE performance of both MVDR and subspace methods as a function of the number of samples used for estimating the covariance matrix.

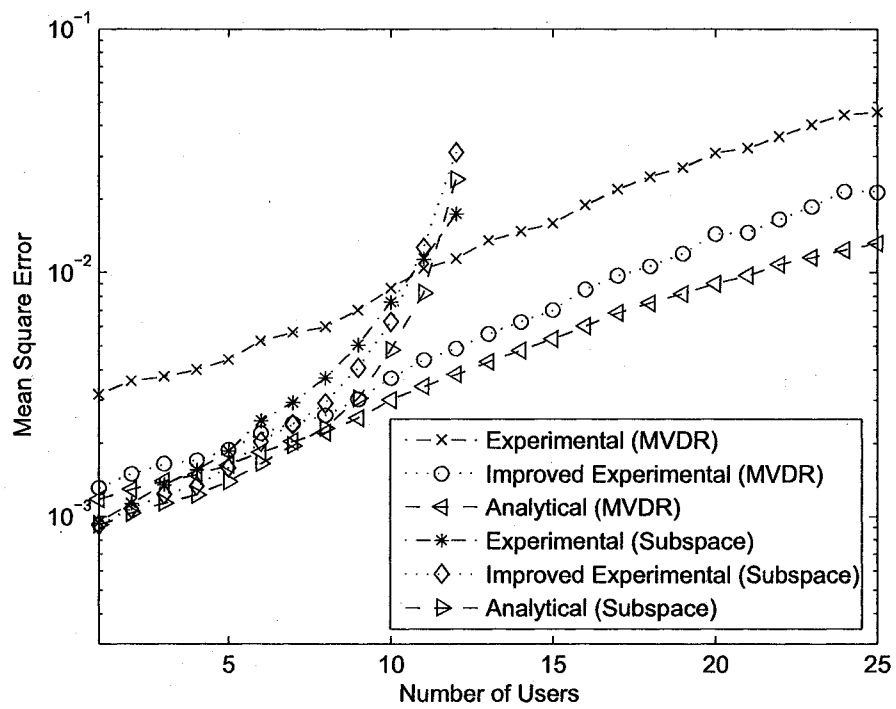


Fig. 4.6 The MSE performance of both MVDR and subspace methods as a function of the number of users in the system.

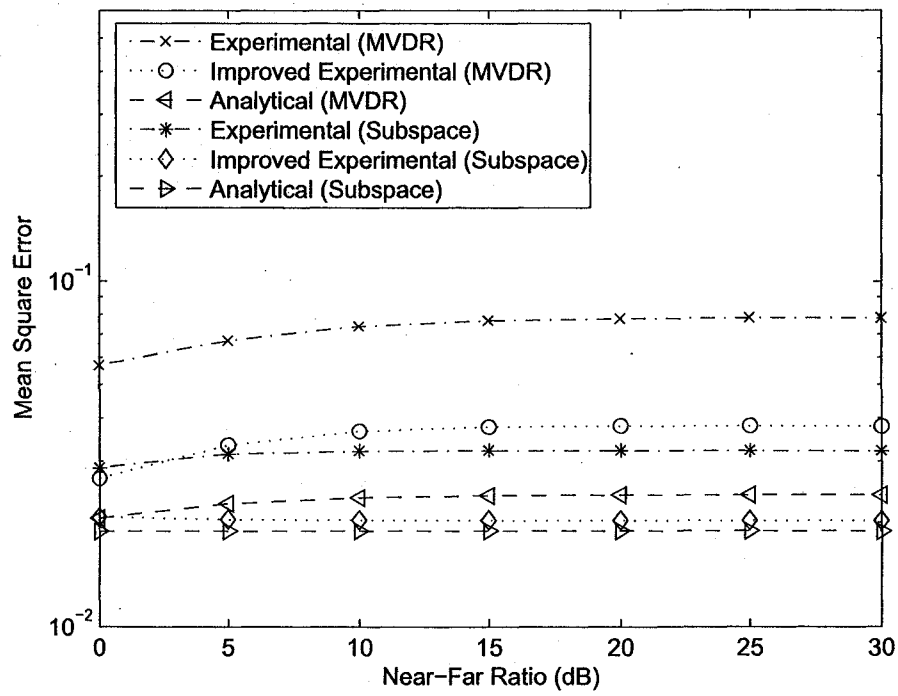


Fig. 4.7 The MSE performance of both MVDR and subspace methods as a function of the Near-Far Ratio.

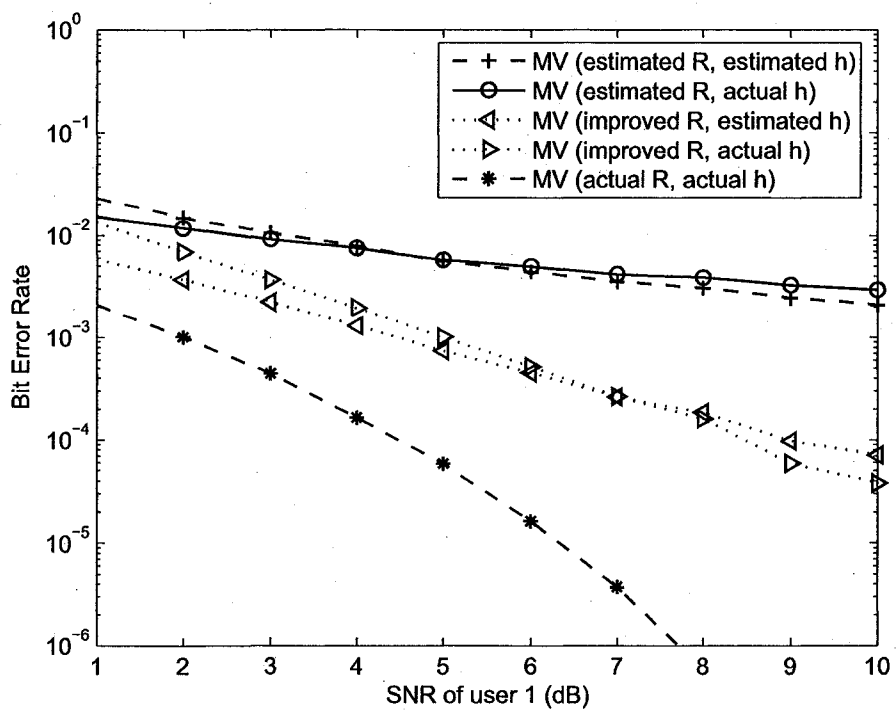


Fig. 4.8 The BER of the MVDR detector as a function of SNR.

Chapter 5

Conclusions and Future Research

In the first part of this thesis, we considered a non-conventional transmission scheme for the downlink of space-time block coded DS/CDMA systems that is based on ST block coding at the chip level. For this scheme, we developed both joint and disjoint space-time decoding and single user detection algorithms. The proposed single-user detectors require only filters of length approximately equal to the processing gain. As a result, the chip-level ST block coding scheme allows the receiver exhibit low decoding delay and improved performance characteristics in short data record adaptation structures compared to its symbol-level counterpart. We have also developed a blind channel estimation technique, and we derived necessary and sufficient conditions for channel identifiability with only a scalar ambiguity. In contrast to symbol-level ST coding transmission schemes where each user is assigned a different signature for each transmit antennas, in our scheme, each user only needs a single spreading code for all transmit antennas. Analytical expressions for the BER performance of decorrelator-type receivers show that these do not come at the expense of detection performance. However, the presented algorithms suffer from the inter-symbol interference (ISI) due to multipath dispersion. This, in turn, increases the effect of multiple access interference (MAI) in a multiuser environment, specially when transmit diversity is involved.

To mitigate the effects of ISI, and consequently MAI, in the second part of this dissertation, we considered a novel transmission scheme for the downlink of MC-CDMA systems with transmit diversity that is based on SF block coding at the chip level. For this scheme, we first developed both disjoint and joint space-frequency decoding and single user detection algorithms. We showed that the joint single-user detectors require only filters of

length approximately equal to the processing gain. As a result, the chip-level SF block coding scheme allows the design of receiver structures that exhibit low decoding delay and improved performance characteristics in short data record compared to their STBC counterparts. Then, we presented a comprehensive study and performance evaluation of two second-order-statistics-based blind channel estimation methods for the downlink of SFBC-MC-CDMA systems. For this purpose, we followed two different approaches for blind channel estimation: (i) a pre-FFT approach (ii) a post-FFT approach. For each approach, we derived necessary and sufficient conditions for channel identifiability with only a scalar ambiguity. Our studies identified two important properties of SFBC MC-CDMA systems: First, the identifiability of the channel is independent of the channel zeros location as long as the sufficient conditions hold. Second, the system is insensitive to antenna order ambiguity (also known as permutation ambiguity) even when there is only one signature assigned to each user. Besides, we showed that the post-FFT approach has the advantage of fully exploiting the inherent structure imposed by SFBC to improve the performance and lower the computational complexity required for practical systems where only an estimate of the received signal covariance matrix is available. The price to be paid for these achievements compared to the pre-FFT approach is some loss in the degrees of freedom of the estimators. Furthermore, we investigated the bias, and MSE under a finite data record size assumption for each estimator. We also showed that the MSE performance derived based on the EVD of autocorrelation matrix of the received signal provides a closer approximation to the actual MSE than SVD-based expressions in low SNRs. Finally, we formulated the CRBs for both unbiased and biased channel estimators that treat the interfering users' spreading codes as unknown deterministic quantities and we demonstrated that for downlink transmissions they always provide tighter bounds than the CRBs which assume the knowledge of all spreading codes.

5.1 Future Research

The research described in this thesis leads naturally to several extensions including:

- In chapters 3 & 4, we employed different strategies in designing linear detectors. As it was shown, in practice, the MVDR approach, as a data-based detector, shows performance degradation due to insufficient number of data samples. Moreover, in the presence of multipath distortion, channel parameters are estimated and resulting unavoidable errors that furthermore affect detectors performance. Thus, joint

performance analysis of detectors and channel estimators for SFBC MC-CDMA systems appears an interesting problem. As for the channel estimators presented in this thesis, perturbation technique can be applied to analyze the effect of finite samples on the performance of the MVDR detector. Specifically, after applying the statistics of sample-based estimated covariance, the expression for Signal-to-Noise-and-Interference Ratio (SINR) or Bit-Error-Rate (BER), as the performance criterion for our analysis, can be derived as a function of the sample size and other system parameters.

- In this thesis, we presented a blind detector, namely, the MVDR scheme, which employs the sample data covariance matrix directly. However, as an alternative, one may design blind detectors using eigen-components of the sample data covariance matrix. In particular, by applying eigenvalue decomposition (EVD) on the data covariance matrix and invoking orthogonality between the signal subspace and noise subspace, an equivalent blind subspace MMSE detection method can be employed. As for the blind channel estimators presented in this thesis which in practice their performance are commonly affected by various factors and each has its own limitations, the detectors that directly or indirectly employ the data covariance matrix could potentially involve similar challenges. Thus, the analytical results presented for each blind channel estimator in this work can to some extent be applied to its detector counterpart.
- In Chapter 4, we identified a unique structure for the covariance matrix of the received signal for SFBC MC-CDMA systems and we applied this structure to develop more efficient SOS-based channel estimation and detection algorithms. Future work can be done to extend the application of our results to other SOS-based channel estimation techniques. In fact, all sample data-based processing algorithms suffer from covariance estimation error due to finite sample effect. Therefore, the certain structure of the covariance matrix in SFBC MC-CDMA systems identified herein plays an important role in improving the performance and lowering the complexity of such algorithms.
- In the derivation of the blind channel estimation algorithms presented in this thesis, we assumed precise knowledge of the channel order at the receiver. In the absence of channel order information, a common approach in practice is to overestimate it.

Thus, it will be interesting to study the robustness of the presented blind channel estimation algorithms to channel order overestimation. More specifically, one could investigate the contribution to the total MSE of the subspace and MVDR channel estimators due to the estimation error caused by channel order overestimation.

References

- [1] N. Al-Dhahir, "Overview and comparison of equalization schemes for space-time-coded signals with application to EDGE," *IEEE Trans. Signal Processing*, vol. 50, pp. 2477–2488, Oct. 2002.
- [2] D. Gesbert, M. Shafi, D.-S. Shiu, P. J. Smith, and A. Naguib, "From theory to practice: An overview of MIMO space-time coded wireless systems," *IEEE J. Select. Areas Commun.*, vol. 21, pp. 281–302, Apr. 2003.
- [3] S. M. Alamouti, "A simple transmit diversity technique for wireless communications," *IEEE J. Select. Areas Commun.*, vol. 16, pp. 1451–1458, Oct. 1998.
- [4] V. Tarokh, H. Jafarkhani, and A. R. Calderbank, "Space-time block codes from orthogonal designs," *IEEE Trans. Inform. Theory*, vol. 45, pp. 1456–1467, July 1999.
- [5] A. Naguib, N. Seshadri, and A. R. Calderbank, "Increasing data rate over wireless channels," *IEEE Signal Processing Mag.*, pp. 76–92, May 2000.
- [6] Y. Gong and K. B. Letaief, "Performance evaluation and analysis of space-time coding in unequalized multipath fading links," *IEEE Trans. Commun.*, vol. 48, pp. 1778–1782, Nov. 2000.
- [7] E. Lindskog and A. Paulraj, "A transmit diversity scheme for channels with intersymbol interference," in *Proc. IEEE Int'l Conf. on Communications*, vol. 1, pp. 307–311, 2000.
- [8] N. Al-Dhahir, "Single-carrier frequency-domain equalization for space-time block-coded transmissions over frequency-selective fading channels," *IEEE Commun. Lett.*, vol. 5, pp. 304–306, July 2001.
- [9] S. Zhou and G. B. Giannakis, "Space-time coding with maximum diversity gains over frequency-selective fading channels," *IEEE Signal Processing Lett.*, vol. 8, pp. 269–272, Oct. 2001.
- [10] Z. Liu, G. Giannakis, S. Barbarossa, and A. Scaglione, "Transmit-antenna space-time block coding for generalized OFDM in the presence of unknown multipath," *IEEE J. Select. Areas Commun.*, vol. 19, pp. 1352–1364, July 2001.

- [11] G. Klang and B. Otterson, "Interference robustness aspects of space-time block code-based transmit diversity," *IEEE Trans. Signal Processing*, vol. 53, pp. 1299–1309, Apr. 2005.
- [12] F. Petre, G. Leus, L. Deneire, M. Engels, M. Moonen, and H. DeMan, "Space-time block-coding for single-carrier block-transmission DS-CDMA downlink," *IEEE J. Select. Areas Commun.*, vol. 21, pp. 350–361, Apr. 2003.
- [13] P. L. Kuffe and A. B. Sesay, "Iterative semiblind multiuser receivers for a space-time block-coded MC-CDMA uplink system," *IEEE Trans. Veh. Technol.*, vol. 53, pp. 601–610, May 2004.
- [14] M. O. Damen, A. Safavi, and K. Abed-Meraim, "On CDMA with space-time codes over multipath fading channels," *IEEE Trans. Commun.*, vol. 2, pp. 11–18, Jan. 2003.
- [15] D. Reynolds, X. Wang, and H. V. Poor, "Blind adaptive space-time multiuser detection with multiple transmitter and receiver antennas," *IEEE Trans. Signal Processing*, vol. 50, pp. 1261–1276, June 2002.
- [16] H. Li, X. Lu, and G. B. Giannakis, "Capon multiuser receiver for CDMA systems with space-time coding," *IEEE Trans. Signal Processing*, vol. 50, pp. 1193–1204, May 2002.
- [17] Y. Gong and K. B. Letaief, "An efficient space-frequency coded ofdm system for broadband wireless communications," *IEEE Trans. Commun.*, vol. 51, pp. 2019–2029, Nov. 2003.
- [18] W. Su, Z. Safar, M. Olfat, and K. J. R. Liu, "Obtaining full-diversity space-frequency codes from space-time codes via mapping," *IEEE Trans. Signal Processing*, vol. 51, pp. 2905–2916, Nov. 2003.
- [19] H. Bolcskei and A. J. Paulraj, "Space-frequency coded broadband OFDM systems," in *IEEE Wireless Communications and Networking Conference*, pp. 1–6, 2000.
- [20] H. Bolcskei and A. Paulraj, "Space-frequency codes for broadband fading channels," in *Proc. IEEE Int'l Symposium on Information Theory*, p. 219, 2001.
- [21] Z. Liu and G. B. Giannakis, "Space-time block coded multiple access through frequency-selective fading channels," *IEEE Trans. Commun.*, vol. 49, pp. 1033–1044, June 2001.
- [22] A. Stamoulis, Z. Liu, and G. B. Giannakis, "Space-time block-coded ofdma with linear precoding for multirate services," *IEEE Trans. Signal Processing*, vol. 50, pp. 119–129, Jan. 2002.

- [23] Z. Yang, B. Lu, and X. Wang, "Bayesian monte carlo multiuser receiver for space-time coded multicarrier CDMA systems," *IEEE J. Select. Areas Commun.*, vol. 19, pp. 1625–1637, Aug. 2001.
- [24] M. K. Tsatsanis and Z. Xu, "Performance analysis of minimum variance CDMA receivers," *IEEE Trans. Signal Processing*, vol. 46, pp. 3014–3022, Nov. 1998.
- [25] E. A. Sourour and M. Nakagawa, "Performance of orthogonal multicarrier CDMA in a multipath fading channel," *IEEE Trans. Commun.*, vol. 44, pp. 356–367, Mar. 1996.
- [26] I. N. Psaromiligkos and S. N. Batalama, "Rapid combined synchronization/ demodulation structures for DS-CDMA systems - part II: finite data-record performance analysis," *IEEE Trans. Commun.*, vol. 51, pp. 1162–1172, July 2003.
- [27] I. R. S. Casella, P. J. E. Jeszensky, and E. S. Sousa, "Evaluation of chip space-time block coding DS-WCDMA in time-varying channels," in *IEEE Personal, Indoor and Mobile Radio Commu. Conf.*, pp. 1588–1592, 2003.
- [28] T. X. Lai and A. B. Sesay, "Space-time block coding over frequency selective fading channel in the downlink WCDMA system," in *IEEE Commun., Computers and signal Processing Conf.*, pp. 372–375, 2003.
- [29] E. A. Lee and D. G. Messerschmitt, eds., *Digital Communication*. 2nd ed., Kluwer, 1994.
- [30] X. Wang and H. V. Poor, "Blind multiuser detection: A subspace approach," *IEEE Trans. Inform. Theory*, vol. 44, pp. 677–690, Mar. 1998.
- [31] P. Xiong, I. N. Psaromiligkos, and S. N. Batalama, "On the relative output SINR of the full and partial decorrelators," *IEEE Trans. Commun.*, vol. 51, pp. 1633–1637, Oct. 2003.
- [32] S. Ulukus and R. Yates, "A blind adaptive decorrelating detector for CDMA systems," *IEEE J. Select. Areas Commun.*, vol. 16, pp. 1530–1541, Oct. 1998.
- [33] B. Muquet, G. B. Giannakis, M. D. Courville, and P. Duhamel, "Cyclic prefixing or zero padding for wireless multicarrier transmissions?," *IEEE Trans. Signal Processing*, vol. 50, pp. 2136–2148, Dec. 2002.
- [34] K. Lee and D. Williams, "A space-frequency transmitter diversity technique for OFDM systems," in *IEEE Global Communications Conf.*, pp. 1473–1477, 2000.
- [35] X. Hu and Y. H. Chew, "On the performance and capacity of an asynchronous space-time block-coded MC-CDMA system in the presence of carrier frequency offset," *IEEE Trans. Veh. Technol.*, vol. 53, pp. 1327–1340, Sept. 2004.

- [36] W. Sun and H. Li, "Space-time coded MC-CDMA: blind channel estimation, identifiability, and receiver design," *EURASIP Journal on Applied Signal Processing*, pp. 1314–1324, Dec. 2002.
- [37] L. Chong and L. B. Milstein, "The effects of channel-estimation errors on a space-time spreading CDMA system with dual transmit and dual receive diversity," *IEEE Trans. Commun.*, vol. 52, pp. 1145–1151, July 2004.
- [38] X. Wang and J. Wang, "Effect of imperfect channel estimation on transmit diversity in CDMA systems," *IEEE Trans. Veh. Technol.*, vol. 53, pp. 1400–1412, Sept. 2004.
- [39] S. Zhou, B. Muquet, and G. B. Giannakis, "Subspace-based (semi-) blind channel estimation for block precoded space-time OFDM," *IEEE Trans. Signal Processing*, vol. 50, pp. 1215–1228, May 2002.
- [40] S. Roy and H. Yan, "Blind channel estimation in multirate CDMA systems," *IEEE Trans. Commun.*, vol. 50, pp. 995–1004, June 2002.
- [41] W. Kang and B. Champagne, "Subspace-based blind channel estimation: generalization and performance analysis," *IEEE Trans. Signal Processing*, vol. 53, pp. 1151–1162, Mar. 2005.
- [42] K. Li and H. Liu, "Joint channel and carrier offset estimation in CDMA communications," *IEEE Trans. Signal Processing*, vol. 47, pp. 1811–1821, July 1999.
- [43] S. Buzzi and H. V. Poor, "On parameter estimation in long-code DS/CDMA systems: Cramr-rao bounds and least-squares algorithms," *IEEE Trans. Signal Processing*, vol. 51, pp. 545–559, Feb. 2003.
- [44] L. Tong and S. Perreau, "Multichannel blind identification: from subspace to maximum likelihood methods," *Proc. IEEE*, vol. 86, pp. 1951–1968, Oct. 1998.
- [45] E. Moulines, P. Duhamel, J.-F. Cardoso, and S. Mayrargue, "Subspace methods for the blind identification of multichannel FIR filters," *IEEE Trans. Signal Processing*, vol. 43, pp. 516–525, Feb. 1995.
- [46] M. Wax and T. Kailath, "Detection of signals by information theoretic criteria," *IEEE Trans. Acoust., Speech, Signal Processing*, vol. 32, pp. 387–392, Apr. 1985.
- [47] H. Akaike, "A new look at the statistical model identification," *IEEE Trans. Automat. Contr.*, vol. 19, pp. 716–723, Dec. 1974.
- [48] B. L. Hughes, "Differential space-time modulation," *IEEE Trans. Inform. Theory*, vol. 46, pp. 2567–2578, Nov. 2000.

- [49] V. Tarokh and H. Jafarkhani, "A differential detection scheme for transmit diversity," *IEEE J. Select. Areas Commun.*, vol. 18, pp. 1169–1174, July 2000.
- [50] Z. Xu, "Perturbation analysis for subspace decomposition with applications in subspace-based algorithms," *IEEE Trans. Signal Processing*, vol. 50, pp. 2820–2830, Nov. 2002.
- [51] Z. Xu, "Asymptotic performance of subspace methods for synchronous multirate CDMA systems," *IEEE Trans. Signal Processing*, vol. 50, pp. 2015–2026, Aug. 2002.
- [52] P. Stoica and A. Nehorai, "Music, maximum likelihood, and cramer-rao bound," *IEEE Trans. Acoust., Speech, Signal Processing*, vol. 37, pp. 720–741, May 1989.
- [53] P. Stoica and A. Nehorai, "Performance study of conditional and unconditional direction-of-arrival estimation," *IEEE Trans. Acoust., Speech, Signal Processing*, vol. 38, pp. 1783–1795, Oct. 1990.
- [54] E. de Carvalho and D. T. M. Slock, "Cramer-rao bounds for semi-blind, blind and training sequence based channel estimation," in *Proc. IEEE Int'l Workshop on Signal Processing Advances for Wireless Communications*, (Paris, France), pp. 129–132, 1997.
- [55] Z. Xu, P. Liu, and X. Wang, "Blind multiuser detection: from MOE to subspace methods," *IEEE Trans. Signal Processing*, vol. 52, pp. 510–524, Feb. 2004.
- [56] H. L. V. Trees, ed., *Detection, Estimation, and Modulation Theory*. Wiley, New York, 1968.
- [57] S. Gazor and H. S. Rad, "Space-time coding ambiguities in joint adaptive channel estimation and detection," *IEEE Trans. Signal Processing*, vol. 52, pp. 372–384, Feb. 2004.